



## King's Research Portal

DOI:

[10.1161/CIRCULATIONAHA.117.028388](https://doi.org/10.1161/CIRCULATIONAHA.117.028388)

*Document Version*

Publisher's PDF, also known as Version of record

[Link to publication record in King's Research Portal](#)

*Citation for published version (APA):*

Aubdool, A. A., Thakore, P., Argunhan, F., Smillie, S.-J., Schnelle, M., Srivastava, S., Alawi, K. M., Wilde, E., Mitchell, J., Farrell-Dillon, K., Richards, D. A., Maltese, G., Siow, R. C., Nandi, M., Clark, J. E., Shah, A. M., Sams, A., & Brain, S. D. (2017). A Novel  $\alpha$ -Calcitonin Gene-Related Peptide Analogue Protects Against End-Organ Damage in Experimental Hypertension, Cardiac Hypertrophy and Heart Failure. *Circulation (Baltimore)*, 136(4), 367-383. <https://doi.org/10.1161/CIRCULATIONAHA.117.028388>

### **Citing this paper**

Please note that where the full-text provided on King's Research Portal is the Author Accepted Manuscript or Post-Print version this may differ from the final Published version. If citing, it is advised that you check and use the publisher's definitive version for pagination, volume/issue, and date of publication details. And where the final published version is provided on the Research Portal, if citing you are again advised to check the publisher's website for any subsequent corrections.

### **General rights**

Copyright and moral rights for the publications made accessible in the Research Portal are retained by the authors and/or other copyright owners and it is a condition of accessing publications that users recognize and abide by the legal requirements associated with these rights.

- Users may download and print one copy of any publication from the Research Portal for the purpose of private study or research.
- You may not further distribute the material or use it for any profit-making activity or commercial gain
- You may freely distribute the URL identifying the publication in the Research Portal

### **Take down policy**

If you believe that this document breaches copyright please contact [librarypure@kcl.ac.uk](mailto:librarypure@kcl.ac.uk) providing details, and we will remove access to the work immediately and investigate your claim.



# A Novel $\alpha$ -Calcitonin Gene-Related Peptide Analogue Protects Against End-Organ Damage in Experimental Hypertension, Cardiac Hypertrophy, and Heart Failure

Editorial, see p 384

**BACKGROUND:** Research into the therapeutic potential of  $\alpha$ -calcitonin gene-related peptide ( $\alpha$ -CGRP) has been limited because of its peptide nature and short half-life. Here, we evaluate whether a novel potent and long-lasting ( $t_{1/2} \geq 7$  hours) acylated  $\alpha$ -CGRP analogue ( $\alpha$ Analogue) could alleviate and reverse cardiovascular disease in 2 distinct murine models of hypertension and heart failure in vivo.

**METHODS:** The ability of the  $\alpha$ Analogue to act selectively via the CGRP pathway was shown in skin by using a CGRP receptor antagonist. The effect of the  $\alpha$ Analogue on angiotensin II-induced hypertension was investigated over 14 days. Blood pressure was measured by radiotelemetry. The ability of the  $\alpha$ Analogue to modulate heart failure was studied in an abdominal aortic constriction model of murine cardiac hypertrophy and heart failure over 5 weeks. Extensive ex vivo analysis was performed via RNA analysis, Western blot, and histology.

**RESULTS:** The angiotensin II-induced hypertension was attenuated by cotreatment with the  $\alpha$ Analogue (50 nmol·kg<sup>-1</sup>·d<sup>-1</sup>, SC, at a dose selected for lack of long-term hypotensive effects at baseline). The  $\alpha$ Analogue protected against vascular, renal, and cardiac dysfunction, characterized by reduced hypertrophy and biomarkers of fibrosis, remodeling, inflammation, and oxidative stress. In a separate study, the  $\alpha$ Analogue reversed angiotensin II-induced hypertension and associated vascular and cardiac damage. The  $\alpha$ Analogue was effective over 5 weeks in a murine model of cardiac hypertrophy and heart failure. It preserved heart function, assessed by echocardiography, while protecting against adverse cardiac remodeling and apoptosis. Moreover, treatment with the  $\alpha$ Analogue was well tolerated with neither signs of desensitization nor behavioral changes.

**CONCLUSIONS:** These findings, in 2 distinct models, provide the first evidence for the therapeutic potential of a stabilized  $\alpha$ Analogue, by mediating (1) antihypertensive effects, (2) attenuating cardiac remodeling, and (3) increasing angiogenesis and cell survival to protect against and limit damage associated with the progression of cardiovascular diseases. This indicates the therapeutic potential of the CGRP pathway and the possibility that this injectable CGRP analogue may be effective in cardiac disease.

Aisah A. Aubdool, BSc, MRes, PhD

Pratish Thakore, BSc, MSc

Fulye Argunhan, BSc, MSc

Sarah-Jane Smillie, BSc, PhD

Moritz Schnelle, MD, PhD

Salil Srivastava, BSc, MRes, PhD

Khadija M. Alawi, BSc, MSc, PhD

Elena Wilde, BSc

Jennifer Mitchell, BSc, MRes

Keith Farrell-Dillon, BSc, MSc

Daniel A. Richards, BSc, MRes, PhD

Giuseppe Maltese, MD

Richard C. Siow, BSc, PhD

Manasi Nandi, BSc, PhD

James E. Clark, BSc, PhD

Ajay M. Shah, MD, FMedSci

Anette Sams, MSc, PhD

Susan D. Brain, BSc, PhD

**Correspondence to:** Susan D. Brain, BSc, PhD, BHF Centre of Excellence and Centre of Integrative Biomedicine, Cardiovascular Division, King's College London, 150 Stamford Street, London SE1 9NH, United Kingdom. E-mail sue.brain@kcl.ac.uk

Sources of Funding, see page 381

**Key Words:** heart failure  
■ hypertension ■ inflammation  
■ oxidative stress ■ receptors, calcitonin gene-related peptide

© 2017 The Authors. *Circulation* is published on behalf of the American Heart Association, Inc., by Wolters Kluwer Health, Inc. This is an open access article under the terms of the [Creative Commons Attribution License](#), which permits use, distribution, and reproduction in any medium, provided that the original work is properly cited.

## Clinical Perspective

### What Is New?

- We have used a novel injectable stabilized  $\alpha$ -calcitonin gene-related peptide (CGRP) agonist, the first to our knowledge, to analyze the effect on cardiovascular disease in 2 distinct murine models.
- We show that the CGRP agonist is well tolerated and selective in the vasculature.
- The CGRP agonist prevented the onset of and limited angiotensin II-induced hypertension.
- The CGRP agonist also protected against heart failure in the abdominal aortic constriction model, suggesting that this  $\alpha$ -CGRP analogue is beneficial in cardiovascular disease.

### What Are the Clinical Implications?

- These preclinical data show that activating the protective CGRP pathway, using selective stabilized agonists, constitutes a novel therapeutic application.
- The results are a stimulus to further develop agonists, including those that are orally active.
- The results highlight the potential development of this injectable stabilized CGRP agonist ( $\alpha$ -CGRP analogue) for the treatment of cardiac dysfunction (eg, in advanced heart failure).

Calcitonin gene-related peptide (CGRP) is a member of the calcitonin family of peptides. CGRP is primarily localized to sensory nerves, although nonneuronal sources are reported.<sup>1</sup> The major CGRP receptor is formed by the coexpression of calcitonin receptor-like receptor (CLR) with receptor activity-modifying protein-1 (RAMP1).<sup>1</sup> These receptors are found throughout the cardiovascular system, specifically in the media, intima, and endothelial layer of blood vessels. Although CGRP is established as a potent vasodilator, there is little evidence that sufficient endogenous CGRP is released to influence physiological blood pressure regulation, although CGRP-containing nerves surround all cardiovascular tissues. Several CGRP receptor antagonists and antibodies developed as migraine therapies have minimal effect on blood pressure in healthy individuals.<sup>1,2</sup> Evidence that CGRP plays a role in cardiovascular protection arises from acute studies where CGRP has been administered in rodent models of hypertension,<sup>3,4</sup> using spontaneously hypertensive rats<sup>5,6</sup> and  $\alpha$ -CGRP-specific knockout (KO) mice.<sup>7</sup> The beneficial effects of the native CGRP peptide have also been observed when administered for up to 24 hours to patients with congestive heart failure with no evidence of tolerance.<sup>8,9</sup>

Although systemic endogenous CGRP levels are raised in some conditions such as pregnancy, it has

proven difficult to raise endogenous CGRP levels to provide cardiovascular benefit. There is little evidence that stimulation of the major sensory nerve-localized transient receptor potential (TRP) channels (TRPV1 or TRPA1) releases CGRP to play a primary protective endogenous role in hypertension.<sup>10,11</sup> This is despite knowledge that activation of TRP channels expressed on sensory nerves induces CGRP-dependent vasodilation in peripheral tissues such as skin.<sup>12</sup> Of note, TRPA1 activation using nitroxyl<sup>13</sup> mediates inotropic effects in the failing heart,<sup>14</sup> but the importance of CGRP is debated.<sup>15</sup> Some CGRP/calcitonin KO mouse strains possess a raised blood pressure at baseline, indicating a potential role of endogenous CGRP.<sup>1,16</sup> We have shown that  $\alpha$ -CGRP-specific KO mice have normal baseline blood pressure but enhanced hypertension following angiotensin II (AngII) infusion for up to 28 days, in comparison with wild-type mice.<sup>7</sup> This was associated with aortic hypertrophy and endothelial dysfunction observed as loss of endothelial nitric oxide synthase and evidence of oxidative stress.<sup>7</sup>

This and related knowledge, together with the understanding that global human RAMP1 transgenic mice are protected from hypertension,<sup>17</sup> led us to hypothesize that a stabilized  $\alpha$ -CGRP agonist with the ability to remain active over prolonged periods would elicit cardioprotective properties. This first  $\alpha$ -CGRP analogue ( $\alpha$ Analogue) is acylated with an albumin-binding fatty acid moiety that allows reversible albumin binding (patent WO 2011/051312 A1).<sup>18,19</sup> It has similar pharmacological properties to the native CGRP peptide, but exhibits prolonged action and improved pharmacokinetic properties with a half-life of >7 hours that benefited a model of type 2 diabetes mellitus.<sup>18,19</sup> The current study demonstrates that the stabilized  $\alpha$ Analogue<sup>18</sup> protects against the development of AngII-induced hypertension and abdominal aortic constriction (AAC)-induced cardiac hypertrophy and heart failure in mice for several weeks. We have determined mechanisms by which this  $\alpha$ Analogue can reverse vascular, renal, and cardiac damage. To our knowledge, this is the first detailed study using an  $\alpha$ -CGRP agonist that has improved stability over the native peptide and illustrates the potential of the CGRP pathway as a therapeutic target and injectable stabilized CGRP agonists as therapeutic agents.

## METHODS

A detailed Methods is provided in the [online-only Data Supplement](#).

## Animals

Experiments complied with ARRIVE (Animal Research: Reporting In vivo Experiments) guidelines, in accordance with the UK Home Office Animals (Scientific Procedures) Act, 1986 and approved by the local Animal Care and Ethics Committee.

Male mice, CD1 or C57BL/6J (12–18 weeks of age; Charles River) were used.

### AngII Murine Hypertension Model

Mice were infused with AngII (1.1 mg·kg<sup>-1</sup>·d<sup>-1</sup>) or saline (control) continuously for 14 days via osmotic mini pumps, as previously.<sup>7</sup> Mice were treated daily with αAnalogue (50 nmol·kg<sup>-1</sup>·d<sup>-1</sup>, SC) or vehicle (0.219 mol/L mannitol, 5% hydroxypropyl-β-cyclodextrin, 1.6% ammonium acetate at pH6.5) for 14 days or at 7 days onward for therapeutic dosing.

### Cardiac Hypertrophy Murine Model

Mice were surgically subjected to pressure overload-induced cardiac hypertrophy and heart failure<sup>20</sup> for 5 weeks and treated daily with αAnalogue (50 nmol·kg<sup>-1</sup>·d<sup>-1</sup>, SC) or vehicle.

### Measurement of Cutaneous Blood Flow

Blood flow was assessed in the ear, leg, or paw using the Full-field Laser Perfusion Imager (Moor Instruments) on anesthetized mice.<sup>12</sup> To investigate the local effects of αAnalogue, mice were pretreated with the CGRP antagonist BIBN4096 (0.3 mg/kg, IV) or control (neutralized saline) followed by αAnalogue injection (100 pmol daily, ipsilateral ear) or vehicle

(contralateral ear). In separate experiments, blood flow in the periphery was measured following systemic treatment of the αAnalogue.

### Measurement of Blood Pressure

Blood pressure, heart rate, and activity were measured using a radiotelemetry (PA-C10, DSI), as previously described<sup>10–12</sup> in AngII-infused C57BL/6J mice. For the characterization of the systemic dose of αAnalogue, blood pressure was measured by tail-cuff plethysmography (CODA 8, Kent Scientific) in conscious mice.<sup>7,10</sup> Following AAC-induced cardiac hypertrophy, blood pressure was measured via carotid artery in anesthetized mice.

### Echocardiography

In vivo cardiac function was assessed using a Vevo 2100 Imaging System with a 40-MHz linear probe (Visualsonics).<sup>20</sup> Data analysis was performed with Vevo 2100 software v.1.2.1 (Visualsonics).

### Light Aversion Assay

Light aversion (10 minutes, 1000 lux) was determined at baseline and 2 hours following injection of αAnalogue, vehicle, or

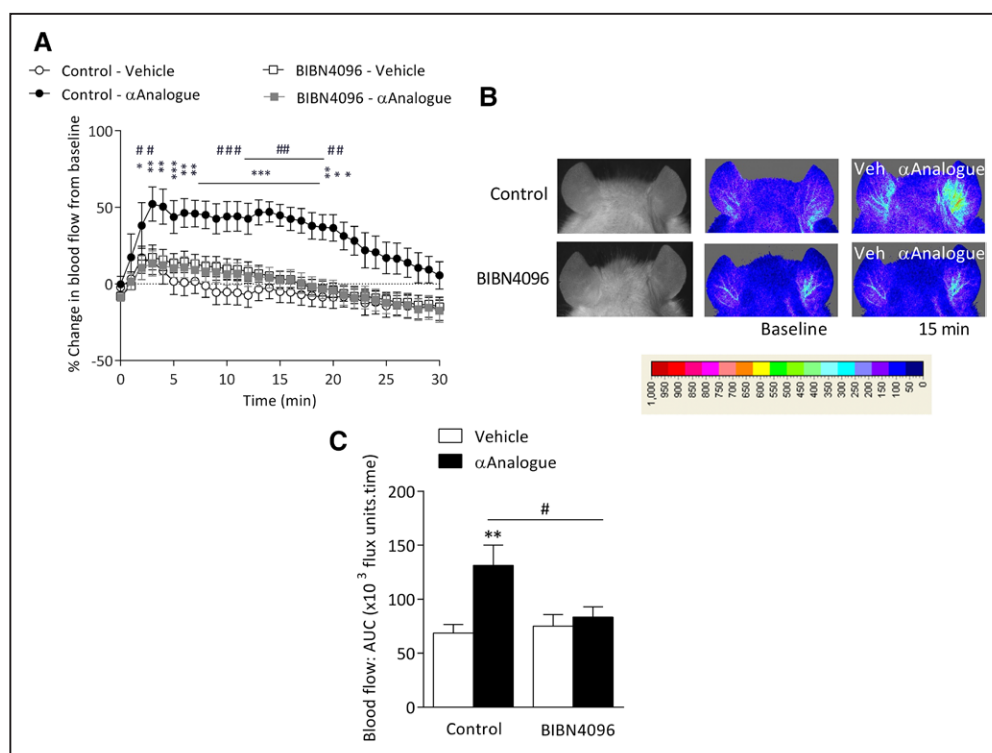


**Figure 1. α-CGRP analogue (αAnalogue) increases vascular blood flow via CGRP receptors.**

Blood flow monitored using Full-field Laser Perfusion Imager in the ear vasculature of mice pretreated with control (saline) or CGRP receptor antagonist BIBN4096 (0.3 mg/kg, IV) at baseline and following intradermal injection of αAnalogue (100 pmol, daily) or vehicle (Veh) (15 μL, n=6). **A**, Blood flow responses expressed as % change from baseline. **B**, Representative Full-field Laser Perfusion Imager pictures alongside gray/black photo showing blood flow at baseline and 15 minutes after treatment. **C**, Blood flow assessed by area under the curve (AUC) for 30 minutes following vehicle or αAnalogue administration (n=6). Data showed as mean±SEM. \**P*<0.05, \*\**P*<0.01, \*\*\**P*<0.001 versus vehicle-treated; #*P*<0.05, ##*P*<0.01, ###*P*<0.001 for αAnalogue treated (**A**, repeated-measures 2-way ANOVA + Bonferroni post hoc test; **C**, 2-way ANOVA + Bonferroni post hoc test). α-CGRP indicates α-calcitonin gene-related peptide.

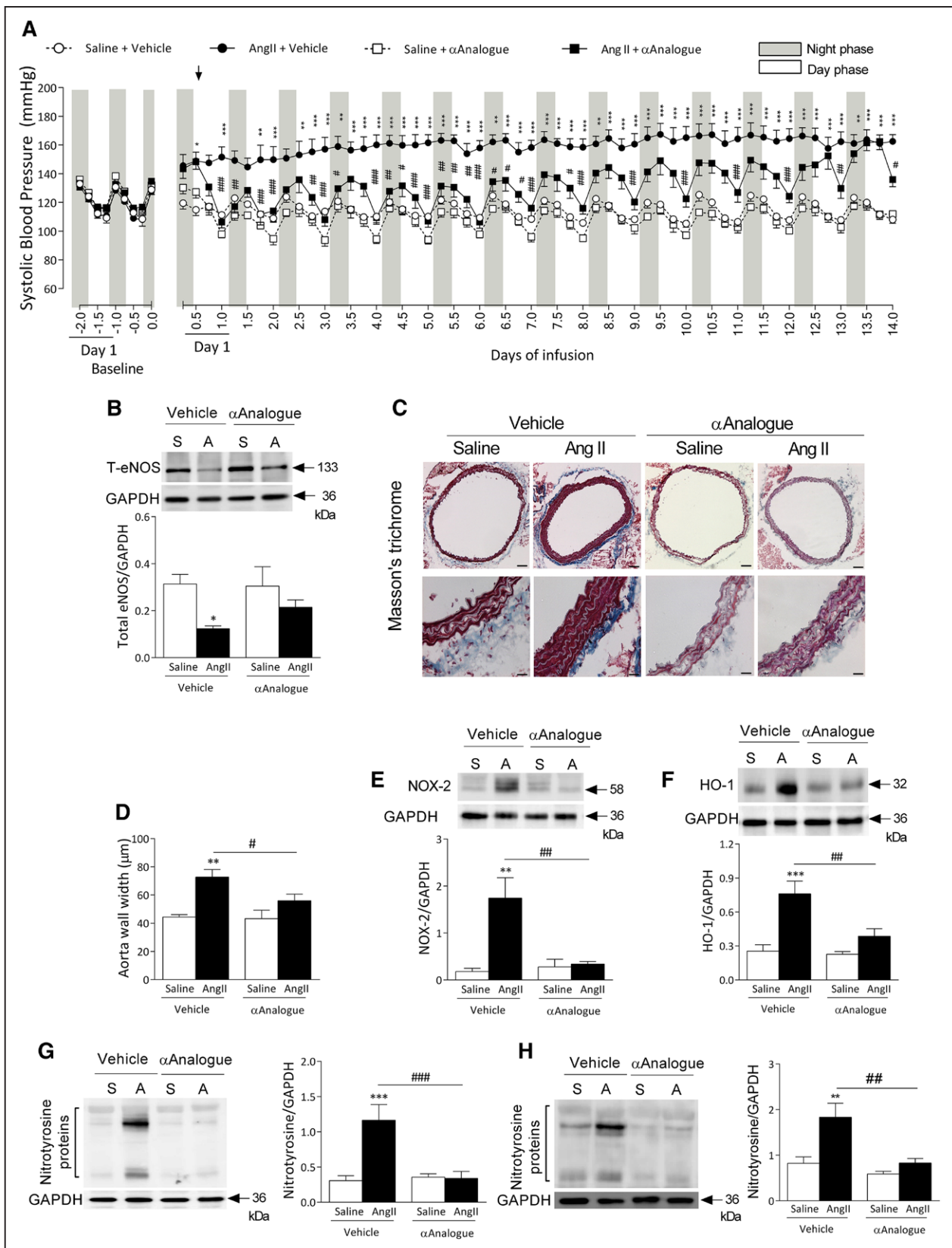


**Figure 2.** Daily systemic treatment with  $\alpha$ -CGRP analogue ( $\alpha$ Analogue) protects against angiotensin II (AngII)-induced hypertension and vascular damage.

Mice were infused with AngII (A, 1.1 mg·kg<sup>-1</sup>·d<sup>-1</sup>) or control (S, saline) for 14 days and treated daily with vehicle (V) or  $\alpha$ Analogue (50 nmol/kg, SC). **A**, Systolic blood pressure was measured by radiotelemetry. Results expressed as 6-hour average. (Continued)

positive control glyceryl trinitrate (320 nmol/kg, IV). See the [online-only Data Supplement](#).

### Glucose Tolerance Test

Mice were fasted for 6 hours and treated with glucose (1 g/kg, IP). Blood glucose level was determined at baseline and stated time points using a One Touch Vita glucose meter (Lifescan).

### RNA Preparation and Real-Time Quantitative Polymerase Chain Reaction

Total RNA was extracted using the Qiagen RNeasy Microarray Mini Kit (Qiagen), followed by reverse transcription into cDNA (Applied Biosystems, Life technologies Ltd). Quantitative polymerase chain reaction was performed with a SYBR-green-based polymerase chain reaction mix (Sensi-Mix, SYBR-green No ROX; Bioline). Primer details are listed in [online-only Data Supplement Table I](#).

### Western Blotting

Western blot analysis was performed in aorta, mesentery, heart, and kidney as previously described.<sup>7</sup> Antibody details are listed in the [online-only Data Supplement](#).

### Quantification of Noradrenaline and Cytokines Using Enzyme-Linked Immunosorbent Assay

After 14 days of AngII or saline infusion, plasma and kidney samples were collected for determination of noradrenaline and inflammatory cytokines (interleukin-6, tumor necrosis factor- $\alpha$ ) by using standard enzyme-linked immunosorbent assay as described in the [online-only Data Supplement](#).

### Histology

Aorta, heart, and kidney tissues were fixed in 4% paraformaldehyde, as previously described.<sup>7</sup> Staining protocol and antibody details are listed in the [online-only Data Supplement](#).

### Statistical Analysis

Results are expressed as mean $\pm$ SEM. Statistical analysis was performed using an unpaired 2-tailed Student *t* test, 1-way or repeated-measures 2-way ANOVA followed by Bonferroni post hoc test. *P*<0.05 was considered to represent a significant difference.

## RESULTS

### Effects of Local Administration of the $\alpha$ Analogue on Vascular Blood Flow

Initial studies determined the ability of the  $\alpha$ Analogue to increase blood flow via the CGRP receptor (CLR/RAMP1) pathway. Intradermal administration of the  $\alpha$ Analogue increased blood flow in a dose-dependent manner in the skin of anesthetized naive mice as determined by laser perfusion imaging (Figure 1A and 1B, [online-only Data Supplement Figure I](#)). This effect was abolished by the selective nonpeptide CGRP receptor antagonist BIBN4096 (Figure 1A through 1C).

### Systemic Treatment With the $\alpha$ Analogue Protects Against Hypertension

Systemic injection of the  $\alpha$ Analogue (10–100 nmol/kg, SC) induced a dose-dependent decrease in blood pressure at 1 to 6 hours, with significance observed at 100 nmol/kg in comparison with vehicle treatment, assessed by tail-cuff in naive mice ([online-only Data Supplement Figure II](#)). A 50 nmol/kg dose was chosen for further studies, because the hypotensive response had recovered by 24 hours in all mice. It is important to note that the blood pressure effects of the  $\alpha$ Analogue (50 nmol/kg, SC) were not significantly different from vehicle-treated mice (Figure 2A, [online-only Data Supplement Figure III](#)). All mice demonstrated normal diurnal variations in cardiovascular hemodynamics at baseline, followed by a hypertensive phenotype post-AngII infusion (Figure 2, [online-only Data Supplement Figure III](#)). Daily systemic treatment with the  $\alpha$ Analogue throughout the 14 days markedly blunted AngII-induced hypertension (Figure 2A, [online-only Data Supplement Figure III](#)). No significant change in heart rate or activity was observed among treatment groups ([online-only Data Supplement Figure III](#)).

In the AngII-infused mice, treatment with the  $\alpha$ Analogue leads to a reproducible reduction in blood pressure, with a similar reduction observed at day 1 to day 14 of treatment ([online-only Data Supplement Figure IV](#)), although there was a reduced hypotensive response to the  $\alpha$ Analogue on the last day. However, the protective activity was clearly maintained, with marked reduction in vascular remodeling and oxidative stress

**Figure 2 Continued.** Mice experience a 12/12 hour light/dark cycle, with the dark cycle shown in the gray striped area. Arrow represents the start of daily treatment. **B**, Protein expression of total eNOS in aorta (n=4–5). **C**, Representative images of Masson trichrome-stained aortic sections. **D**, Quantification of smooth muscle wall width (n=4–5; scale bars, 100  $\mu$ m). Protein expression of NADPH oxidase-2 (NOX-2) (**E**), heme oxygenase-1 (HO-1) (**F**), nitrotyrosine in aorta (n=4–6) (**G**). **H**, Protein expression of nitrotyrosine in mesenteric vessels (n=6–7). Results shown as mean $\pm$ SEM. \**P*<0.05, \*\**P*<0.01, \*\*\**P*<0.001 versus vehicle-treated saline-infused; #*P*<0.05, ###*P*<0.01, ####*P*<0.001 for  $\alpha$ Analogue-treated AngII-infused versus vehicle-treated AngII-infused (**A**, repeated-measures 2-way ANOVA + Bonferroni post hoc test; **B** through **H**, 2-way ANOVA + Bonferroni post hoc test).  $\alpha$ -CGRP indicates  $\alpha$ -calcitonin gene-related peptide; and eNOS, endothelial nitric oxide synthase.

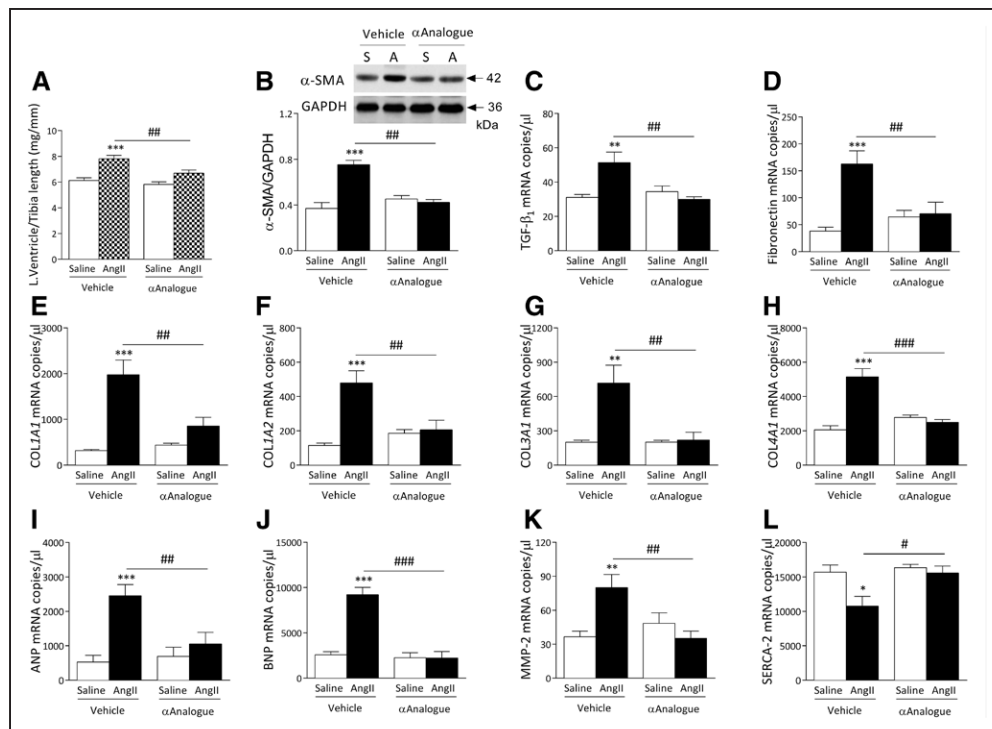


**Figure 3. α-CGRP analogue (αAnalogue) protects against angiotensin II (AngII)-induced cardiac hypertrophy and fibrosis.**

Mice were treated as in Figure 2 (AngII, A; Saline, S). **A**, Left ventricle weight normalized to tibia length ratio (mg/mm). **B**, Protein expression of α-smooth muscle actin (α-SMA) in heart (n=5). mRNA expression measured by real-time quantitative polymerase chain reaction for transforming growth factor-β<sub>1</sub> (TGF-β<sub>1</sub>) (**C**), fibronectin (**D**), collagen type 1 α<sub>1</sub> (COL1A1) (**E**), collagen type 1 α<sub>2</sub> (COL1A2) (**F**), collagen type 3 α<sub>1</sub> (COL3A1) (**G**), collagen type 4 α<sub>1</sub> (COL4A1) (**H**), atrial natriuretic peptide (ANP) (**I**), brain natriuretic peptide (BNP) (**J**), matrix metalloproteinase-2 (MMP-2) (**K**), and sarcoplasmic reticulum Ca<sup>2+</sup> ATPase-2 (SERCA-2) (**L**) in heart (n=5–11). Results expressed as copy numbers per microliter normalized to hypoxanthine-guanine phosphoribosyltransferase, β<sub>2</sub>M and β-actin, and showed as mean±SEM. \*P<0.05, \*\*P<0.01, \*\*\*P<0.001 versus vehicle-treated saline-infused; #P<0.05, ##P<0.01, ###P<0.001 versus vehicle-treated AngII-infused (2-way ANOVA + Bonferroni post hoc test). α-CGRP indicates α-calcitonin gene-related peptide.

(Figure 2). AngII infusion increased water consumption from day 3, consistent with previous findings,<sup>21</sup> and this was reduced by the αAnalogue treatment throughout the time course (online-only Data Supplement Figure VA and VB). Typically, AngII reduced body weight, which was absent in αAnalogue-treated mice (online-only Data Supplement Figure VC). Food intake was not affected in any treatment groups (online-only Data Supplement Figure VD).

### Systemic Treatment With the αAnalogue Does Not Affect Normal Behavioral Responses or Glucose Homeostasis

One of the limiting factors in the potential use of CGRP agonists therapeutically is that they may cause indications relevant to migraine, flushing, or metabolic changes.<sup>1</sup> We therefore examined its effects on activity and core body temperature by radiotelemetry, behavioral responses using a light aversion assay, and signs of flushing by assessing peripheral blood flow.

Treatment with the αAnalogue (50 nmol/kg, SC) had no effect on activity (online-only Data Supplement Figure IIID) or light avoidance in comparison with baseline (online-only Data Supplement Figure VI), unlike glyceryl trinitrate, an established inducer of migraine symptoms. Neither acute nor chronic systemic treatment of the αAnalogue had a significant effect on skin blood flow (online-only Data Supplement Figure VII). We found no significant change in core body temperature (online-only Data Supplement Figure VIII) or in glucose homeostasis (online-only Data Supplement Figure IX) with the αAnalogue treatment in comparison with vehicle.

### αAnalogue Protects Against AngII-Induced Vascular Changes in the Aorta and Mesentery

AngII infusion caused endothelial dysfunction, revealed by a significant decrease in endothelial nitric oxide synthase expression and vascular hypertrophy,

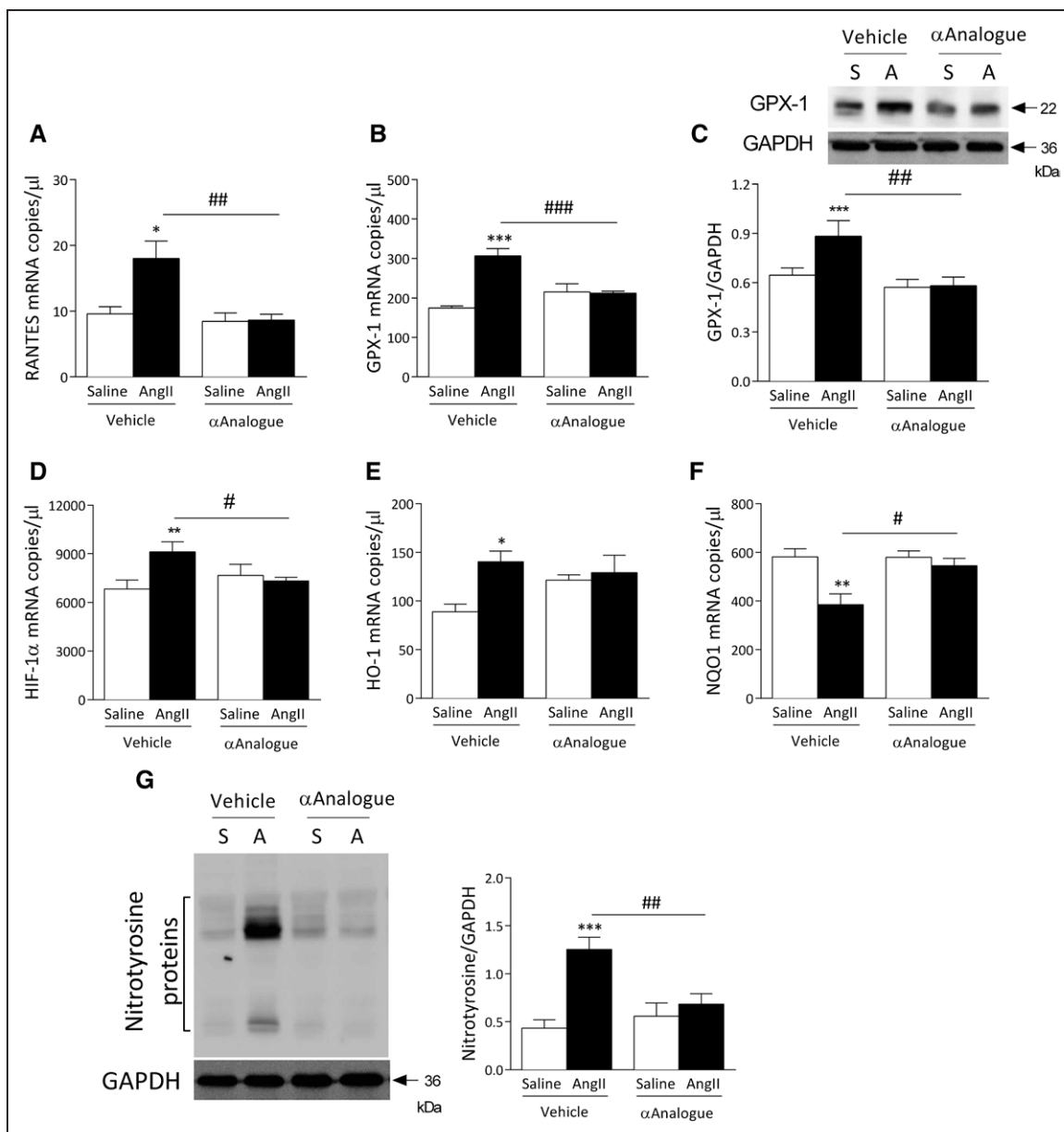


**Figure 4. Daily systemic treatment with α-CGRP analogue (αAnalogue) protects against angiotensin II (AngII)-induced cardiac inflammation and oxidative stress.**

Mice were treated as in Figure 2 (AngII, A; Saline, S). mRNA expression measured by real-time quantitative polymerase chain reaction (n=5–11) for RANTES (A) and glutathione peroxidase-1 (GPX-1) (n=6–11) (B). C, Protein expression of GPX-1 in heart (n=5). mRNA expression for hypoxia-inducible factor-1 (HIF-1α) (D), heme oxygenase-1 (HO-1) (E), and NADPH dehydrogenase quinone-1 (NQO1) (n=5–11) (F). Results expressed as copy numbers per microliter normalized to hypoxanthine-guanine phosphoribosyltransferase, B<sub>2</sub>M and β-actin, and showed as mean±SEM. G, Protein expression of nitrotyrosine (n=5) in heart (n=6–7). \*P<0.05, \*\*P<0.01, \*\*\*P<0.001 versus vehicle-treated saline-infused; #P<0.05, ###P<0.01, ####P<0.001 versus vehicle-treated AngII-infused (2-way ANOVA + Bonferroni post hoc test). α-CGRP indicates α-calcitonin gene-related peptide.

with increased aortic wall thickness. These were not observed in mice treated with the αAnalogue (Figure 2B through 2D). AngII upregulated NADPH oxidase-2 (NOX-2) expression, accompanied by increased vascular aortic oxidative stress, as reflected by an increase in the stress-response protein heme oxygenase-1 (HO-1) and nitration of protein tyrosine residues, an indication of peroxynitrite formation in

vehicle-treated AngII-infused mice. These responses were attenuated by the αAnalogue (Figure 2E through 2G). Although we observed no changes in endothelial nitric oxide synthase expression following AngII infusion in mesenteric vessels (online-only Data Supplement Figure X), there was a marked increase in nitrosative stress, which was blocked by the αAnalogue (Figure 2H).



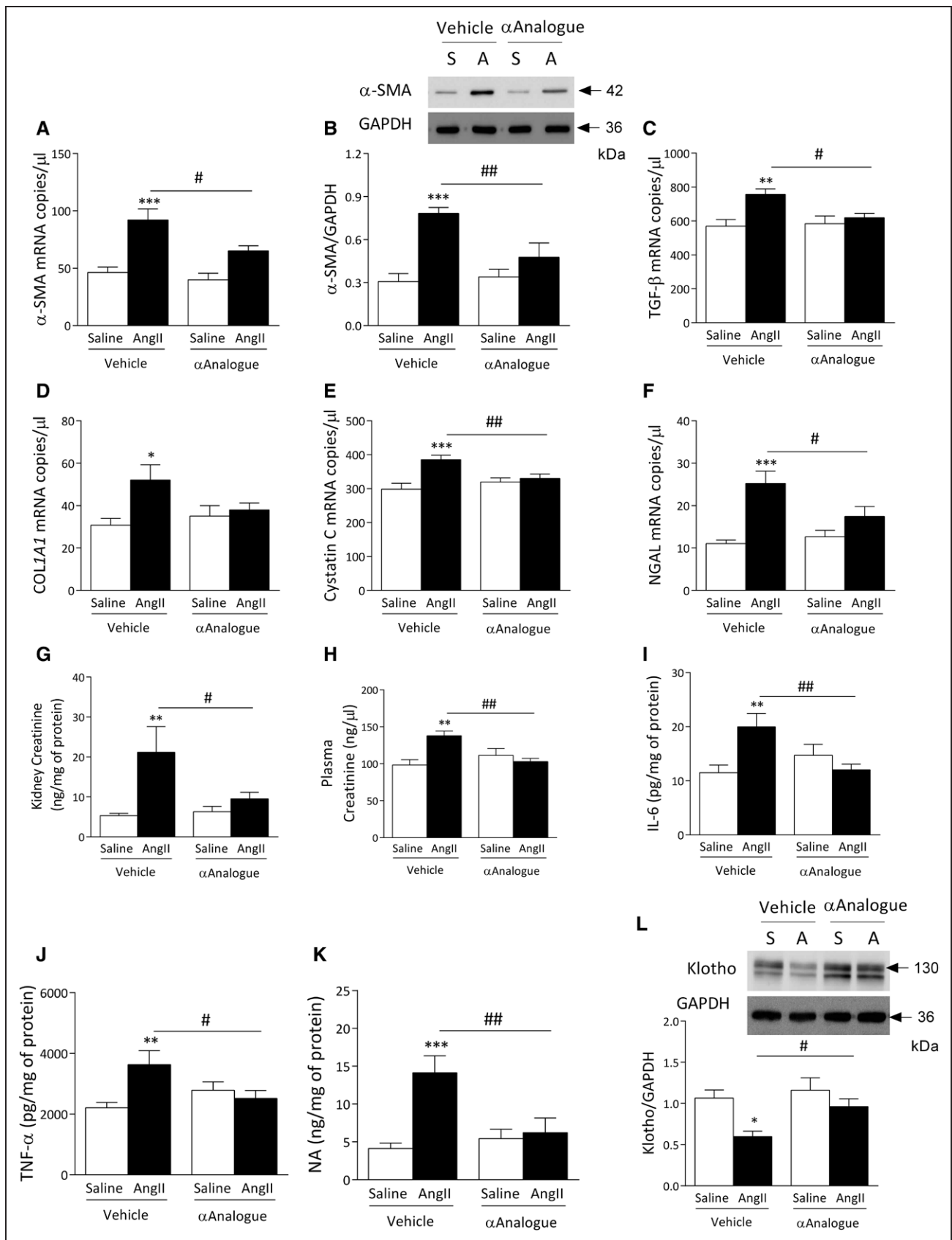


**Figure 5. Daily systemic treatment with  $\alpha$ -CGRP analogue ( $\alpha$ Analogue) protects against angiotensin II (AngII)-induced renal fibrosis, dysfunction, and inflammation.** Mice were treated as in Figure 2 (AngII, A; Saline, S). mRNA (A) and protein expression of  $\alpha$ -SMA (B) in kidney. mRNA (Continued)

## $\alpha$ Analogue Treatment Protects Against AngII-Induced Cardiac Remodeling, Fibrosis, and Oxidative Stress

AngII-induced cardiac hypertrophy was reduced by the  $\alpha$ Analogue (Figure 3A, [online-only Data Supplement Table II](#)). Hearts of vehicle-treated but not  $\alpha$ Analogue-treated AngII-infused mice showed increased protein expression of  $\alpha$ -smooth muscle actin and mRNA expression of several cardiac stress markers, including transforming growth factor- $\beta_1$ , a major driver of cardiac fibrosis, extracellular matrix remodeling markers such as connective tissue growth factor, fibronectin, collagen type 1, 3, and 4, and natriuretic peptides such as atrial natriuretic peptide and brain natriuretic peptide (Figure 3B through 3J, [online-only Data Supplement Table III](#)). Transforming growth factor- $\beta_1$  induces matrix metalloproteinase-2 in fibroblasts contributing to cardiac remodeling.<sup>22</sup> Daily treatment with the  $\alpha$ Analogue protected against AngII-induced changes in matrix metalloproteinase-2 and the corresponding tissue inhibitor of metalloproteinase-2 mRNA expression in the hearts (Figure 3K, [online-only Data Supplement Table III](#)). The cardiac muscle-specific sarcoplasmic reticulum Ca<sup>2+</sup> ATPase-2 is important in Ca<sup>2+</sup> handling, and its expression decreases under pathological conditions, leading to contractile dysfunction.<sup>23</sup> The  $\alpha$ Analogue protected against AngII-induced decrease in sarcoplasmic reticulum Ca<sup>2+</sup> ATPase-2 mRNA expression (Figure 3L).

The  $\alpha$ Analogue protected against AngII-induced inflammation, as shown by reduced mRNA expression of the nuclear factor kappa B cells and the chemokine RANTES (Figure 4A, [online-only Data Supplement Table III](#)). Treatment with the  $\alpha$ Analogue caused no change in the apoptosis regulator B-cell lymphoma-2 (Bcl-2) but resulted in a significant reduction in apoptotic markers such as p53 in AngII-infused hearts ([online-only Data Supplement Table III](#)). We next determined the effects of the  $\alpha$ Analogue on oxidative stress. AngII-induced increase in the antioxidant enzyme glutathione peroxidase-1 expression was absent in  $\alpha$ Analogue-treated groups (Figure 4B and 4C). An increase in hypoxia-inducible factor 1 $\alpha$  was attenuated by  $\alpha$ Analogue treatment (Figure 4D). AngII-induced changes in the mRNA expression of HO-1 and the phase II detoxifying enzymes NADPH dehydroge-

nase quinone-1 were absent by daily treatment with the  $\alpha$ Analogue (Figure 4E and 4F). Cardiac nitrosative stress was absent by the  $\alpha$ Analogue treatment in AngII-infused mice (Figure 4G). Collectively, these results show a marked protective effect on the proinflammatory and oxidative pathways associated with AngII-induced cardiovascular disease.

## $\alpha$ Analogue Protects Against AngII-Induced Renal Fibrosis and Injury

AngII infusion caused renal fibrosis, indicated by upregulation of  $\alpha$ -smooth muscle actin expression, increased transforming growth factor- $\beta_1$  and collagen mRNA expression, which were absent in mice cotreated with the  $\alpha$ Analogue (Figure 5A through 5D). The kidneys of AngII-infused mice exhibited renal damage, with increased mRNA expression of cystatin C and neutrophil gelatinase-associated lipocalin, plasma and renal creatinine levels, and mesangial matrix expansion in the glomeruli, which were all absent in mice treated with the  $\alpha$ Analogue (Figure 5E through 5H, [online-only Data Supplement Figure XI](#)). AngII infusion resulted in renal inflammation, highlighted by increased interleukin-6 and tumor necrosis factor- $\alpha$  concentrations, which were abolished by the  $\alpha$ Analogue (Figure 5I and 5J). There was a significant increase in localized sympathetic nerve activity, shown by increased noradrenaline content in AngII-infused kidney but not plasma, which was blocked by  $\alpha$ Analogue treatment (Figure 5K, [online-only Data Supplemental Figure XII](#)). The decreased noradrenaline levels in the kidney provides evidence that CGRP was able to attenuate the sympathetic activity. Downregulation of renal klotho expression can aggravate AngII-induced renal damage.<sup>24</sup> Here, the  $\alpha$ Analogue protects against this downregulation (Figure 5L).

## $\alpha$ Analogue Protects Against AngII-Induced Upregulation of CGRP Receptor RAMP1

RAMP1 determines the CGRP receptor phenotype when associated with CLR, and CGRP receptors are upregulated in cardiovascular disease models.<sup>1</sup> We observed a significant increase in CGRP receptor RAMP1 protein expression in the aorta, mesentery, and heart of vehicle-treated AngII-infused mice but not the  $\alpha$ Analogue

**Figure 5 Continued.** expression of TGF- $\beta_1$  (C), collagen type 1a1 (COL1A1) (D), cystatin C (E), and neutrophil gelatinase-associated lipocalin (NGAL) (F) in kidney. Creatinine levels in kidney (G) and plasma (H) (n=6–8). IL-6 (I), TNF- $\alpha$  (J), and noradrenaline (NA) (K) levels in kidney (n=6–9). L, Protein expression of klotho in kidney. mRNA expression measured by real-time quantitative polymerase chain reaction (n=6–8), expressed as copy numbers per microliter normalized to hypoxanthine-guanine phosphoribosyltransferase, B<sub>2</sub>M, and  $\beta$ -actin. Results shown as mean $\pm$ SEM. \* $P$ <0.05, \*\* $P$ <0.01, \*\*\* $P$ <0.001 versus vehicle-treated saline-infused; # $P$ <0.05, ## $P$ <0.01 versus vehicle-treated AngII-infused (2-way ANOVA + Bonferroni post hoc test).  $\alpha$ -CGRP indicates  $\alpha$ -calcitonin gene-related peptide; IL-6, interleukin 6;  $\alpha$ -SMA,  $\alpha$ -smooth muscle actin; TGF- $\beta_1$ ; transforming growth factor- $\beta_1$ ; and TNF- $\alpha$ , tumor necrosis factor- $\alpha$ .

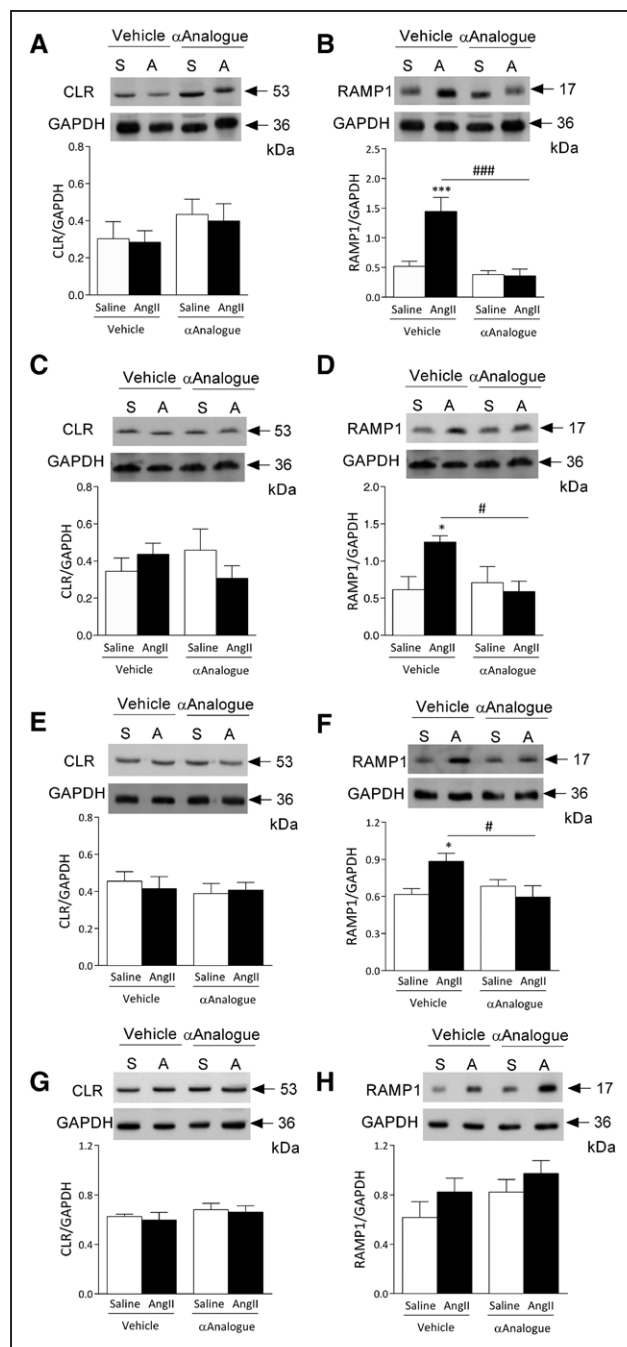


**Figure 6. Effects of daily systemic treatment with  $\alpha$ -CGRP analogue ( $\alpha$ Analogue) on CGRP receptor expression in angiotensin II (AngII)-induced hypertension.**

Mice were treated as in Figure 2 (AngII, A; saline, S, V, vehicle;  $\alpha$ -CGRP analogue; C). Protein expression of calcitonin receptor-like receptor (CLR) (A) and receptor-associated membrane protein-1 (RAMP1) (B) in aorta (n=6). Protein expression of CLR (C) and RAMP1 (D) in mesenteric vessels (n=6). Protein expression of CLR (E) and RAMP1 (F) in heart (n=6–7). Protein expression of CLR (G) and RAMP1 (H) in kidney (n=5–6). Results showed as mean $\pm$ SEM. \* $P$ <0.05, \*\*\* $P$ <0.001 versus vehicle-treated saline-infused; # $P$ <0.05, ### $P$ <0.001 versus vehicle-treated AngII-infused (2-way ANOVA + Bonferroni post hoc test).  $\alpha$ -CGRP indicates  $\alpha$ -calcitonin gene-related peptide.

(Figure 6). There was no significant change in CLR expression observed in different tissues, regardless of treatment (Figure 6). We found no change in endothelin-1 expression in heart or aorta treated with vehicle or the  $\alpha$ Analogue (online-only Data Supplement Figure XIII).

### **$\alpha$ Analogue Limits AngII-Induced Hypertension and Associated Cardiac Remodeling**

To determine whether the  $\alpha$ Analogue influences established hypertension, we assessed its effects by starting treatment at day 7 of AngII infusion. Treatment with the  $\alpha$ Analogue attenuated AngII-induced hypertension (Figure 7A, online-only Data Supplement Figure XIV). We observed a significant decrease in Akt and osteopontin, remodeling, and fibrotic markers (transforming growth factor- $\beta_1$ , connective tissue growth factor,  $\alpha$ -smooth muscle actin, collagen type 1 and 3), NOX-2, and markers of oxidative stress (HO-1, NADPH dehydrogenase quinone-1) in aorta (online-only Data Supplement Table IV). Accordingly, a substantial decrease in cardiac hypertrophy was found, with a significant reduction in left ventricular weight:tibia length ratio (Figure 7B, online-only Data Supplement Table V) and in cardiac fibrosis, remodeling, and inflammation, shown by a significant reduction in collagen type 3, atrial natriuretic peptide, and NOX-2 mRNA expression (online-only Data Supplement Table VI). It is notable that the  $\alpha$ Analogue reduced AngII-mediated increase in cardiomyocyte size and collagen deposition, revealed by wheat germ agglutinin and Picrosirius Red staining, respectively (Figure 7C and 7D). Cardiac nitrosative stress was reversed by the  $\alpha$ Analogue in hypertensive mice (Figure 7E).

### **$\alpha$ Analogue Protects Against AAC-Induced Cardiac Hypertrophy and Heart Failure**

To investigate the cardioprotective effect of CGRP in heart failure, mice were subjected to sham or AAC-induced cardiac hypertrophy and heart failure for 5 weeks. Quantification of in vivo cardiac function revealed that ejection fraction was better preserved in  $\alpha$ Analogue-treated AAC mice, with a reduction in septum wall thickness as shown by echocardiography (Figure 8A and 8B, online-only Data Supplement Figure XV, and online-only Data Supplement Table VII). Chronic treatment with the  $\alpha$ Analogue for 5 weeks was well tolerated, with no significant change in body weight, food and water intake, light avoidance, or blood pressure (online-only Data Supplement Figures XVI and XVII).  $\alpha$ Analogue-treated mice consistently developed less cardiac hypertrophy and fibrosis after AAC than vehicle-treated groups (Figure 8C, 8E through 8H, online-

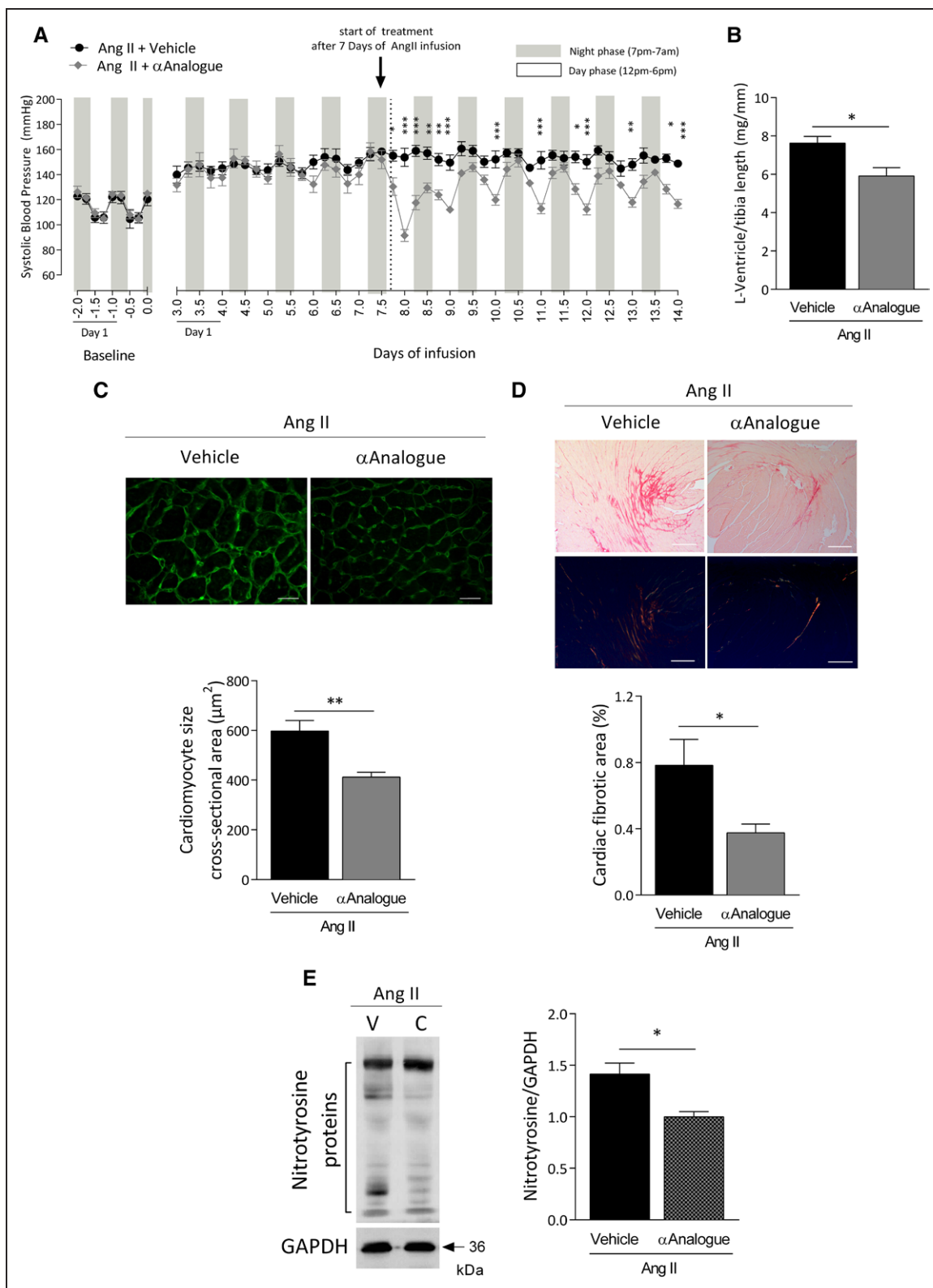


**Figure 7. α-CGRP analogue (αAnalogue) limits angiotensin II (AngII)-induced hypertension.**

Mice were infused with AngII (1.1 mg·kg<sup>-1</sup>·d<sup>-1</sup> for 14 days) and treated daily with vehicle or αAnalogue (50 nmol/kg, SC) at day 7 to 14 of infusion (n=4). **A**, Systolic blood pressure was measured by radiotelemetry. Results expressed as 6-hour average. Mice experience a 12/12 hour light/dark cycle, with the dark cycle shown in the gray striped area. Arrow represents the start of daily treatment. **B**, Left ventricle weight normalized to tibia length ratio (mg/mm). Representative heart sections (**Top**) and analysis (**Bottom**) showing cardiac hypertrophy by cardiomyocyte borders outlined using wheat germ agglutinin (scale (Continued)

only Data Supplement Table VIII, and online-only Data Supplement Figure XVIII). Insufficient angiogenesis is known as a driver of heart failure,<sup>20</sup> and left ventricular heart sections subjected to AAC showed reduced capillary density that was reversed by  $\alpha$ Analogue treatment (Figure 8I and 8J). Quantitative immunoblotting showed that phosphorylated p38 mitogen-activated protein kinase levels were significantly increased in  $\alpha$ Analogue-treated AAC hearts (online-only Data Supplement Figure XIX). Mice subjected to AAC showed an increase in cardiac inflammation, oxidative, nitrosative stress, and apoptosis in vehicle-treated but not  $\alpha$ Analogue-treated groups (Figure 8K through 8N, online-only Data Supplement Figure XVIII).

## DISCUSSION

CGRP is one of the most potent microvascular dilators known, and its protective properties are well established in vitro. However, it has been difficult to harness this information in drug discovery projects involving the cardiovascular system to date, primarily because of the instability of the peptide. This study presents novel mechanistic evidence that chronic systemic treatment with an injected stabilized  $\alpha$ -CGRP agonist is effective in the onset and ongoing AngII-induced hypertension and AAC-induced cardiac hypertrophy and heart failure in vivo. The  $\alpha$ Analogue, which possesses a considerably longer half-life than the native CGRP peptide (>7 hours in comparison with <30 minutes) is well tolerated. Specifically, the agonist did not lower systemic blood pressure in naive mouse, but exerted beneficial protective effects at the vascular, renal, and cardiac levels by alleviating fibrosis, remodeling, inflammation, oxidative stress, apoptosis, and preserving overall function in 2 distinct cardiovascular disease models. Our results are consistent with the concept that the CGRP receptor can be an influential regulatory component in cardiovascular disease and that CGRP agonists have potential therapeutic benefits.

The  $\alpha$ Analogue acted as a selective CGRP agonist via the CGRP receptor to mediate vasodilatation. Because the  $\alpha$ Analogue is not orally active, a systemic injectable dose that elicited an initial decrease in blood pressure with full recovery by 24 hours was chosen. This allowed baseline blood pressure to be maintained over the 2- to 5-week protocols in the control/sham mice. Although systemic CGRP infusion previously led to flushing in humans,<sup>25</sup> we found no undesirable side effects at the selected dose.

Although  $\alpha$ -CGRP-specific KO mice have normal basal cardiovascular hemodynamics, they exhibit an

enhanced hypertensive phenotype in AngII-induced hypertension.<sup>7</sup> Indeed, acute injection of the native CGRP peptide was beneficial in hypertensive rats<sup>26</sup> but effects were short lasting (<10 minutes) because of its short half-life.<sup>27</sup> In contrast, CGRP infusion for 6 days had beneficial effects in hypertensive rats.<sup>3</sup> To build on this and elucidate the mechanisms, we show that the  $\alpha$ Analogue protects against AngII-induced increase in blood pressure for 2 weeks. We tested for potential desensitization by the daily administration of the  $\alpha$ Analogue in naive mice and found a reproducible hypotensive effect, with no signs of downregulation of the CGRP pathway in the vasculature. However, there was a reduced effect on hypertension at the 14-day time point, leading us to investigate for other markers of disease. AngII-induced hypertension is associated with weight loss and increased water intake, in addition to hypertension. These were reversed by the  $\alpha$ Analogue throughout. Of interest, blocking the CGRP pathway with antagonists/antibodies against CGRP and its receptor (currently in clinical trials for prevention of migraine<sup>2</sup>) may interfere with this protective pathway and thereby increase cardiovascular risk. However, in the limited clinical studies performed to date, no evidence has been found. It is possible that endogenous levels of CGRP do not reach sufficient levels in humans to mediate protective effects. To our knowledge, this is the first in-depth study in cardiovascular models with a long-acting CGRP agonist where there has been a sustained benefit in protective cardiovascular effects.

AngII-induced vascular dysfunction and remodeling were reversed by the  $\alpha$ Analogue, in keeping with reports that CGRP inhibits smooth muscle cell proliferation by increasing cAMP or inhibiting the ERK1/2 signaling cascade.<sup>28</sup> CGRP has direct anti-inflammatory and antioxidant effects in endothelial progenitor cells.<sup>29</sup> Accordingly, the  $\alpha$ Analogue reduced the AngII-induced increase in the endogenous source of ROS<sup>30</sup> NOX-2, oxidative stress-associated proteins, and nitrosative stress in hypertensive aorta, which was consistent with less nitrosative stress in the hypertensive mesenteric vessels. There was no change in vascular endothelial dysfunction in resistance vessels, complementing our previous findings.<sup>7</sup>

CGRP receptors are upregulated in cardiovascular disease,<sup>1</sup> with evidence of a pressure-dependent regulation.<sup>12</sup> This may amplify responses to CGRP, especially in hypertension.<sup>7,17</sup> Accordingly, RAMP1 expression was increased in hypertensive resistance and conduit vessels. The  $\alpha$ Analogue reduced this effect such that RAMP1 returned to normal expression levels as the cardiovas-

**Figure 7 Continued.** bars, 20  $\mu$ m) (C) and cardiac fibrosis by Picrosirius Red staining (scale bars, 200  $\mu$ m) (D). E, Protein expression of nitrotyrosine in heart. Results showed as mean $\pm$ SEM. \* $P$ <0.05, \*\* $P$ <0.01, \*\*\* $P$ <0.001 versus vehicle-treated (A, repeated-measures 2-way ANOVA + Bonferroni post hoc test; B through E, 2-way ANOVA + Bonferroni post hoc test).  $\alpha$ -CGRP indicates  $\alpha$ -calcitonin gene-related peptide.

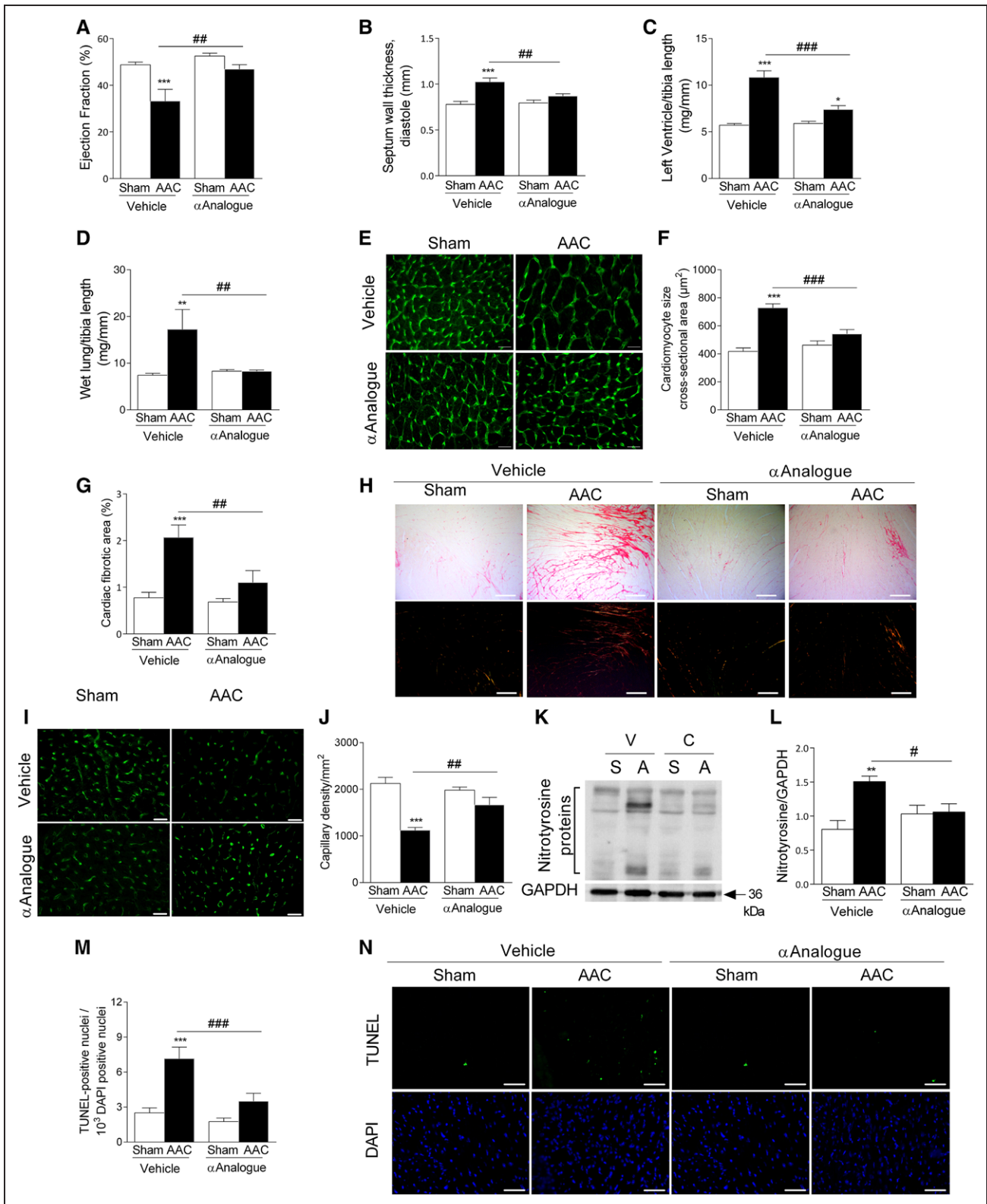


**Figure 8.** α-CGRP analogue (αAnalogue) preserves heart function post-AAC-induced cardiac hypertrophy and heart failure.

Mice were treated daily with vehicle and αAnalogue (50 nmol/kg, SC) postsurgery for 5 weeks (n=6–8). Ejection fraction (%) (A), septum wall thickness at diastole (mm) (B), left ventricle mass normalized to tibia length (mg/mm) (C), and wet lung mass (mg) normalized to tibia length (D). Representative images (E) and quantification of cardiomyocyte cross-sectional area (F) in heart using wheat germ agglutinin staining (scale bars, 20 μm). Quantification (G) and representative images (Continued)

cular system benefited, irrespective of the continuing presence of AngII. This finding suggests that CGRP may act in an autoregulatory manner depending on CGRP peptide/agonist availability.

CGRP has positive chronotropic effects,<sup>31</sup> and  $\alpha$ -CGRP KO mice exhibit exacerbated cardiac dysfunction in pressure overload-induced hypertrophy<sup>32</sup> and deoxycorticosterone acetate salt-induced hypertension.<sup>33,34</sup> Here, the  $\alpha$ Analogue had no effect on in vivo heart function, as observed by radiotelemetry or echocardiography in sham mice, but protected against cardiac hypertrophy in AngII-induced hypertension. The  $\alpha$ Analogue downregulated markers of fibrosis, remodeling, and hypertrophy, and protected against the reduction in the cardiac contractile dysfunction marker sarcoplasmic reticulum  $\text{Ca}^{2+}$  ATPase-2 in hypertensive hearts, as well. Our results correlate with previous in vitro findings<sup>35–37</sup> and provide in vivo evidence that the  $\alpha$ Analogue has influential antiremodeling effects in the stressed heart, while not directly modulating normal heart activity in control mice.

The  $\alpha$ Analogue reduces cardiac inflammation, as shown by reducing AngII-induced increase in the chemokine RANTES. AngII increases hypoxia-inducible factor 1 $\alpha$  mRNA expression, indicating the involvement of fibrotic and oxidative stress pathways, and this was reduced by the  $\alpha$ Analogue. CGRP regulates oxidative stress by the PI3K/Akt and mitogen-activated protein kinase signaling pathways,<sup>38</sup> and deletion of the CGRP gene exacerbates cardiac oxidative stress in ischemia-reperfusion injury.<sup>39</sup> The  $\alpha$ Analogue protects against AngII-induced changes in the endogenous antioxidant defense responses and nitrosative stress. A link between CGRP and HO-1 is known.<sup>40</sup> Activation of HO-1 and NADPH dehydrogenase quinone-1 can counteract hypertension, potentially through generating the vasodilator carbon monoxide<sup>41,42</sup> and improved endothelial nitric oxide synthase coupling.<sup>43</sup> Our data build on earlier findings in cardiomyocytes, smooth muscle cells, and  $\alpha$ -CGRP KO mice, implying that the  $\alpha$ Analogue acts directly via its receptors on the heart and reduces stress-activated kinases induced by oxidative stress,<sup>44</sup> adverse tissue remodeling to preserve cardiac function.

Hypertension is associated with renal fibrosis and inflammation that were reduced by the  $\alpha$ Analogue, complementing knowledge that CGRP promotes renal protection in hypertension independently of its vasodilator action.<sup>33,45</sup> The  $\alpha$ Analogue preserved renal function by reducing mesangial matrix expansion, plasma and kid-

ney creatinine levels, and expression of cystatin C and neutrophil gelatinase-associated lipocalin, the early biomarker of acute kidney injury. AngII increases renal adrenergic receptors<sup>46</sup> and we found a significant increase in renal noradrenaline content, which was reversed by the  $\alpha$ Analogue. Hence, the  $\alpha$ Analogue may preserve renal function by reducing sympathetic activity. Klotho has nephroprotective effects, and AngII-induced downregulation of klotho aggravates renal damage in hypertension.<sup>24</sup> This downregulation was rescued by the  $\alpha$ Analogue, and our results further confirm the link between klotho and CGRP.<sup>29</sup> The upregulation of klotho associated with the use of  $\alpha$ Analogue may translate into enhanced renal protection in hypertension. The primary functional source of CGRP was reported to be independent of the kidney, because chemical denervation of renal sensory afferents removed tissue CGRP but without any beneficial effect in hypertensive mice.<sup>46</sup> However, our study highlights that mimicking sensory nerve efferent function by using an  $\alpha$ -CGRP analogue protects against end-organ damage in hypertension, especially renal fibrosis, a strong predictor of clinical progression of kidney disease.

Strikingly, the  $\alpha$ Analogue limits AngII-induced cardiovascular pathologies, ameliorating cardiac remodeling and fibrosis. This highlights the therapeutic potential of the  $\alpha$ Analogue when given in established hypertension. Although the  $\alpha$ Analogue was unable to reduce vascular endothelial dysfunction, it reduced markers of damage such as osteopontin, the downstream regulator of Akt activity,<sup>47</sup> remodeling, fibrosis, and oxidative stress.<sup>7</sup> The  $\alpha$ Analogue reduced both vascular and cardiac NOX-2 expression. It is possible that many of the beneficial effects of the  $\alpha$ Analogue in both early or late onset of hypertension are primarily related to a decrease in blood pressure and the resultant reduction in pressure-induced damage in the vasculature, kidney, and heart. Although it is presently difficult to separate the direct effects of the  $\alpha$ Analogue on pressure and cardiac function, it is evident that CGRP has antihypertensive effects and induces protection in a comprehensive manner.

To investigate the cardioprotective effects of the  $\alpha$ Analogue, we subjected mice to AAC and examined cardiac function. The adverse structural remodeling and hypertrophy at 5 weeks post-AAC, with significant reduction in ejection fraction and increasing heart mass with fibrosis, were markedly attenuated in  $\alpha$ Analogue-treated mice, under conditions where blood pressure was similar to  $\alpha$ Analogue and

**Figure 8 Continued.** of fibrosis in heart (**H**) using picrosirius red staining (scale bars, 200  $\mu\text{m}$ ). Representative images (**I**) and quantification of capillary density in heart (**J**) using isolectin-B<sub>4</sub> staining (scale bars, 20  $\mu\text{m}$ ). **K** and **L**, Protein expression of nitrotyrosine in heart. Quantification (**M**) and representative images of apoptosis (**N**) using TUNEL staining (scale bars, 50  $\mu\text{m}$ ). Results showed as mean $\pm$ SEM. \* $P$ <0.05, \*\* $P$ <0.01, \*\*\* $P$ <0.001 versus vehicle-treated sham mice; # $P$ <0.05, ## $P$ <0.01, ### $P$ <0.001 versus vehicle-treated AAC mice (2-way ANOVA + Bonferroni post hoc test). AAC indicates abdominal aorta constriction;  $\alpha$ -CGRP,  $\alpha$ -calcitonin gene-related peptide; and TUNEL, terminal deoxynucleotidyl transferase dUTP nick-end labeling.

vehicle-treated sham mice. This is consistent with findings where  $\alpha$ -CGRP/calcitonin KO mice showed adverse cardiac dysfunction with increased mortality following transverse aortic constriction.<sup>32</sup> Although CGRP infusion for 24 hours previously improved cardiac performance in patients with chronic congestive heart failure,<sup>8,9</sup> this is the first demonstration that chronic treatment with a long-lasting CGRP agonist is beneficial and well tolerated. Myocyte apoptosis is well documented in heart failure and CGRP regulates cell survival signaling and antiapoptotic pathway via CLR/RAMP1 in cardiomyocytes.<sup>38,48</sup> Although the  $\alpha$ Analogue reduces nuclear factor kappa B cells and apoptotic marker p53 expression in our acute AngII model, here, the  $\alpha$ Analogue reduced apoptosis, as revealed in terminal deoxynucleotidyl transferase dUTP nick-end labeling staining with increased p38 mitogen-activated protein kinase phosphorylation in the hypertrophic heart. Similarly, the  $\alpha$ Analogue maintained its antioxidant effects. Development of cardiac hypertrophy is associated with increased cardiomyocyte size and reduced capillary density, which ultimately lead to hypoxia and cell death.<sup>20</sup> These changes were markedly reduced by the  $\alpha$ Analogue. This finding supports earlier studies where CGRP acted as a proangiogenic factor<sup>32,49</sup> and suggests that CGRP promotes normal cardiac microvessel development, perhaps via angiogenesis in hypertrophic hearts. Further gene expression studies on ventricle tissues demonstrate that markers of heart failure were abrogated by the  $\alpha$ Analogue.

To our knowledge, this is the first study demonstrating that a long-lasting and stable  $\alpha$ -CGRP agonist has the potential to act as a novel therapeutic agent, targeting key mechanisms to benefit cardiovascular dysfunction, with limited adverse pathological changes and side effects. The results support the concept provided by in vitro studies that CGRP protects against adverse remodeling, inflammation, oxidative stress, apoptosis, and end-organ damage in cardiovascular disease, in addition to its vasodilator activity. We thus propose that the CGRP pathway is a therapeutic target for the clinical treatment of cardiovascular disease and, more specifically, that injectable CGRP agonists may benefit heart failure.

## SOURCES OF FUNDING

This work was supported by British Heart Foundation (Grant#-PG/12/34/29557 and RE/13/2/30182).  $\alpha$ Analogue was supplied by Novo Nordisk. Dr Schnelle was supported by a Deutsche Forschungsgemeinschaft Joint PhD Studentship (IRTG1816). F.A. is an MRC PhD student. E.W. is an MRC NC3Rs PhD student.

## DISCLOSURES

None.

## AFFILIATIONS

From Cardiovascular Division, BHF Centre of Research Excellence and Centre of Integrative Biomedicine, King's College London, United Kingdom (A.A.A., F.A., S.-J.S., S.S., K.M.A., E.W., J.M., K.F.-D., G.M., R.C.S., S.D.B.); Institute of Pharmaceutical Sciences, King's College London, United Kingdom (P.T., M.N.); Cardiovascular Division, BHF Centre of Research Excellence, James Black Centre, King's College London, United Kingdom (M.S., D.A.R., A.M.S.); Department of Cardiology and Pneumology, Medical Center Goettingen, Germany (M.S.); Cardiovascular Division, BHF Centre of Research Excellence, Rayne Institute, St Thomas' Hospital, King's College London, United Kingdom (J.E.C.); Novo Nordisk A/S, Diabetic Complications Biology, Novo Nordisk Park, Maaloev, Denmark (A.S.); and Department of Clinical Experimental Research, Glostrup Research Institute, Rigshospitalet, Denmark (A.S.).

## FOOTNOTES

Received July 28, 2016; accepted April 17, 2017.

The online-only Data Supplement is available with this article at <http://circ.ahajournals.org/lookup/suppl/doi:10.1161/CIRCULATIONAHA.117.028388/-/DC1>.

*Circulation* is available at <http://circ.ahajournals.org>.

## REFERENCES

- Russell FA, King R, Smillie SJ, Kodji X, Brain SD. Calcitonin gene-related peptide: physiology and pathophysiology. *Physiol Rev*. 2014;94:1099–1142. doi: 10.1152/physrev.00034.2013.
- Diener HC, Charles A, Goadsby PJ, Holle D. New therapeutic approaches for the prevention and treatment of migraine. *Lancet Neurol*. 2015;14:1010–1022. doi: 10.1016/S1474-4422(15)00198-2.
- Fujioka S, Sasakawa O, Kishimoto H, Tsumura K, Morii H. The antihypertensive effect of calcitonin gene-related peptide in rats with norepinephrine- and angiotensin II-induced hypertension. *J Hypertens*. 1991;9:175–179.
- Supowit SC, Katki KA, Hein TW, Gupta P, Kuo L, Dickerson IM, Dipette DJ. Vascular reactivity to calcitonin gene-related peptide is enhanced in subtotal nephrectomy-salt induced hypertension. *Am J Physiol Heart Circ Physiol*. 2011;301:H683–H688. doi: 10.1152/ajpheart.00598.2009.
- Hobara N, Gesssei-Tsutsumi N, Goda M, Takayama F, Akiyama S, Kurosaki Y, Kawasaki H. Long-term inhibition of angiotensin prevents reduction of periarterial innervation of calcitonin gene-related peptide (CGRP)-containing nerves in spontaneously hypertensive rats. *Hypertens Res*. 2005;28:465–474. doi: 10.1291/hypres.28.465.
- Kawasaki H, Inaizumi K, Nakamura A, Hobara N, Kurosaki Y. Chronic angiotensin II inhibition increases levels of calcitonin gene-related peptide mRNA of the dorsal root ganglia in spontaneously hypertensive rats. *Hypertens Res*. 2003;26:257–263.
- Smillie SJ, King R, Kodji X, Outzen E, Pozsgai G, Fernandes E, Marshall N, de Winter P, Heads RJ, Dessapt-Baradez C, Gnudi L, Sams A, Shah AM, Siow RC, Brain SD. An ongoing role of  $\alpha$ -calcitonin gene-related peptide as part of a protective network against hypertension, vascular hypertrophy, and oxidative stress. *Hypertension*. 2014;63:1056–1062. doi: 10.1161/HYPERTENSIONAHA.113.02517.
- Gennari C, Nami R, Agnusdei D, Fischer JA. Improved cardiac performance with human calcitonin gene related peptide in patients with congestive heart failure. *Cardiovasc Res*. 1990;24:239–241.
- Shekhar YC, Anand IS, Sarma R, Ferrari R, Wahi PL, Poole-Wilson PA. Effects of prolonged infusion of human alpha calcitonin gene-related peptide on hemodynamics, renal blood flow and hormone levels in congestive heart failure. *Am J Cardiol*. 1991;67:732–736.
- Marshall NJ, Liang L, Bodkin J, Dessapt-Baradez C, Nandi M, Collet-Teixeira S, Smillie SJ, Lalgi K, Fernandes ES, Gnudi L, Brain SD. A role for TRPV1



- in influencing the onset of cardiovascular disease in obesity. *Hypertension*. 2013;61:246–252. doi: 10.1161/HYPERTENSIONAHA.112.201434.
11. Bodkin JV, Thakore P, Aubdool AA, Liang L, Fernandes ES, Nandi M, Spina D, Clark JE, Aaronson PI, Shattock MJ, Brain SD. Investigating the potential role of TRPA1 in locomotion and cardiovascular control during hypertension. *Pharmacol Res Perspect*. 2014;2:e00052. doi: 10.1002/prp2.52.
  12. Aubdool AA, Graepel R, Kodji X, Alawi KM, Bodkin JV, Srivastava S, Gentry C, Heads R, Grant AD, Fernandes ES, Bevan S, Brain SD. TRPA1 is essential for the vascular response to environmental cold exposure. *Nat Commun*. 2014;5:5732. doi: 10.1038/ncomms6732.
  13. Eberhardt M, Dux M, Namer B, Miljkovic J, Cordasic N, Will C, Kichko TI, de la Roche J, Fischer M, Suarez SA, Bikiel D, Dorsch K, Leffler A, Babes A, Lampert A, Lennerz JK, Jacobi J, Marti MA, Doctorovich F, Hogestatt ED, Zygmunt PM, Ivanovic-Burmazovic I, Messlinger K, Reeh P, Filipovic MR. H2S and NO cooperatively regulate vascular tone by activating a neuroendocrine HNO-TRPA1-CGRP signalling pathway. *Nat Commun*. 2014;5:4381. doi:10.1038/ncomms5381.
  14. Paolucci N, Saavedra WF, Miranda KM, Martignani C, Isoda T, Hare JM, Espey MG, Fukuto JM, Feelisch M, Wink DA, Kass DA. Nitroxyl anion exerts redox-sensitive positive cardiac inotropy *in vivo* by calcitonin gene-related peptide signaling. *Proc Natl Acad Sci USA*. 2001;98:10463–10468. doi: 10.1073/pnas.181191198.
  15. Katori T, Hoover DB, Ardell JL, Helm RH, Belardi DF, Tocchetti CG, Forfia PR, Kass DA, Paolucci N. Calcitonin gene-related peptide *in vivo* positive inotropy is attributable to regional sympatho-stimulation and is blunted in congestive heart failure. *Circ Res*. 2005;96:234–243. doi: 10.1161/01.RES.0000152969.42117.ca.
  16. Oh-hashii Y, Shindo T, Kurihara Y, Imai T, Wang Y, Morita H, Imai Y, Kayaba Y, Nishimatsu H, Suematsu Y, Hirata Y, Yazaki Y, Nagai R, Kuwaki T, Kurihara H. Elevated sympathetic nervous activity in mice deficient in alpha-CGRP. *Circ Res*. 2001;89:983–990.
  17. Sabharwal R, Zhang Z, Lu Y, Abboud FM, Russo AF, Chapple MW. Receptor activity-modifying protein 1 increases baroreflex sensitivity and attenuates Angiotensin-induced hypertension. *Hypertension*. 2010;55:627–635. doi: 10.1161/HYPERTENSIONAHA.109.148171.
  18. Nielsen AS, Kruse T, Kodra JT, Lau JF, Kofoed J, Raun K, Nilsson C, inventors; Novo Nordisk, assignee. Derivatives of cgrp. *WO Patent* 2,011,051,312. May 5, 2011.
  19. Nilsson C, Hansen TK, Rosenquist C, Hartmann B, Kodra JT, Lau JF, Clausen TR, Raun K, Sams A. Long acting analogue of the calcitonin gene-related peptide induces positive metabolic effects and secretion of the glucagon-like peptide-1. *Eur J Pharmacol*. 2016;773:24–31. doi: 10.1016/j.ejphar.2016.01.003.
  20. Zhang M, Brewer AC, Schröder K, Santos CX, Grieve DJ, Wang M, Anilkumar N, Yu B, Dong X, Walker SJ, Brandes RP, Shah AM. NADPH oxidase-4 mediates protection against chronic load-induced stress in mouse hearts by enhancing angiogenesis. *Proc Natl Acad Sci USA*. 2010;107:18121–18126. doi: 10.1073/pnas.1009700107.
  21. Cassis LA, Marshall DE, Fettingier MJ, Rosenbluth B, Lodder RA. Mechanisms contributing to angiotensin II regulation of body weight. *Am J Physiol*. 1998;274(5 pt 1):E867–E876.
  22. Overall CM, Wrana JL, Sodek J. Transcriptional and post-transcriptional regulation of 72-kDa gelatinase/type IV collagenase by transforming growth factor-beta 1 in human fibroblasts. Comparisons with collagenase and tissue inhibitor of matrix metalloproteinase gene expression. *J Biol Chem*. 1991;266:14064–14071.
  23. Domenighetti AA, Wang Q, Egger M, Richards SM, Pedrazzini T, Delbridge LM. Angiotensin II-mediated phenotypic cardiomyocyte remodeling leads to age-dependent cardiac dysfunction and failure. *Hypertension*. 2005;46:426–432. doi: 10.1161/01.HYP.0000173069.53699.d9.
  24. Mitani H, Ishizaka N, Aizawa T, Ohno M, Usui S, Suzuki T, Amaki T, Mori I, Nakamura Y, Sato M, Nangaku M, Hirata Y, Nagai R. *In vivo* klothe gene transfer ameliorates angiotensin II-induced renal damage. *Hypertension*. 2002;39:838–843.
  25. Gennari C, Fischer J. Cardiovascular action of calcitonin gene-related peptide in humans. *Calcif Tissue Int*. 1985;37:581–584.
  26. Li J, Wang DH. Development of angiotensin II-induced hypertension: role of CGRP and its receptor. *J Hypertens*. 2005;23:113–118.
  27. Kraenzlin ME, Ch'ng JL, Mulderry PK, Ghatei MA, Bloom SR. Infusion of a novel peptide, calcitonin gene-related peptide (CGRP) in man. Pharmacokinetics and effects on gastric acid secretion and on gastrointestinal hormones. *Regul Pept*. 1985;10:189–197.
  28. Li XW, Hu CP, Wu WH, Zhang WF, Zou XZ, Li YJ. Inhibitory effect of calcitonin gene-related peptide on hypoxia-induced rat pulmonary artery smooth muscle cells proliferation: role of ERK1/2 and p27. *Eur J Pharmacol*. 2012;679:117–126. doi: 10.1016/j.ejphar.2012.01.015.
  29. Zhou Z, Hu CP, Wang CJ, Li TT, Peng J, Li YJ. Calcitonin gene-related peptide inhibits angiotensin II-induced endothelial progenitor cells senescence through up-regulation of klothe expression. *Atherosclerosis*. 2010;213:92–101. doi: 10.1016/j.atherosclerosis.2010.08.050.
  30. Bendall JK, Cave AC, Heymes C, Gall N, Shah AM. Pivotal role of a gp91(phox)-containing NADPH oxidase in angiotensin II-induced cardiac hypertrophy in mice. *Circulation*. 2002;105:293–296.
  31. Franco-Cereceda A, Gennari C, Nami R, Agnusdei D, Pernow J, Lundberg JM, Fischer JA. Cardiovascular effects of calcitonin gene-related peptides I and II in man. *Circ Res*. 1987;60:393–397.
  32. Li J, Levick SP, DiPette DJ, Janicki JS, Supowit SC. Alpha-calcitonin gene-related peptide is protective against pressure overload-induced heart failure. *Regul Pept*. 2013;185:20–28. doi: 10.1016/j.regpep.2013.06.008.
  33. Supowit SC, Rao A, Bowers MC, Zhao H, Fink G, Steficek B, Patel P, Katki KA, Dipette DJ. Calcitonin gene-related peptide protects against hypertension-induced heart and kidney damage. *Hypertension*. 2005;45:109–114. doi: 10.1161/01.HYP.0000151130.34874.fa.
  34. Bowers MC, Katki KA, Rao A, Koehler M, Patel P, Spiekerman A, DiPette DJ and Supowit SC. Role of calcitonin gene-related peptide in hypertension-induced renal damage. *Hypertension*. 2005;46:51–57. doi:10.1161/01.HYP.0000168926.44648.ed.
  35. Matsui S, Yamane T, Kobayashi-Hattori K, Oishi Y. Calcitonin gene-related peptide regulates mitogen-activated protein kinase pathway to decrease transforming growth factor  $\beta$ 1-induced hepatic plasminogen activator inhibitor-1 mRNA expression in HepG2 cells. *Biosci Biotechnol Biochem*. 2014;78:787–790. doi: 10.1080/09168451.2014.910096.
  36. Piao FL, Cao C, Han JH, Kim SZ, Kim SH. Calcitonin gene-related peptide-induced suppression of atrial natriuretic peptide release through receptors for CGRP1 but not for calcitonin and amylin. *Eur J Pharmacol*. 2004;483:295–300.
  37. Vega AV, Ramos-Mondragón R, Calderón-Rivera A, Zarain-Herzberg A, Avila G. Calcitonin gene-related peptide restores disrupted excitation-contraction coupling in myotubes expressing central core disease mutations in RyR1. *J Physiol*. 2011;589(pt 19):4649–4669. doi: 10.1113/jphysiol.2011.210765.
  38. Umoh NA, Walker RK, Millis RM, Al-Rubaiee M, Gangula PR, Haddad GE. Calcitonin gene-related peptide regulates cardiomyocyte survival through regulation of oxidative stress by PI3K/Akt and MAPK signaling pathways. *Ann Clin Exp Hypertens*. 2014;2:1007.
  39. Huang R, Karve A, Shah I, Bowers MC, DiPette DJ, Supowit SC, Abela GS. Deletion of the mouse alpha-calcitonin gene-related peptide gene increases the vulnerability of the heart to ischemia-reperfusion injury. *Am J Physiol Heart Circ Physiol*. 2008;294:H1291–H1297. doi: 10.1152/ajp-heart.00749.2007.
  40. Peng J, Lu R, Ye F, Deng HW, Li YJ. The heme oxygenase-1 pathway is involved in calcitonin gene-related peptide-mediated delayed cardioprotection induced by monophosphoryl lipid A in rats. *Regul Pept*. 2002;103:1–7.
  41. Vera T, Kelsen S, Yanes LL, Reckelhoff JF, Stec DE. HO-1 induction lowers blood pressure and superoxide production in the renal medulla of angiotensin II hypertensive mice. *Am J Physiol Regul Integr Comp Physiol*. 2007;292:R1472–R1478. doi: 10.1152/ajpregu.00601.2006.
  42. Yang L, Quan S, Nasjletti A, Laniado-Schwartzman M, Abraham NG. Heme oxygenase-1 gene expression modulates angiotensin II-induced increase in blood pressure. *Hypertension*. 2004;43:1221–1226. doi: 10.1161/01.HYP.0000126287.62060.e6.
  43. Kim YH, Hwang JH, Kim KS, Noh JR, Gang GT, Oh WK, Jeong KH, Kwak TH, Choi HS, Lee IK, Lee CH. Enhanced activation of NAD(P)H: quinone oxidoreductase 1 attenuates spontaneous hypertension by improvement of endothelial nitric oxide synthase coupling via tumor suppressor kinase liver kinase B1/adenosine 5'-monophosphate-activated protein kinase-mediated guanosine 5'-triphosphate cyclohydrolase 1 preservation. *J Hypertens*. 2014;32:306–317. doi: 10.1097/HJH.000000000000018.
  44. Schaeffer C, Vandroux D, Thomassin L, Athias P, Rochette L, Connat JL. Calcitonin gene-related peptide partly protects cultured smooth muscle cells from apoptosis induced by an oxidative stress via activation of ERK1/2 MAPK. *Biochim Biophys Acta*. 2003;1643:65–73.
  45. Li J, Carnevale KA, Dipette DJ, Supowit SC. Renal protective effects of  $\alpha$ -calcitonin gene-related peptide in deoxycorticosterone-salt hypertension. *Am J Physiol Renal Physiol*. 2013;304:F1000–F1008. doi: 10.1152/ajprenal.00434.2012.

46. Xiao L, Kirabo A, Wu J, Saleh MA, Zhu L, Wang F, Takahashi T, Loperena R, Foss JD, Mernaugh RL, Chen W, Roberts J 2nd, Osborn JW, Itani HA, Harrison DG. Renal denervation prevents immune cell activation and renal inflammation in angiotensin II-induced hypertension. *Circ Res*. 2015;117:547–557. doi: 10.1161/CIRCRESAHA.115.306010.
47. de Castro Brás LE. Osteopontin: a major player on hypertension-induced vascular remodeling. *J Mol Cell Cardiol*. 2015;85:151–152. doi: 10.1016/j.yjmcc.2015.05.020.
48. Sueur S, Pesant M, Rochette L, Connat JL. Antiapoptotic effect of calcitonin gene-related peptide on oxidative stress-induced injury in H9c2 cardiomyocytes via the RAMP1/CRLR complex. *J Mol Cell Cardiol*. 2005;39:955–963. doi: 10.1016/j.yjmcc.2005.09.008.
49. Toda M, Suzuki T, Hosono K, Hayashi I, Hashiba S, Onuma Y, Amano H, Kurihara Y, Kurihara H, Okamoto H, Hoka S, Majima M. Neuronal system-dependent facilitation of tumor angiogenesis and tumor growth by calcitonin gene-related peptide. *Proc Natl Acad Sci USA*. 2008;105:13550–13555. doi: 10.1073/pnas.0800767105.

## A Novel $\alpha$ -Calcitonin Gene-Related Peptide Analogue Protects Against End-Organ Damage in Experimental Hypertension, Cardiac Hypertrophy, and Heart Failure

Aisah A. Aubdool, Pratish Thakore, Fulye Argunhan, Sarah-Jane Smillie, Moritz Schnelle, Salil Srivastava, Khadija M. Alawi, Elena Wilde, Jennifer Mitchell, Keith Farrell-Dillon, Daniel A. Richards, Giuseppe Maltese, Richard C. Siow, Manasi Nandi, James E. Clark, Ajay M. Shah, Anette Sams and Susan D. Brain

*Circulation*. 2017;136:367-383; originally published online April 26, 2017;  
doi: 10.1161/CIRCULATIONAHA.117.028388

*Circulation* is published by the American Heart Association, 7272 Greenville Avenue, Dallas, TX 75231  
Copyright © 2017 American Heart Association, Inc. All rights reserved.  
Print ISSN: 0009-7322. Online ISSN: 1524-4539

The online version of this article, along with updated information and services, is located on the  
World Wide Web at:

<http://circ.ahajournals.org/content/136/4/367>

Free via Open Access

Data Supplement (unedited) at:

<http://circ.ahajournals.org/content/suppl/2017/04/26/CIRCULATIONAHA.117.028388.DC1>

**Permissions:** Requests for permissions to reproduce figures, tables, or portions of articles originally published in *Circulation* can be obtained via RightsLink, a service of the Copyright Clearance Center, not the Editorial Office. Once the online version of the published article for which permission is being requested is located, click Request Permissions in the middle column of the Web page under Services. Further information about this process is available in the [Permissions and Rights Question and Answer](#) document.

**Reprints:** Information about reprints can be found online at:  
<http://www.lww.com/reprints>

**Subscriptions:** Information about subscribing to *Circulation* is online at:  
<http://circ.ahajournals.org/subscriptions/>

## SUPPLEMENTAL MATERIAL

### Supplemental Methods

#### Animals

Male mice, CD1 (#022) or C57BL/6J (#027) (12-18 weeks of age), purchased from Charles River (Kent, UK) were used in all experiments. Blood flow experiments were performed on CD1 mice, whilst all other experiments with C57BL/6J mice. Mice were housed in a climatically controlled environment, on a 12-h light/dark cycle, with free access to water and standard food *ad libitum*. All experiments were conducted in accordance with the UK Home Office Animals (Scientific Procedures) Act, 1986 and were approved by the King's College London Animal Care and Ethics Committee. All experiments were conducted in a blinded manner. Animals were randomly assigned to control or treatment groups and the experimenter was blinded towards treatment at the time of experiment.

#### Cutaneous blood flow measurement by Full-field Laser Perfusion Imager

Cutaneous blood flow was assessed in the whole area of ear, leg or paw area using the Full-field Laser Perfusion Imager (FLPI, Moor Instruments) on anaesthetised mice in their ventral positioned placed on a heating mat, maintained at 36°C, as previously described.<sup>1-3</sup>

*Local effects of  $\alpha$ -CGRP analogue ( $\alpha$ Analogue, Figure 1, Supplemental Figure 1):* CD1 mice were anaesthetised intraperitoneally (*i.p.*) with ketamine (75 mg/kg) and medetomidine (1 mg/kg).<sup>1</sup> Following recording of baseline blood flow in both ears to ensure the haemodynamic vascular responses have stabilised after anaesthesia, mice were injected intravenously (*i.v.*) with vehicle (neutralised saline) or CGRP receptor antagonist (BIBN4096, 0.3mg/kg)<sup>1, 4, 5</sup> and blood flow was resumed for another 5 min. The ipsilateral ear was then injected intradermally (*i.d.*) with  $\alpha$ Analogue<sup>6</sup> (100pmol in 15 $\mu$ l, Novo Nordisk), whilst the contralateral ear received vehicle (0.219M Mannitol, 5% HPCD, 1.6% ammonium acetate at pH6.5). Initial experiments investigated other doses of  $\alpha$ Analogue (1-100pmol in 15 $\mu$ l). Changes in blood flow after these treatments were followed for 30 min. Results are expressed as (1) a measure of maximum % increase in blood flow from baseline or (2) arbitrary flux units ( $\times 10^3$  flux units) measured as area under the recorded flux (response curve) versus time for the entire recording period for 30 min following *i.d.* injection.

*Systemic effects of  $\alpha$ Analogue (Supplemental Figure 7):* C57BL/6J mice were anaesthetised with isoflurane (2%, Abbott Laboratories) in 2l/min O<sub>2</sub> and blood flow in the ear was measured for 5 min. Mice were allowed to recover and injected subcutaneously (*s.c.*) with vehicle (0.219M Mannitol, 5% HPCD, 1.6% ammonium acetate at pH 6.5) or  $\alpha$ Analogue (50nmol/kg, *s.c.*, Novo Nordisk). At 1h following treatment, mice were anaesthetised and blood flow was measured for a further 5 min.

In other experiments, blood flow was measured for 5 min in the paw, leg and ear of mice treated daily with vehicle or  $\alpha$ Analogue (50nmol/kg, *s.c.*, Novo Nordisk) for 14 days. Results are expressed as an average blood flow (flux units) for the 5 min for each area.

### **Measurement of blood pressure via tail-cuff plethysmography**

Blood pressure was measured by tail-cuff plethysmography, using the CODA 8 non-invasive blood pressure acquisition technique system for mice (Kent Scientific), as previously described.<sup>7, 8</sup> All measurements were taken at a thermoneutral ambient room temperature (25-27°C). C57BL/6J mice were warmed on a heating pad for 10 min prior to and during blood pressure recordings. Mice were trained for at least 10 consecutive days prior to baseline blood pressure measurements, to reduce stress-induced changes caused by restraint.

*Dose-response characterisation of  $\alpha$ Analogue:* Measurements were taken at baseline and 1, 6, 24 and 30h following administration of vehicle (0.219M Mannitol, 5% HPCD, 1.6% ammonium acetate at pH 6.5) or  $\alpha$ Analogue (10-100nmol/kg, *s.c.*, Novo Nordisk).

### **Measurement of blood pressure via carotid artery cannulation**

After 5 weeks of abdominal aortic construction (AAC)-cardiac hypertrophy and heart failure, mice were anaesthetised using isoflurane (2%, Abbott laboratories, UK) in 2L/min O<sub>2</sub>, where systemic blood pressure was monitored invasively<sup>9</sup>. The core temperature of the mice was maintained at 37°C with a homeothermic blanket (Havard apparatus, Cambridge, UK). Briefly, the left carotid artery was isolated and fluid-filled (heparin; 100U/ml diluted in 0.9% saline) cannula with an outer diameter of 0.7mm and internal diameter of 0.28mm (Smiths Medical-Portex, Hythe, UK) was introduced into the carotid artery. After a 5-min stabilisation period, systemic pressures were measured using PowerLab data acquisition system and LabChart 8 Pro software (ADInstruments Ltd, Oxfordshire, UK). Data was represented as an average of 10 min continuous recording.

### **Measurement of blood pressure via radiotelemetry**

Blood pressure, heart rate and activity were measured using a radiotelemetry device (PA-C10, DSI, NL), with the catheter placed in the left carotid artery and advanced towards the aortic arch, as previously described<sup>1, 8, 10</sup> in C57BL/6J mice. The catheter was secured using surgical braided silk (5.0, waxed, Pearsalls sutures) and the outer wound closed with absorbable sutures (5.0, Ethicon, Johnson and Johnson) in a discontinuous pattern. The transmitter was placed *s.c.* in the right flank and the transmitter pocket was irrigated with sterile saline (0.9% saline; sodium chloride, pyrogen free). All procedures were conducted using aseptic techniques under isoflurane anaesthesia (2%, Abbott Laboratories, UK) in 2l/min O<sub>2</sub>. Surgical anaesthesia was assessed by loss of the paw pinch reflex. Buprenorphine was administered intramuscularly (50  $\mu$ g/kg, *i.m.*, Vetergesic, Alstoe Animal Health)

for pain relief. All animals were singly housed and allowed to recover for 7-10 days before recording baseline blood pressure for three 3 nights and 2 days in a quiet room. Blood pressure, heart rate activity was monitored at 10 min intervals, for duration of 2 min using the DSI software (DSI Dataquest A.R.T.) and data analysed in Microsoft Excel and GraphPad Prism 5. Data are represented as an average of 6h measurement.

### **Angiotensin-II murine hypertension model**

Following baseline blood pressure measurement using radiotelemetry, C57BL/6J mice were implanted *s.c.* in the mid-scapular region under isoflurane anaesthesia, with osmotic pump (1002; Alzet) containing Angiotensin II (AngII, Sigma) at a dose of 1.1mg/kg/day or saline (control) for 14 days, as previously described.<sup>7, 10</sup> Blood pressure measurement using radiotelemetry was resumed. Mice were treated daily with vehicle (0.219M Mannitol, 5% HPCD, 1.6% ammonium acetate at pH 6.5) or  $\alpha$ Analogue<sup>6</sup> (50nmol/kg, *s.c.*, Novo Nordisk) at different time-points, as detailed below.

*Experimental design 1:* Animals were divided into four groups: vehicle (saline), vehicle (AngII),  $\alpha$ Analogue (saline) and  $\alpha$ Analogue (AngII). Following, saline or AngII osmotic pump infusion, mice received daily treatment of vehicle or  $\alpha$ Analogue (50nmol/kg, *s.c.*, Novo Nordisk) at Day 1 to Day 14 of AngII infusion (Figure 2). Total food intake (g), water consumption (ml) and body weight (g) was recorded throughout the study.

*Experimental design 2:* Animals were divided into two groups: vehicle (AngII) and  $\alpha$ Analogue (AngII). All mice received osmotic pumps containing AngII (1.1mg/kg/day) and at day 7 following AngII infusion when mice showed a significant increase in blood pressure from baseline, they received daily treatment of vehicle or  $\alpha$ Analogue (50nmol/kg, *s.c.*, Novo Nordisk) at Day 7 to Day 14 of AngII infusion (Figure 6).

At the end of the study (Day 15), mice were briefly anaesthetised with isoflurane (Abbott Laboratories) in 2l/min O<sub>2</sub> and blood was collected via cardiac puncture. Mice were culled by cervical dislocation and organs (heart and aorta) were harvested for post-analysis. Heart, lung, kidney and spleen from each mouse was excised, dried on filter paper and weighed. Organs' weights were normalised to body weight and tibia length.

### **Cardiac hypertrophy murine model**

Mice were surgically subjected to pressure-overload induced-cardiac hypertrophy and heart failure as previously described.<sup>11</sup> Briefly, suprarenal aortic constriction was performed in anaesthetised mice (2% isoflurane carried in O<sub>2</sub>, Abbott Laboratories), where the abdominal aorta was ligated to the width of a 28G needle (0.36mm) using suture thread (8-0, Ethilon Sutures, Ethicon) in between the superior mesenteric and celiac bifurcation. Sham surgeries were performed in the same manner, excluding the

constriction. Post-surgery analgesia was provided in the form of buprenorphine (50 µg/kg, *i.m.*, Vetergesic). Following surgery, mice were treated daily with vehicle (0.219M Mannitol, 5% HPCD, 1.6% ammonium acetate at pH 6.5) or  $\alpha$ Analogue<sup>6</sup> (50nmol/kg, *s.c.*, Novo Nordisk) for 5 weeks. Body weight, food and water intake were measured throughout the study. At the end of week 5, mice were briefly anaesthetised with isoflurane (Abbott Laboratories) in 2l/min O<sub>2</sub> and blood was collected via cardiac puncture. Mice were culled by cervical dislocation and organs were harvested for post-analysis. Heart, lung, kidney and spleen from each mouse was excised and weighed. Organs' weights were normalised to body weight and tibia length.

### **Echocardiography**

Anesthesia in mice was induced in a chamber with 5% isoflurane for 1 min, afterwards maintained with 1.5% on a heated platform. Imaging was performed 10 min after induction using a Vevo 2100 Imaging System with a 40-MHz linear probe (Visualsonics, Canada), as previously described.<sup>11, 12</sup> Cardiac dimensions as well as systolic function were assessed using M-mode imaging in long axis views. The relative wall thickness (RWT) in diastole was calculated as follows:  $RWT = (\text{septal wall thickness} + \text{posterior wall thickness}) / \text{left ventricular diameter}$ . Data analysis was performed with Vevo®2100 software v.1.2.1 (Visualsonics).

### **Light aversion assay**

The light aversion assay is based on rodents' natural preference for darker areas compared to lighter areas<sup>13, 14</sup> and was used to study photophobia in rodents, a common symptom of migraine.<sup>15</sup> The apparatus consisted of two equal compartments: one-half (20 (d) x 20 (w) x 14 (h) cm) black plexiglass, with a black lid on top, the remaining half was transparent to enable behavioural assessment and recording. Mice were able to move freely between the two compartments through a small doorway (5 × 5 cm) in the center of the black plexiglass wall separating the two compartments, as described previously.<sup>14</sup> Lighting conditions (1000 lux) were established with the aid of 100-watt incandescent lamp, placed 45 cm above the centre of the box floor to the test arena and confirmed with a luxmeter (Mastech Light Meter, LX1010B, Mestech UK). At 1000 lux, light intensities in the dark zone were about 200 lux immediately inside the opening, 30 lux at the back wall across from the opening, and 10 lux at all four corners.

Mice were trained in the light/dark box under a range of lighting conditions (500-1000 lux) twice for 7 days. Mice that displayed equal preference between light/dark compartments (>40% light preference) were used in our study. Following acclimation in the testing room for 1h (200 lux), baseline recordings (10 min) were obtained, followed by systemic administration of vehicle (0.219M Mannitol, 5% HPCD, 1.6% ammonium acetate at pH 6.5) or  $\alpha$ Analogue (50 nmol/kg, *s.c.*) or the positive control glyceryl trinitrate (GTN, 320 nmol/kg, *i.v.*). Behavioural responses were resumed for 10min at 2h following

treatment.<sup>16</sup>

To evaluate the effects of chronic administration of the  $\alpha$ Analogue (5 weeks), sham mice were assessed on week 5 for light aversion at 1h following systemic administration of vehicle (0.219M Mannitol, 5% HPCD, 1.6% ammonium acetate at pH 6.5) or  $\alpha$ Analogue (50 nmol/kg, *s.c.*); behavioural responses were recorded for 10min.

Mouse behaviour was digitally recorded using an IPEVO camera (IPEVO, UK), placed 30cm above the light/dark box and attached to a laptop. Videos were continuously recorded at 30 frames/s and decomposed to individual frames of 1s interval. Each 10min experimental interval was taken to start immediately after the mouse entered the dark chamber. Behavioural experiments were conducted by a blinded observer and analysis was conducted procedurally with a custom ImageJ script, applying foreground extraction to determine the presence of the mouse against the white background of the light box floor across sequential frames. Absolute duration and % dwell time within the light and dark chambers was automatically calculated, as was the number of transitions, interpreted as crossings. Data was represented as the % of time spent in light during the 600s test session.

### **Glucose tolerance test**

Glucose tolerance tests (GTT) were performed following a 6h fast (from 08:30 to 14:30), as previously described.<sup>17</sup> Glucose (1g/kg, Sigma) was injected *i.p.* and blood glucose levels were monitored for 2h (from 08:30 to 14:30) at the indicated time points after injection with a One Touch Vita glucose meter (Lifescan, UK). GTT was determined at baseline and at Day 14 following daily treatment with the  $\alpha$ Analogue (50nmol/kg, *s.c.*) or its respective vehicle (0.219M Mannitol, 5% HPCD, 1.6% ammonium acetate at pH 6.5).

### **Core body temperature measurement using radiotelemetry**

Core body temperature and activity were measured using radio-telemetry as described previously.<sup>18</sup> Briefly, animals were anaesthetised by isoflurane (2%, Abbott Laboratories, UK) in 2l/min O<sub>2</sub>, placed on a homeothermic heating pad and buprenorphine (50 $\mu$ g/kg, *i.m.*, Vetergesic, Alstoe, Animal Health, UK) was administered peri-operatively. The abdomen was shaved and scrubbed using surgical scrub and a small ventral midline abdominal incision (< 2 cm) was made to expose the abdominal muscle wall. A ventral incision was made on the abdominal wall and a small volume of (< 80  $\mu$ l) sterile saline was applied to facilitate the insertion of the radio telemetry transmitter (TA10TA-F10; DSI, St Paul, Minnesota, USA). Following implantation, the abdominal wall and skin were sutured separately using absorbable sutures (Vicryl<sup>®</sup> 4.0, Ethicon, Johnson & Johnson, UK). The mice were monitored until ambulatory and were individually housed with food and water *ad libitum*. Mice were weighed and examined daily, and were allowed a minimum 7 days post-surgical recovery period. Cages containing the telemetered animals were placed on the receiver plates (RPC-1; Data Sciences Incorporated (DSI,



Minnesota, USA); radio signals from the implanted transmitters were monitored via a fully automated data acquisition system (DataquestART, version 3.1; DSI, Minnesota, USA). Locomotor activity and core body temperature were monitored at 10 min intervals, for duration of 2 min.

Following baseline measurement for 1h, the  $\alpha$ Analogue (50nmol/kg, *s.c.*) and its respective vehicle (0.219M Mannitol, 5% HPCD, 1.6% ammonium acetate at pH 6.5) were administered *s.c.* and measurements were recorded for 24h thereafter.

### **Measurement of gene expression using Real-time reverse transcription polymerase chain reaction**

Real-time reverse transcription polymerase chain reaction (RT-qPCR) was carried out as previously described.<sup>3, 7, 10</sup>

Total ribonucleic acid (RNA) was extracted from aorta, heart and kidney tissue using the Qiagen RNeasy Microarray tissue mini Kit (Qiagen), according to manufacturer's instructions. Total RNA (1 $\mu$ g) was then reverse transcribed into cDNA using the High Capacity RNA-to-cDNA Kit (Applied Biosystems, Life technologies Ltd) as per manufacturer's instructions. A thermal cycler (DNA Engine Tetrad 2 Peltier Thermal Cycler) was used for reverse transcription to complementary DNA (cDNA). Negative RT samples were carried out as a control to exclude possible contamination of genomic DNA. cDNA was then diluted 1:40 in nuclease-free water for RT-qPCR. Quantitative PCR (qPCR) was then conducted using a SYBR-green-based PCR mix (Sensi-Mix, SYBR-green No ROX; Bioline) and primers from the specific gene of interest pipetted into 100-well gene disks (Qiagen) by an automated robot (CAS1200; Qiagen Corbett), followed by PCR in a Corbett Rotor-gene 6000. Settings were as follows; initial denaturation: 10min at 95°C; cycling: 45 cycles- 10 s at 95°C, 15 s at 57°C, and 5s at 72°C; melt: 68-90°C. Samples were subjected to melting curve analysis to confirm amplification specificity. Data were collected as copies/ $\mu$ l and normalised against murine hypoxanthine phosphor-ribosyltransferase (HPRT),  $\beta$ -2-microglobulin (B<sub>2</sub>M) and  $\beta$ -actin expression using GeNorm3.4 software. A list of primers are summarised in Supplemental Table I.

### **Western blotting**

Western blot analysis was performed as previously described.<sup>1, 2, 7</sup> Briefly, aorta, mesentery, heart and kidney tissue was homogenised in SDS lysis buffer containing protease inhibitor (1 tablet/50ml, Roche, Germany) and protein concentrations were determined. Samples were loaded onto a 7-12% Tris SDS-polyacrylamide gel electrophoresis and transferred to polyvinylidene difluoride (PVDF) membranes using a semi-dry technique (Bio-Rad). After blocking with 5% non-fat dry milk, membranes were incubated with a primary antibody (4°C, overnight), and incubated with the secondary antibody at room temperature for 1h. Proteins were detected by enhanced chemiluminescence (ECL, Piercenet) and developed using the Syngene gel doc dark room system. Densitometric analysis was performed using Image J analysis software (NIH, USA). Antibodies against eNOS (1:500, Ab5589), HO-1 (1:500,

Ab13248), nitrotyrosine (1:500, Ab61392)<sup>2</sup>, GPX-1 (1:1000, Ab22604), CLR (1:500, Ab173562) and RAMP1 (1:1000, Ab156575) were purchased from Abcam. Antibodies against NOX-2 (gp91phox, 1:500, 611414) were obtained from BD Transduction,  $\alpha$ -SMA (1:1000, A2547) from Sigma and klotho (1:500, KM2076) from Cosmo Bio Co. Ltd. p-p38 (1:1000, 9216) and total-p38 (1:1000, 9212) were purchased from Cell Signalling. GAPDH (1:4000, AM4300) was purchased from Life Technologies Ltd and used for a loading control. Note that for nitrosylated proteins detected using anti-nitrotyrosine antibody, densitometric analysis was conducted for the entire lane and normalised to GAPDH.

### **Quantification of noradrenaline using ELISA**

Plasma and renal noradrenaline (NA) content were quantified using a commercially available NA ELISA kit (RE59261; IBL International, Hamburg, Germany), as previously described.<sup>1</sup> Briefly, kidneys were homogenised in phosphate buffered saline (1M), supplemented with protease inhibitors (Roche, Germany). Lysates were cleared by centrifugation at 2,600 g for 15 min at 4°C. NA content was extracted from both plasma and kidney tissue lysate and assessed by standard ELISA technique, according to the manufacturer instructions. The limit of sensitivity was 20 pg/ml and the linearity limit was 8.0 ng/ml. Cross-reactivity to other catecholamines or metabolites was manufacturer tested as <0.02%. Protein concentration of each kidney samples were determined by Bradford dye-binding method (Bio-rad) and noradrenaline content was normalised to mg of protein.

### **Quantification of IL-6 and TNF- $\alpha$ using ELISA**

Briefly, frozen kidney tissues were homogenised in phosphate buffered saline (1M), supplemented with protease inhibitors (Roche, Germany). Lysates were cleared by centrifugation at 2,600 g for 15 min at 4°C. Renal interleukin-6 (IL-6) and Tumour necrosis factor- $\alpha$  (TNF- $\alpha$ ) content were quantified using a commercially available ELISA kit (RAB0308 & RAB0477, Sigma, UK), following manufacturer's protocol. Protein concentration of each kidney samples were determined by Bradford dye-binding method (Bio-rad). The final concentrations of both IL-6 and TNF- $\alpha$  were calculated with respect to the total amount of protein (mg).

### **Histology**

Aorta, heart and kidney tissues were fixed in 4% paraformaldehyde (overnight, 4°C), as previously described.<sup>7, 19, 20</sup> For heart and kidney samples, after routine paraffin wax embedding, transverse sections (6 $\mu$ m) were prepared using a Reichert-Jung 2030 Biocut microtome onto poly-L-lysine slides. For aorta samples, following fixation aorta segments were embedded in optimal cutting temperature compound (OCT, VWR), frozen on dry ice in a cryomould and cryosectioned on a microtome cryostat (6 $\mu$ m, Bright, UK) on Superfrost Plus glass slides. Sections were allowed to dry overnight. Approximately 8-10 transverse sections were obtained from each heart or aorta per mouse for staining.

*Aorta Staining:* Sections of aorta were stained with Masson's trichrome, as previously described<sup>7,21</sup>. All slides were imaged using an Olympus Colourview III camera, connected to an Olympus BX51 microscope (x10 magnification). Images were taken using CellSens Dimension viewing software (Version 1.1.3, Olympus). Aortic wall width (medial thickness) were measured (mean of 8 measurements taken from at least 3 sections for each 4 mice/group) using ImageJ analysis software (scale bars, 100µm; NIH, USA).

*Heart Staining:* Picrosirius Red (0.1% w/v) staining was used to visualise collagen fibres in the heart<sup>20</sup> and fibrosis was assessed blindly. All slides were imaged using a Leica Diaplan microscope (x10 magnification) and images captured using ProgRes Capture Pro viewing software (Version 2.8.8, JENOPTIK) under bright light and circular polarised light according to a modified Junqueira method.<sup>22</sup> <sup>23</sup> Cardiac fibrosis was quantified on circular polarised light images using Image J analysis software (scale bars, 200µm; NIH, USA).

Conjugated wheat germ agglutinin (WGA, CF488A, Biotium) staining was applied to outline cardiomyocyte boundaries and quantify cross-sectional area.<sup>20</sup> All slides were imaged using an Olympus Colourview III camera, connected to an Olympus BX51 microscope (x40 magnification). Images were taken using CellSens Dimension viewing software (Version 1.1.3, Olympus). Myocyte cross-sectional area was employed as an index of cardiac hypertrophy and determined on fibres with circular shapes in a blinded fashion by quantitative image analysis using Image J (scale bars, 20µm; NIH, USA).

Capillaries were immunostained with isolectin B4 (Vector B-1205) and capillary density was quantified as the number of capillaries per mm<sup>2</sup> of LV sections<sup>11</sup>. All slides were imaged using an Olympus Colourview III camera, connected to an Olympus BX51 microscope (x40 magnification). Images were taken using CellSens Dimension viewing software (Version 1.1.3, Olympus). Number of capillaries were manually counted in a blinded fashion by quantitative image analysis using Image J (scale bars, 20µm; NIH, USA).

Apoptosis was detected by using terminal deoxyribonucleotide transferase (TdT)-mediated dUTP nick-end labelling (TUNEL) staining (Millipore S7111 kit) in LV sections<sup>24</sup>. All slides were imaged using an Olympus Colourview III camera, connected to an Olympus BX51 microscope (x20 magnification). Images were taken using CellSens Dimension viewing software (Version 1.1.3, Olympus). TUNEL-positive myocytes and DAPI-stained nuclei were manually counted by quantitative image analysis using Image J (scale bars, 50µm; NIH, USA).

*Kidney Staining:* Sections of kidney were stained with Periodic acid–Schiff's (PAS) and counter stained with hematoxylin, as previously described<sup>25</sup>. All slides were imaged using an Olympus Colourview III camera, connected to an Olympus BX51 microscope (x40 magnification). Images were taken using

CellSens Dimension viewing software (Version 1.1.3, Olympus). A semi quantitative system was used to grade mesangial expansion by either diffuse (irregular streaks) or segmental (localized to a lobule) type. In each of the experimental animals, 20 glomeruli were examined for mesangial expansion and each glomerulus was graded 0 to 4 corresponding to the percentage of mesangial matrix covering/occupying the urinary space of the Bowman's capsule. Glomeruli were assessed and graded 1-4, as follows: grade 1, involvement of 0-24%; grade 2, 25-29%; grade 3, 50-74% or grade 4; 75-100% of mesangial area to Bowman's capsule (scale bars, 20 $\mu$ m; NIH, USA). Mean glomerular score index was determined for each kidney<sup>26</sup>.

All morphometric measurements were performed in a blinded manner.

### **Statistical analysis**

Data in the manuscript is expressed as mean  $\pm$  SEM. Statistical analysis was performed using a two-tailed Student's *t*-test (2 unpaired groups), one-way or repeated measures two-way analysis of variance (ANOVA) followed by Bonferroni's comparison *post hoc* test (multiple groups comparison).  $p < 0.05$  was considered to represent a significant difference.

Supplemental Tables

Supplemental Table 1. Gene primer sequences		
Target Gene	Primer Sequence	Accession number
<b>Akt</b>	F: CGTCGCCAAGGATGAGGTTG R: GTCGTGGGTCTGGAATGAGT	NM_001165894.1
<b><math>\alpha</math>-MHC</b>	F: GCTGGAAGAAAAGCTCAAGAAGAAA R: TCTCTATCTGCACGGATGTGG	NM_001164171.1
<b><math>\beta</math>-MHC</b>	F: CACCTACCAGACAGAGGAAGA R: GGAGCTGGGTAGCACAAGA	NM_080728.2
<b><math>\alpha</math>-skeletal actin</b>	F: CTAAATCCAAGTCCTGCAAGTG R: ACATGGTGTCTAGTTTCAGAGG	NM_001272041.1
<b>ANP</b>	F: GGATTTCAAGAACCTGCTAGACC R: GCAGAGCCCTCAGTTTGCT	NM_008725.3
<b>B<sub>2</sub>M</b>	F: GTCGCTTCAGTCGTCAGCA R: TTGAGGGGTTTTCTGGATAGCA	NM_009735.3
<b>Bcl-2</b>	F: AGGCTGGGATGCCTTTGTGG R: TGTTTGGGGCAGGTTTGTCTG	NM_009741.5
<b>BNP</b>	F: TGGGCTGTAACGCACTGAA R: TGTTGTGGCAAGTTTGTGCTT	NM_001287348.1
<b>Collagen Type 1 <math>\alpha</math>1</b>	F: TCTGACTGGAAGAGCGGAGAG R: AGACGGCTGAGTAGGGAACA	NM_007742.4
<b>Collagen Type 1 <math>\alpha</math>2</b>	F: TGGATACGCGGACTCTGTTG R: CCCTTTCGTA CTGATCCCGATT	NM_007743.2
<b>Collagen Type 3 <math>\alpha</math>1</b>	F: GGGAGGAATGGGTGGCTATC R: CTGGGCCTTTGATACCTGGA	NM_009930.2
<b>Collagen Type 4 <math>\alpha</math>1</b>	F: CTGGAGAAAAGGGCCAGAT R: TCCTTAACTTGTGCCTGTCC	NM_009931.2
<b>CTGF</b>	F: GGGCCTCTTCTGCGATTC R: ATCCAGGCAAGTGCATTGGTA	NM_010217.2
<b>Cystatin C</b>	F: GAGTACAACAAGGGCAGCAAC R: AGCAGAGTGCCTTCCTCATCA	NM_009976.4
<b>eNOS</b>	F: GACCCTCACCGCTACAA AT R: GTCCTGGTGTCCAGATCCAT	NM_008713.4
<b>Fibronectin</b>	F: CCGGTGGCTGTCAGTCAGA R: CCGTTCCCACTGCTGATTTATC	NM_006495700.2
<b>GPX-1</b>	F: TTCGGACACCAGGAGAATGG R: TAAAGAGCGGGTGAGCCTTC	NM_008160.6
<b>HIF-1<math>\alpha</math></b>	F: CGAGAACGAGAAGAAAAAGATGAGT R: CGTAAATAACTGATGGTGAGCCT	NM_010431.2
<b>HO-1</b>	F: CAACATTGAGCTGTTTGAGGAG R: CTCTGACCAAGTGACGCCAT	NM_010442.2
	F: CCTGGTTCATCATCGCTAATC	NM_013556.2

<b>HPRT</b>	R: TCCTCCTCAGACCGCTTTT	
<b>MMP-2</b>	F: GACAAGTTCTGGAGATACAATGAAGTG R: CAGGTTATCAGGGATGGCATTTC	NM_006530751.1
<b>NGAL</b>	F: AATGTCACCTCCATCCTGGTCA R: GACAGCTCCTTGGTTCTTCCATAC	NM_008491.1
<b>NF-κB</b>	F: CCTACGGAAGTGGGCAAATGT R: TCCCCTCTGTTTTGGTTGCT	NM_008689.2
<b>NOX-2</b>	F: ACTCCTTGGGTCAGCACTGG R: GTTCCTGTCCAGTTGTCTTCG	NM_007807.5
<b>NQO1</b>	F: TCATTCTCTGGCCGATTCA R: TGCTGTAAACCAGTTGAGGTTC	NM_008706.5
<b>Osteopontin</b>	F: AAACCAGCCAAGGTAAGCCT R: GCAAAAGCAATCACTGCCA	NM_001204201.1
<b>p53</b>	F: ATGCCCATGCTACAGAGGAG R: AGACTGGCCCTTCTTGGTCT	NM_001127233.1
<b>RANTES</b>	F: TGCTCCAATCTTGCAGTCGT R: GCGTATACAGGGTCAGAATCAAG	NM_013653.3
<b>SERCA-2</b>	F: TGGAACCTTTGCCGCTCATTT R: CAGAGGCTGGTAGATGTGTT	NM_009722.3
<b>TGF-β<sub>1</sub></b>	F: TCAGACATTCGGGAAGCAGT R: GCCCTGTATTCCGTCTCCTTG	NM_011577.2
<b>TIMP-2</b>	F: GATTCAGTATGAGATCAAGCAGATAAAGA R: GCGAGACCCCGCACACT	NM_011594.3
<b>α-SMA</b>	F: ACTACTGCCGAGCGTGA R: ATAGGTGGTTTCGTGGATGC	NM_007392.3
<b>β-actin</b>	F: CACAGCTTCTTTGCAGCTCCTT R: TCAGGATACCTCTCTTGCTCT	NM_007393.5

**Supplemental Table 1. List of gene primer sequences used for qRT-PCR studies.**

**Supplemental Table 2: Changes in organ weight in AngII and saline-infused mice pre-treated with  $\alpha$ Analogue or vehicle**

Organs	Vehicle		$\alpha$ Analogue	
	Saline	AngII	Saline	AngII
Total Heart:Body Weight (mg/g)	4.4 $\pm$ 0.3	6.3 $\pm$ 0.2 ***	4.5 $\pm$ 0.2	5.2 $\pm$ 0.2 ††
Total Heart:Tibia length (mg/mm)	7.9 $\pm$ 0.4	10.0 $\pm$ 0.4 ***	7.5 $\pm$ 0.2	8.4 $\pm$ 0.3 ††
Left Ventricle:Body Weight (mg/g)	3.4 $\pm$ 0.2	4.9 $\pm$ 0.1 ***	3.5 $\pm$ 0.2	4.2 $\pm$ 0.1 †††
Lung Oedema (Wet:Dry Ratio)	4.2 $\pm$ 0.1	4.2 $\pm$ 0.1	4.1 $\pm$ 0.1	4.1 $\pm$ 0.1
Kidney:Body Weight (mg/g)	5.8 $\pm$ 0.3	5.8 $\pm$ 0.3	5.8 $\pm$ 0.3	5.7 $\pm$ 0.2
Kidney:Tibia length (mg/mm)	10.8 $\pm$ 0.3	9.1 $\pm$ 0.4	9.4 $\pm$ 0.2	9.4 $\pm$ 0.6
Spleen:Body Weight (mg/g)	2.5 $\pm$ 0.2	3.1 $\pm$ 0.2	2.7 $\pm$ 0.2	3.1 $\pm$ 0.3
Spleen:Tibia length (mg/mm)	4.7 $\pm$ 0.2	4.8 $\pm$ 0.3	4.5 $\pm$ 0.3	5.1 $\pm$ 0.4

**Supplemental Table 2. Changes in organ weight in the heart of AngII and saline-infused mice treated daily with  $\alpha$ -CGRP analogue ( $\alpha$ Analogue, 50nmol/kg) or vehicle (*s.c.*) daily for 14 days.** Mice were implanted with osmotic pumps containing saline or AngII (1.1mg/kg/day) and treated daily with vehicle or  $\alpha$ Analogue (50nmol/kg, *s.c.*) for 14 days (n=6-9). At day 15, mice were sacrificed, organs were weighed and normalised to body weight (mg/g) or tibia length (mg/mm). Results show mean  $\pm$  SEM. \*\*\*p<0.001 vs vehicle-treated saline-infused mice; ††p<0.01, †††p<0.001 vs vehicle-treated AngII-infused mice (2-way ANOVA + Bonferroni *post hoc* test).

<b>Supplemental Table 3: Changes in gene expression in the heart of AngII and saline-infused mice pre-treated with <math>\alpha</math>Analogue or vehicle</b>				
<b>Gene</b>	<b>Vehicle</b>		<b><math>\alpha</math>Analogue</b>	
	<b>Saline</b>	<b>AngII</b>	<b>Saline</b>	<b>AngII</b>
CTGF	89.3 $\pm$ 14.6	220.3 $\pm$ 44.0 *	152.0 $\pm$ 42.9	67.6 $\pm$ 20.1 †
Akt	499.1 $\pm$ 80.1	721.8 $\pm$ 96.6	666.7 $\pm$ 78.6	365.7 $\pm$ 59.3 †
TIMP-2	337.6 $\pm$ 22.5	396.2 $\pm$ 33.5	391.5 $\pm$ 52.1	223.5 $\pm$ 30.0 *, ††
NF- $\kappa$ B	231.6 $\pm$ 16.5	263.6 $\pm$ 25.2	276.9 $\pm$ 14.6	185.3 $\pm$ 12.7 **, †
Bcl-2	16.0 $\pm$ 1.5	17.3 $\pm$ 2.0	13.5 $\pm$ 2.1	12.7 $\pm$ 1.7
p53	5082 $\pm$ 569.4	7267 $\pm$ 543.1 *	6475 $\pm$ 518.5	4926 $\pm$ 359.5 ††

**Supplemental Table 3. Changes in gene expression in in the heart of AngII and saline-infused mice treated daily with  $\alpha$ -CGRP analogue ( $\alpha$ Analogue, 50nmol/kg) or vehicle (s.c.) daily for 14 days.** Mice implanted with osmotic pumps containing saline (S) or AngII (A, 1.1mg/kg/day) and treated daily with vehicle or  $\alpha$ Analogue (50nmol/kg, s.c.) for 14 days. mRNA expression measured by qRT-PCR (n=5-11) for connective tissue growth factor (CTG), Protein Kinase B (PKB, Akt), tissue inhibitor of metalloproteinase-2 (TIMP-2), nuclear factor kappa B cells (NF- $\kappa$ B), apoptosis regulator B-cell lymphoma 2 (Bcl-2) and apoptotic marker p53 in the mice heart. Results expressed as copy numbers per  $\mu$ l normalised to HPRT, B<sub>2</sub>M and  $\beta$ -actin. Results show mean  $\pm$  SEM. \*p<0.05 vs vehicle-treated saline-infused mice; †p<0.05, ††p<0.01 vs vehicle-treated AngII-infused mice (2-way ANOVA + Bonferroni *post hoc* test).



<b>Supplemental Table 4. Changes in gene expression in the aorta of vehicle and <math>\alpha</math>Analogue treated AngII-infused mice</b>		
<b>Gene</b>	<b>AngII</b>	
	<b>Vehicle</b>	<b><math>\alpha</math>Analogue</b>
<i>Vascular dysfunction</i>		
eNOS	210.2 $\pm$ 14.4	162.2 $\pm$ 31.5
Akt	663.3 $\pm$ 23.6	567.9 $\pm$ 30.1 *
<i>Remodelling and fibrosis</i>		
TGF- $\beta$	3282.2 $\pm$ 395.3	1567.4 $\pm$ 412.6 *
CTGF	2957.2 $\pm$ 270.3	1513.3 $\pm$ 412.6 *
COL1A1	8869.7 $\pm$ 2537.2	5253.2 $\pm$ 1553.8
COL3A1	2765.6 $\pm$ 802.5	1139.5 $\pm$ 325.45
$\alpha$ -SMA	5288.1 $\pm$ 343.5	3272.2 $\pm$ 271.6 **
<i>Vascular Inflammation</i>		
RANTES	2524.6 $\pm$ 1132.0	928.9 $\pm$ 228.8
Osteopontin	36.0 $\pm$ 10.9	4.8 $\pm$ 2.4 *
<i>Oxidative Stress</i>		
HO-1	1169.0 $\pm$ 349.0	226.3 $\pm$ 68.2 *
NOX-2	52.8 $\pm$ 1.4	32.3 $\pm$ 2.8 **

**Supplemental Table 4. Changes in gene expression in the aorta of vehicle and  $\alpha$ -CGRP analogue ( $\alpha$ Analogue) treated Angiotensin II (AngII)-infused mice.** Mice infused with AngII (1.1mg/kg/day) and treated daily with vehicle or  $\alpha$ Analogue (50nmol/kg, *s.c.*) at day 7 to 14. mRNA expression measured by qRT-PCR (n=4) for endothelial nitric oxide (eNOS), Protein kinase B (PKB, Akt), transforming growth factor beta-1 (TGF- $\beta$ 1), connective tissue growth factor (CTGF), collagen type 1  $\alpha$ 1 (COL1A1), collagen type 3  $\alpha$ 1 (COL3A1), alpha-smooth muscle actin ( $\alpha$ -SMA), RANTES, osteopontin, haem-oxygenase 1 (HO-1), NAD(P)H dehydrogenase, quinone-1 (NQO1) and NADPH oxidase-2 (NOX-2) in the mice aorta. Results expressed as copy numbers per  $\mu$ l normalised to HPRT, B2M and  $\beta$ -actin. Results are shown as mean  $\pm$  SEM. \*p<0.05, \*\*p<0.01 vs vehicle-treated AngII-infused mice (two-tailed Student *t*-test).

<b>Supplemental Table 5: Changes in organ weight in <math>\alpha</math>Analogue or vehicle-treated AngII-induced hypertensive mice</b>		
<b>Organs</b>	<b>AngII</b>	
	<b>Vehicle</b>	<b><math>\alpha</math>Analogue</b>
Total Heart:Body Weight (mg/g)	6.3 $\pm$ 0.5	4.9 $\pm$ 0.2 *
Total Heart:Tibia length (mg/mm)	9.4 $\pm$ 0.4	7.5 $\pm$ 0.6 *
Left Ventricle:Body Weight (mg/g)	5.2 $\pm$ 0.4	3.9 $\pm$ 0.1 *
Lung Oedema (Wet:Dry Ratio)	3.7 $\pm$ 0.2	3.9 $\pm$ 0.3
Kidney:Body Weight (mg/g)	5.8 $\pm$ 0.3	5.3 $\pm$ 0.3
Kidney:Tibia length (mg/mm)	8.4 $\pm$ 0.2	8.2 $\pm$ 0.1
Spleen:Body Weight (mg/g)	2.6 $\pm$ 0.3	2.9 $\pm$ 0.2
Spleen:Tibia length (mg/mm)	3.8 $\pm$ 0.3	4.5 $\pm$ 0.6

**Supplemental Table 5. Changes in organ weight in the heart of  $\alpha$ -CGRP analogue ( $\alpha$ Analogue, 50nmol/kg) or vehicle (s.c.)-treated AngII-infused mice.** Mice were infused with AngII (1.1mg/kg/day) osmotic pumps for 14 days and treated with vehicle or  $\alpha$ Analogue (50nmol/kg) on Day 7-14 (n=4). At day 15, mice were sacrificed, organs were weighed and normalised to body weight (mg/g) or tibia length (mg/mm). Results show mean  $\pm$  SEM. \*p<0.05 vs vehicle-treated AngII-infused mice (two-tailed Student t-test).

<b>Supplemental Table 6: Changes in gene expression in the heart of vehicle and <math>\alpha</math>Analogue treated AngII-infused mice</b>		
<b>Gene</b>	<b>AngII</b>	
	<b>Vehicle</b>	<b><math>\alpha</math>Analogue</b>
<i>Remodelling and fibrosis</i>		
CTGF	1118 $\pm$ 85.6	719.0 $\pm$ 206.3
Fibronectin	586.0 $\pm$ 62.0	330.6 $\pm$ 87.6
COL1A1	825.5 $\pm$ 140.0	569.3 $\pm$ 157.8
COL3A1	852.2 $\pm$ 140.0	282.5 $\pm$ 91.9 *
COL4A1	4670.9 $\pm$ 415.7	4108.7 $\pm$ 512.0
SERCA-2	189.2 $\pm$ 13.5	163.7 $\pm$ 18.7
ANP	40224 $\pm$ 7485.1	6026.7 $\pm$ 2559.2 **
BNP	1365.6 $\pm$ 220.9	1517.8 $\pm$ 641.2
<i>Oxidative Stress</i>		
NOX-2	67.7 $\pm$ 7.1	44.4 $\pm$ 3.9 *

**Supplemental Table 6. Changes in gene expression in the heart of vehicle and  $\alpha$ -CGRP analogue ( $\alpha$ Analogue) treated Angiotensin II (AngII)-infused mice.** Mice infused with AngII (1.1mg/kg/day) and treated daily with vehicle or  $\alpha$ Analogue (50nmol/kg, s.c.) at day 7 to 14 (n=4). mRNA expression measured by qRT-PCR for connective tissue growth factor (CTGF), fibronectin, collagen type 1  $\alpha$ 1 (COL1A1), collagen type 3  $\alpha$ 1 (COL3A1), collagen type 4  $\alpha$ 1 (COL4A1), sarcoplasmic reticulum Ca<sup>2+</sup> ATPase-2 (SERCA-2), atrial natriuretic peptide (ANP), brain natriuretic peptide (BNP) and NADPH oxidase-2 (NOX-2) in heart. Results expressed as copy numbers per  $\mu$ l normalised to HPRT, B2M and  $\beta$ -actin. Data represent mean + S.E.M. \*p<0.05, \*\*p<0.01 vs vehicle-treated AngII-infused (two-tailed Student t-test).

**Supplemental Table 7. Echocardiographic parameters of left ventricular size and function 5 weeks post AAC-induced hypertrophy and heart failure in mice treated with  $\alpha$ Analogue or vehicle**

Parameters	Vehicle		$\alpha$ Analogue	
	Sham	AAC	Sham	AAC
n	8	6	8	8
HR [bpm]	430.3 $\pm$ 11.59	455.5 $\pm$ 36.49	452.9 $\pm$ 10.37	457.9 $\pm$ 17.49
LVID;d [mm]	4.18 $\pm$ 0.10	4.36 $\pm$ 0.13	4.10 $\pm$ 0.11	4.32 $\pm$ 0.07
LVID;s [mm]	3.16 $\pm$ 0.08	3.68 $\pm$ 0.21*	3.01 $\pm$ 0.09	3.32 $\pm$ 0.09
LVV;d [ $\mu$ l]	40.14 $\pm$ 2.43	59.04 $\pm$ 7.82**	35.76 $\pm$ 2.80	45.13 $\pm$ 3.04
LVV;s [ $\mu$ l]	78.41 $\pm$ 4.39	86.44 $\pm$ 5.97	75.00 $\pm$ 4.98	84.61 $\pm$ 3.16
septW [mm]	0.78 $\pm$ 0.03	1.02 $\pm$ 0.04 ***	0.79 $\pm$ 0.03	0.87 $\pm$ 0.03 ††
postW [mm]	0.74 $\pm$ 0.03	1.03 $\pm$ 0.06 ***	0.71 $\pm$ 0.03	0.78 $\pm$ 0.02 †††
rWT	0.37 $\pm$ 0.02	0.47 $\pm$ 0.02 **	0.37 $\pm$ 0.02	0.38 $\pm$ 0.01 ††
SV [ $\mu$ l]	38.27 $\pm$ 2.30	27.40 $\pm$ 2.7 **	39.24 $\pm$ 2.43	39.48 $\pm$ 1.34 ††
EF [%]	48.80 $\pm$ 1.17	33.10 $\pm$ 5.17 ***	52.51 $\pm$ 1.24	46.87 $\pm$ 1.96 ††
FS [%]	24.39 $\pm$ 0.72	15.91 $\pm$ 2.92 ***	26.67 $\pm$ 0.79	23.37 $\pm$ 1.17 ††

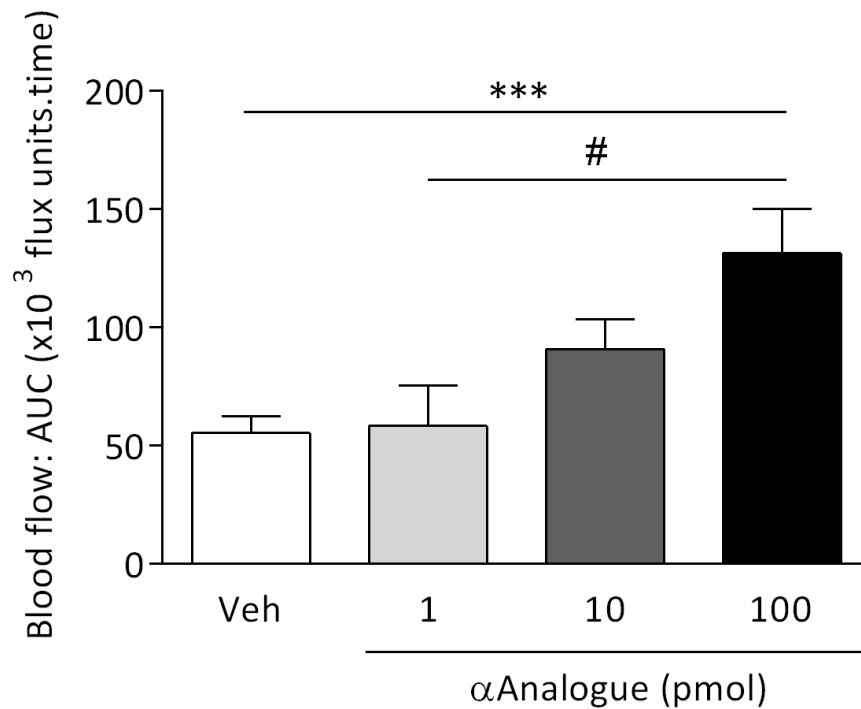
**Supplemental Table 7. Echocardiographic parameters of left ventricular size and function 5 weeks post AAC-induced hypertrophy and heart failure.** Mice were treated daily with vehicle or  $\alpha$ -CGRP analogue ( $\alpha$ Analogue, 50nmol/kg/day, *s.c.*) post surgery (n=6-8). (HR: heart rate, LVID;d: left ventricular dimension in diastole, LVID;s: left ventricular dimension in systole, LVV;d: left ventricular volume in diastole, LVV;s: left ventricular volume in systole, septW: septal wall thickness, postW: posterior wall thickness, rWT: relative wall thickness, SV: stroke volume, EF: ejection fraction, FS: fractional shortening. Data represented as mean  $\pm$  SEM (n=6-8). \*p<0.05, \*\*p<0.01, \*\*\*p<0.001 vs respective sham-treated; ††p<0.01, †††p<0.001 vs vehicle-treated AAC (2-way ANOVA + Bonferroni *post hoc* test).

**Supplemental Table 8: Changes in organ weight in AAC and sham-treated WT mice pre-treated with  $\alpha$ Analogue or vehicle**

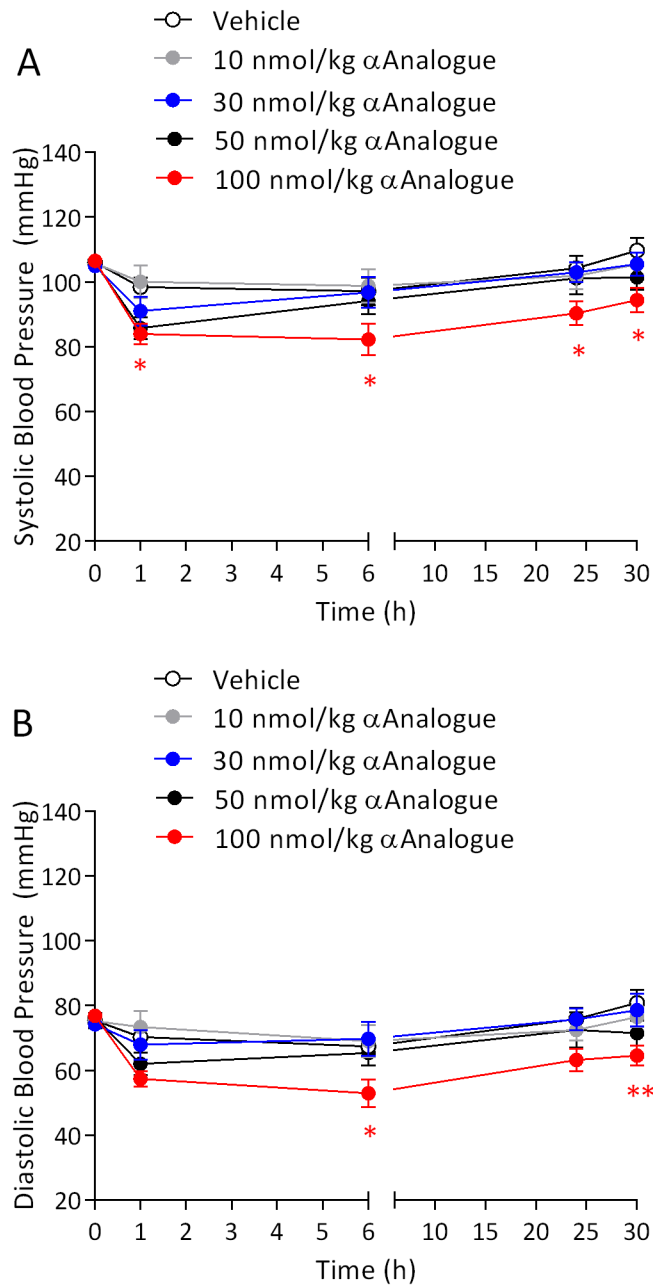
Organs	Vehicle		$\alpha$ Analogue	
	Sham	AAC	Sham	AAC
Total Heart:Body Weight (mg/g)	4.7 $\pm$ 0.1	9.1 $\pm$ 0.1***	4.7 $\pm$ 0.2	5.9 $\pm$ 0.3†††
Total Heart:Tibia length (mg/mm)	7.6 $\pm$ 0.2	13.8 $\pm$ 1.2***	7.8 $\pm$ 0.3	9.6 $\pm$ 0.5†††
LV:Body Weight (mg/g)	3.5 $\pm$ 0.1	7.1 $\pm$ 0.6***	3.5 $\pm$ 0.1	4.5 $\pm$ 0.3*,†††
Lung Oedema (Wet:Dry Ratio)	4.3 $\pm$ 0.0	4.5 $\pm$ 0.3	4.2 $\pm$ 0.1	4.3 $\pm$ 0.1
Dry Lung:Tibia length (mg/g)	1.7 $\pm$ 0.1	3.8 $\pm$ 0.8***	2.0 $\pm$ 0.1	1.9 $\pm$ 0.1††

**Supplemental Table 8. Changes in organ weight in  $\alpha$ -CGRP analogue ( $\alpha$ Analogue, 50nmol/kg) or vehicle (*s.c.*)-treated sham or AAC-induced cardiac hypertrophy and heart failure mice.** Mice were treated daily for 5 weeks post surgery. Organs were weighed and normalised to body weight (mg/g) or tibia length (mg/mm). Results show mean + SEM (n=6-8). \*p<0.05, \*\*\*p<0.001 vs respective sham-treated; ††p<0.01, †††p<0.001 vs vehicle-treated AAC mice (2-WAY ANOVA + Bonferroni *post hoc* test).

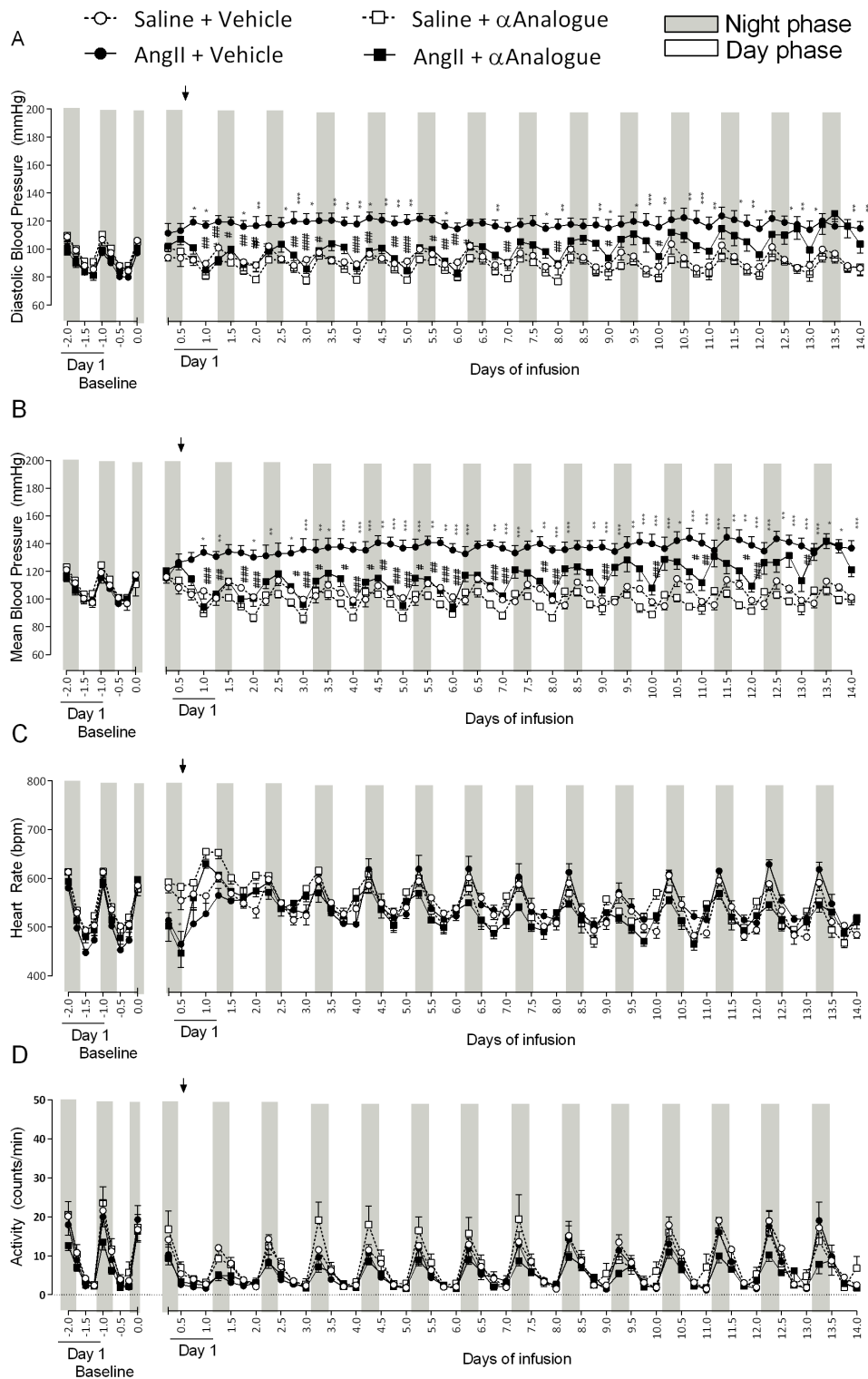
## Supplemental Figures



**Supplemental Figure 1. Effect of local administration  $\alpha$ -CGRP analogue ( $\alpha$ Analogue) on vascular skin blood flow in naïve mice.** Blood flow was monitored using Full-field Laser Perfusion Imager (FLPI) in the ear skin of anaesthetised mice ( $n=4-6$ ) at baseline (5 min) and following intradermal injection of  $\alpha$ Analogue (1-100pmol) in the ipsilateral ear and vehicle (0.219M Mannitol, 5% HPCD, 1.6% ammonium acetate at pH 6.5) in the contralateral ear. Results show mean  $\pm$  SEM for area under the curve (AUC) for the 30 min recording. \*\*\* $p<0.001$  vs vehicle-treated ear; # $p<0.05$  vs  $\alpha$ Analogue treated ear (One-way ANOVA + Bonferroni *post hoc* test).

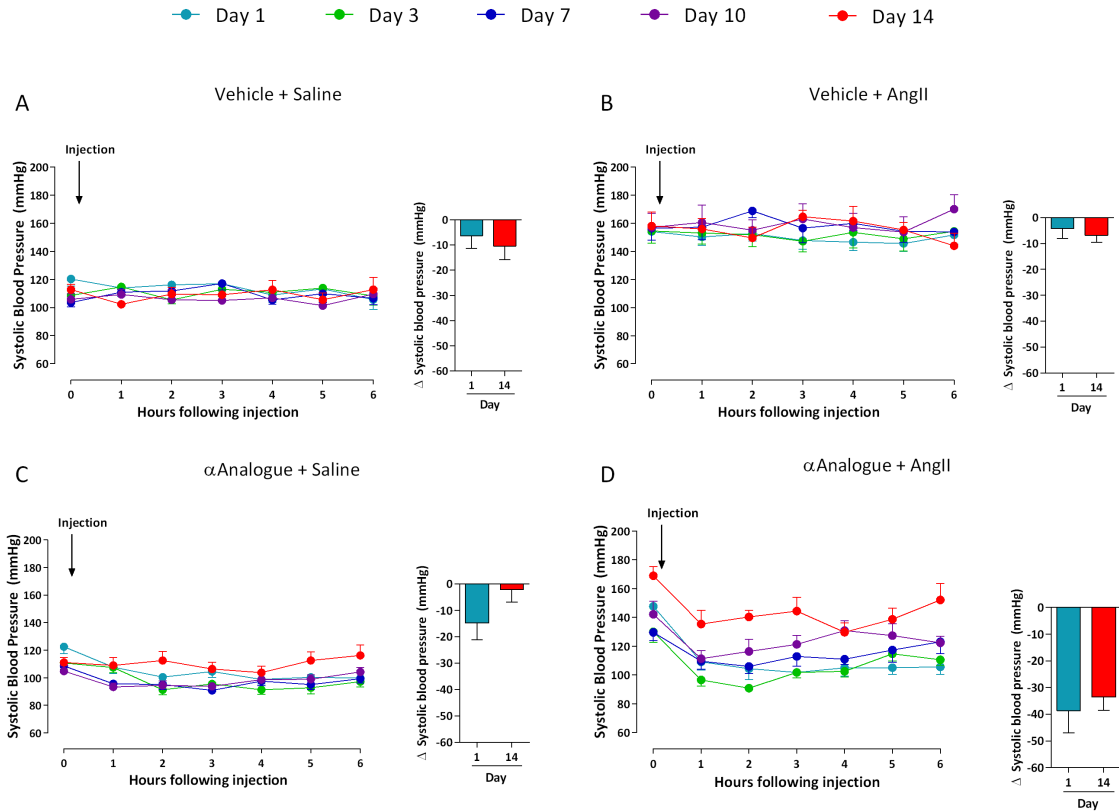


**Supplemental Figure 2. Effect of systemic administration of  $\alpha$ -CGRP analogue ( $\alpha$ Analogue) on blood pressure in naïve mice. (A) Systolic and (B) diastolic blood pressure was monitored using tail-cuff plethysmography in trained conscious restrained mice at baseline and 1, 6, 24 and 30h following vehicle (0.219M Mannitol, 5% HPCD, 1.6% ammonium acetate at pH 6.5) or  $\alpha$ Analogue administration (10, 30, 50 or 100nmol/kg, *s.c.*). Blood pressure values were obtained for each animal and results show mean  $\pm$  SEM for each group of mice (n=7). \* $p$ <0.05, \*\* $p$ <0.01 vehicle vs 100nmol/kg  $\alpha$ Analogue treatment (Repeated measures 2-way ANOVA + Bonferroni *post hoc* test).**

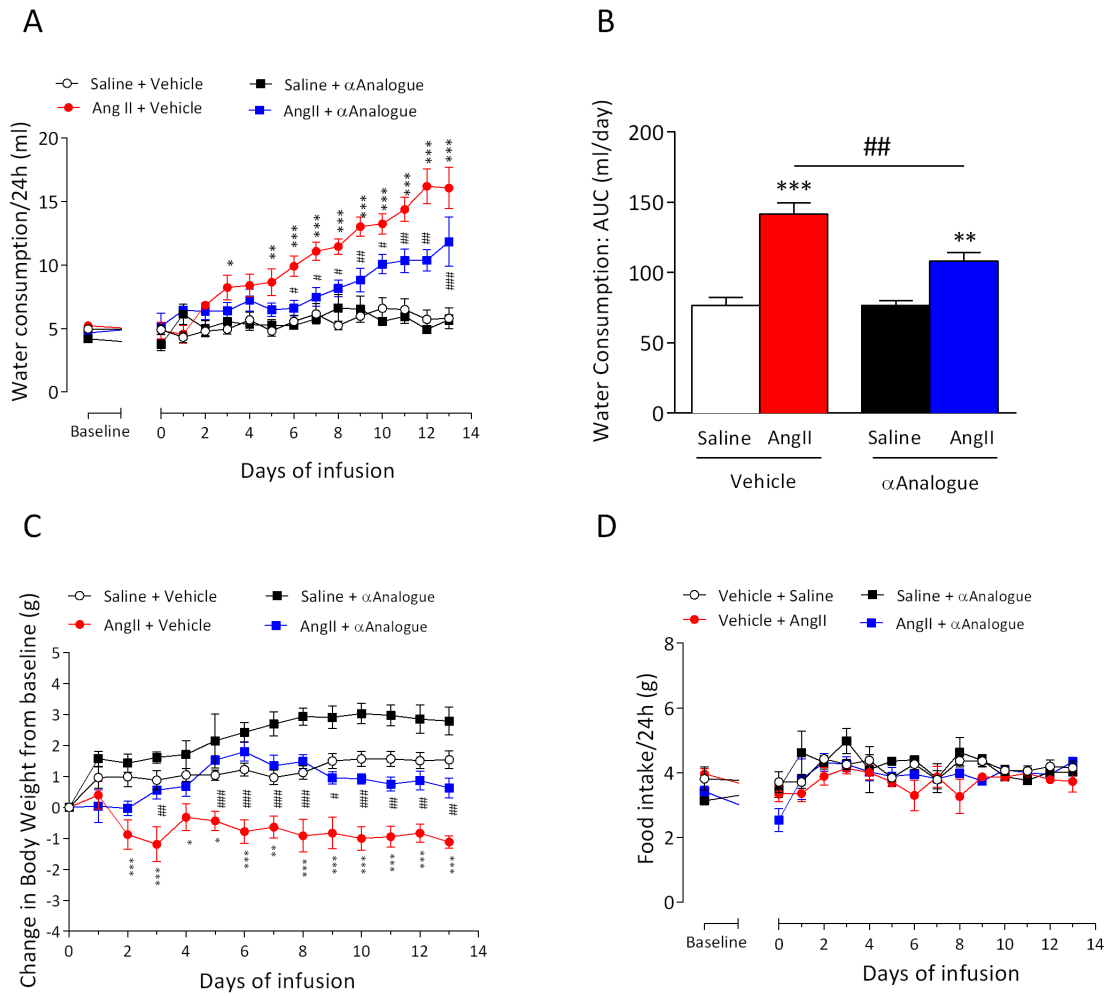


**Supplemental Figure 3. Effect of daily systemic treatment with  $\alpha$ -CGRP analogue ( $\alpha$ Analogue, 50nmol/kg) on cardiovascular haemodynamics in angiotensin II (AngII)-induced hypertension.** Mice were infused with either AngII (1.1mg/kg/day) or control (saline) with osmotic pumps for 14 days and treated daily with vehicle or  $\alpha$ Analogue (50nmol/kg, *s.c.*). (A) Diastolic blood pressure, (B) mean blood pressure, (C) heart rate and (D) activity were measured by radiotelemetry. Results show measurement taken every 10 min, expressed as 6h average. Mice experience a 12/12h light/dark cycle, with the dark cycle shown in the grey striped area. Arrow represents the start of daily treatment. Results show mean  $\pm$  SEM (n=4-7). \**p*<0.05, \*\**p*<0.01, \*\*\**p*<0.001 vs vehicle-treated saline-infused mice; #*p*<0.05, ###*p*<0.01, ####*p*<0.001 for  $\alpha$ Analogue-treated mice AngII-infused vs vehicle-treated AngII-infused mice (Repeated measures 2-way ANOVA + Bonferroni *post hoc* test).

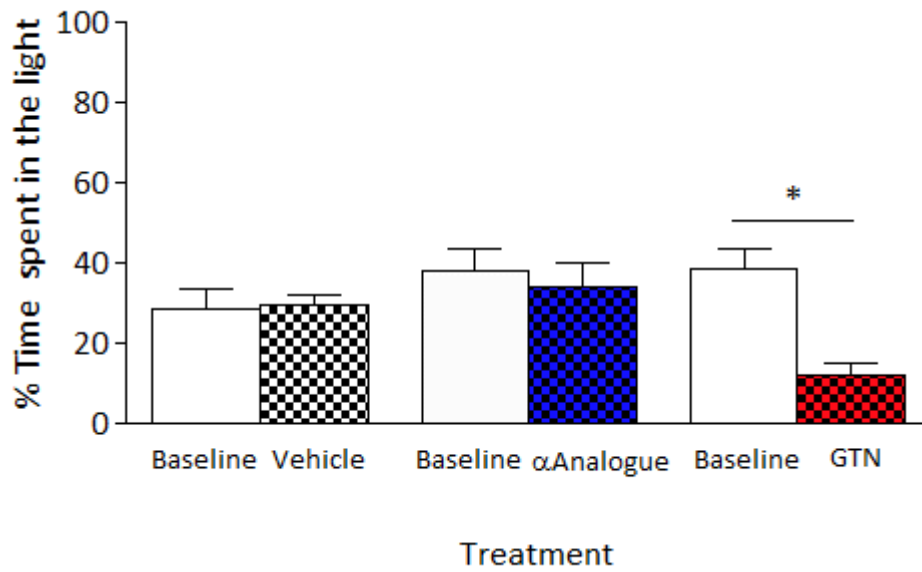




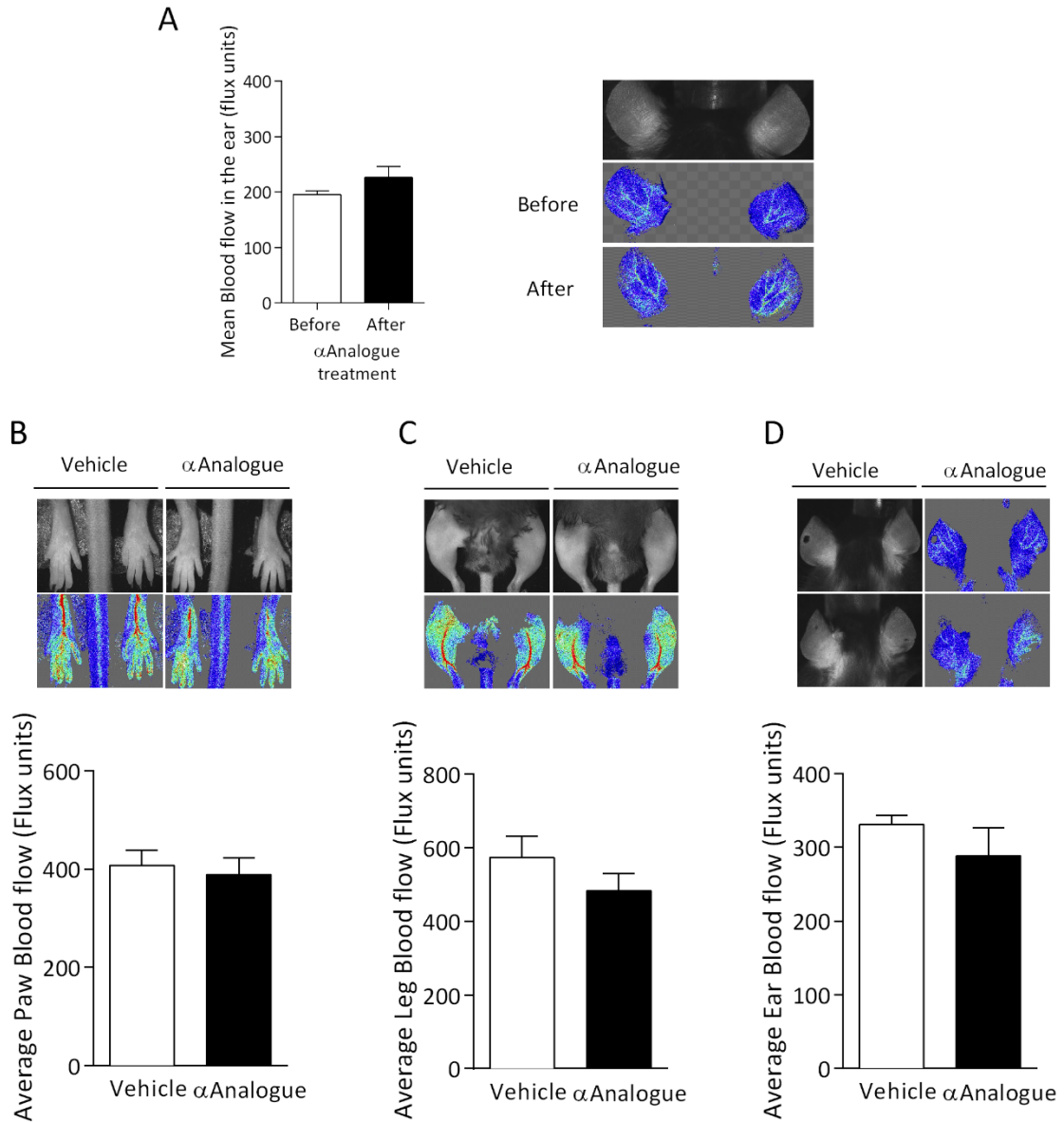
**Supplemental Figure 4. Daily systemic treatment with the  $\alpha$ -CGRP analogue ( $\alpha$ Analogue) produces a reproducible reduction in blood pressure in Angiotensin II (AngII)-induced hypertension in mice.** 6h time course profile of systolic blood pressure following injection of vehicle or  $\alpha$ Analogue (50nmol/kg) at Day 1, 3, 7, 10 and 14 in mice infused with saline (**A and C**) or AngII (**B and D**). **Left Panels**, Detailed analysis of SBP changes pre-and up to 6h post-  $\alpha$ Analogue or vehicle injection in mice infused with saline or AngII. **Right Panels**, Change ( $\Delta$ ) in SBP at Day 1 and Day 14 at 1h following injection from baseline (n=4-7). Results show mean  $\pm$  SEM.



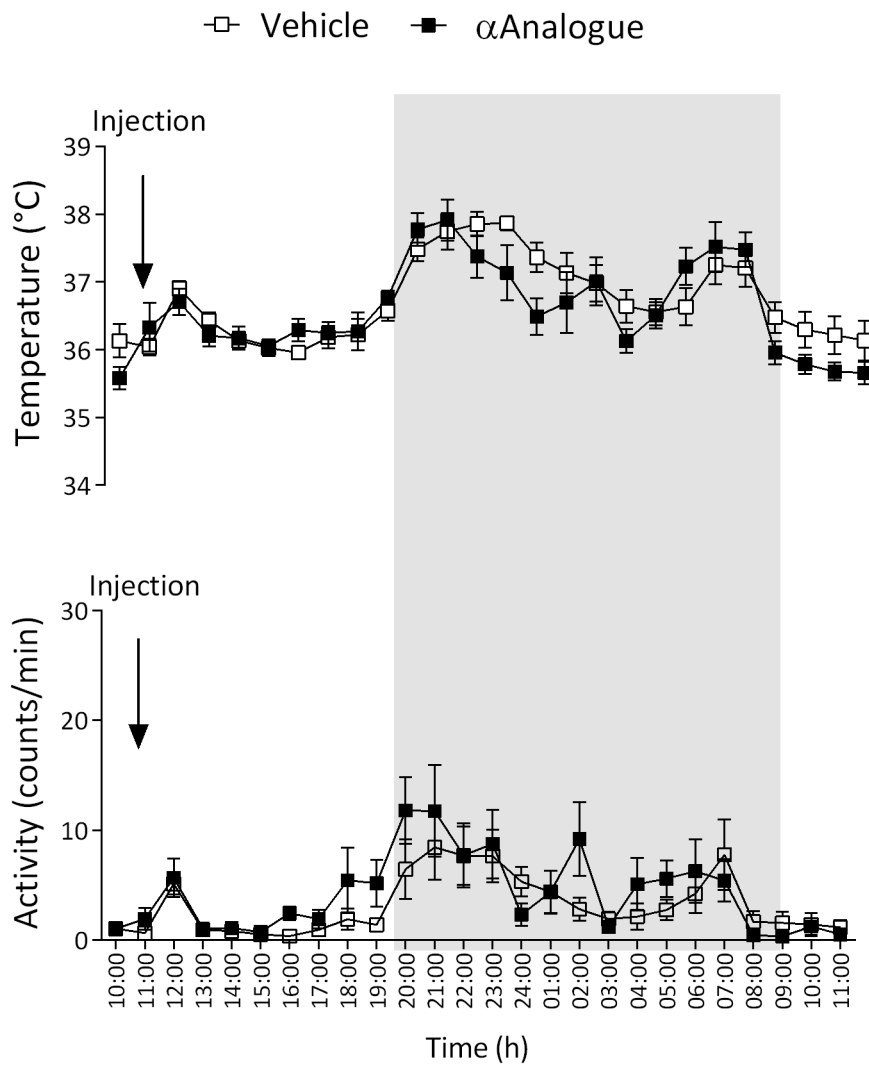
**Supplemental Figure 5. Effects of the  $\alpha$ -CGRP analogue ( $\alpha$ Analogue) or vehicle on (A-B) water consumption, (C) body weight and (D) food intake in Angiotensin II (AngII)-induced hypertension in mice.** Baseline measurements of body weight, food and water intake were taken for 7 days prior to osmotic pump implantation. Mice were administered with osmotic pumps containing saline or AngII (1.1 mg/kg/day for 14 day). Measurements were taken daily. Data are mean  $\pm$  S.E.M from n=5-7. AUC represents area under the curve results throughout the 14 day recording. Results show mean  $\pm$  SEM. \*p<0.05, \*\*p<0.01, \*\*\*p<0.001 versus vehicle-treated group, #p<0.05, ##p<0.01, ###p<0.001 versus  $\alpha$ Analogue-treated group (Repeated measures 2-way ANOVA + Bonferroni *post hoc* test for A,C-D and 2-way ANOVA + Bonferroni *post hoc* test for B).



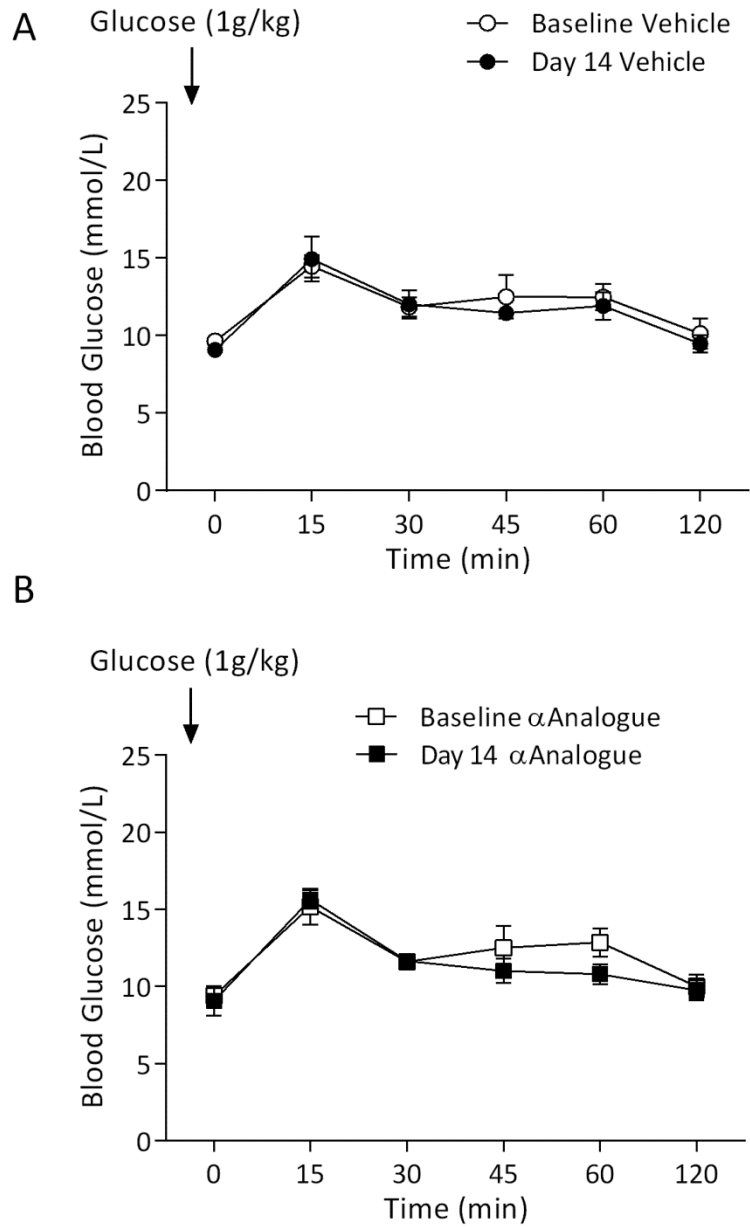
**Supplemental Figure 6. Effects of the  $\alpha$ -CGRP analogue ( $\alpha$ Analogue) on light-aversion.** Mice were trained twice daily for 5 days to enable an even distribution to enter the dark covered zone or bright light uncovered area (n=6-7). On the test day, time (s) spent in the light (1000 lux) was recorded for 600s at baseline and 1h following administration of  $\alpha$ Analogue (50nmol/kg, *s.c.*) or glyceryl trinitrate (GTN, 352nmol/kg, *i.v.*). Results show % time spent in light in mice, mean  $\pm$  SEM (n=6-7). \*p<0.05 vs respective baseline (paired t-tests).



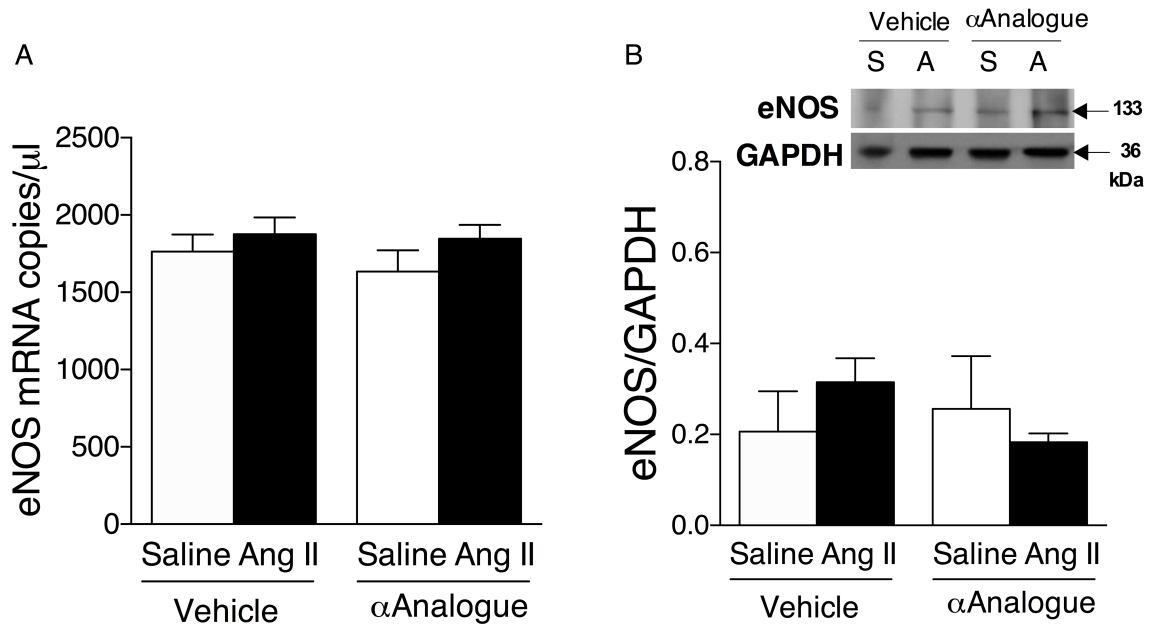
**Supplemental Figure 7. Effects of the  $\alpha$ -CGRP analogue ( $\alpha$ Analogue) on peripheral blood flow in mice.** Mice were briefly anaesthetised with isoflurane (2%) and blood flow was monitored using Full-field Laser Perfusion Imager (FLPI) for 5 min. **(A)** Average blood flow in the ear vasculature at baseline (before) and 1h following a single treatment of  $\alpha$ Analogue (50nmol/kg, *s.c.*) in mice (n=6). Average blood flow in the **(B)** paw, **(C)** leg and **(D)** ear of mice at day 14 following daily treatment of vehicle or  $\alpha$ Analogue (50nmol/kg, *s.c.*). Representative FLPI pictures alongside grey/black 'photo' showing blood flow for vehicle and  $\alpha$ Analogue treatment. Results represent mean  $\pm$  SEM for average measurement (flux units) for 5 min recording.  $p > 0.05$  ns (two-tailed Student's *t*-test).



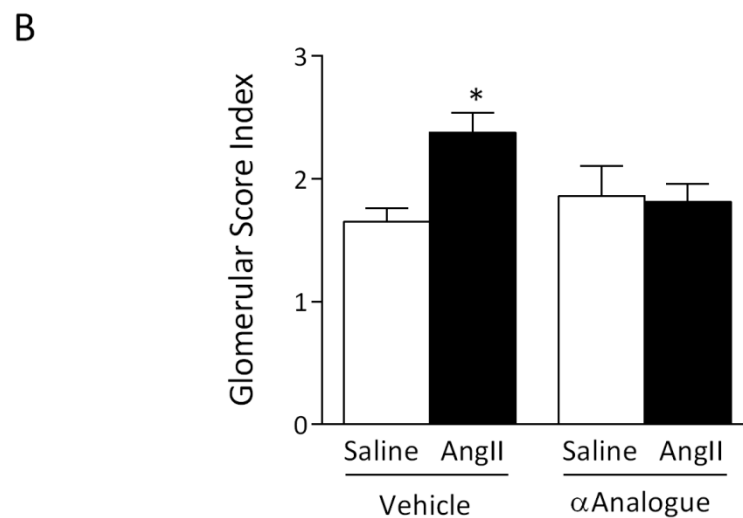
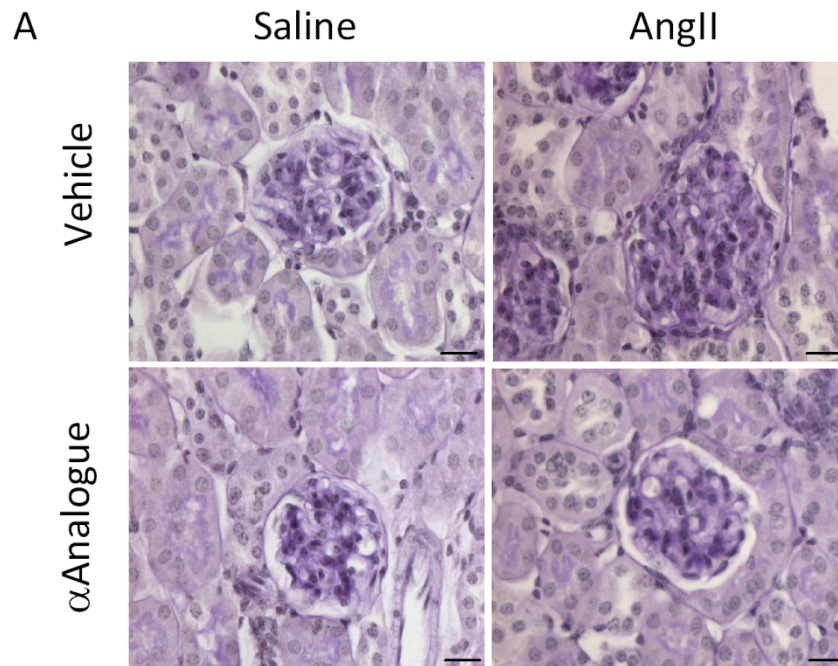
**Supplemental Figure 8. Effects of  $\alpha$ -CGRP analogue ( $\alpha$ Analogue) on core body temperature and activity in mice** Core body temperature and activity recordings over 24h at baseline and following vehicle or  $\alpha$ Analogue (50nmol/kg, *s.c.*) treatment in conscious mice (n=5). Results represent average 1h recording, mean  $\pm$  SEM. Arrow denotes time of treatment and grey area represents night/dark period. NS  $p > 0.05$  vs vehicle treatment (Repeated measures 2-way ANOVA + Bonferroni *post hoc* test).



**Supplemental Figure 9. Effects of cardiovascular active dose of  $\alpha$ -CGRP analogue ( $\alpha$ Analogue) on glucose tolerance test in mice.** Time course of plasma glucose concentrations (mmol/L) following systemic administration of glucose (1g/kg, *i.p.*) in mice treated daily with **(A)** vehicle (n=4) and **(B)**  $\alpha$ Analogue (50nmol/kg/day, *s.c.*, n=5) for 14 days. Results show mean  $\pm$  SEM. Arrow denotes treatment time of glucose administration. NS  $p > 0.05$  vs baseline (Repeated measures 2-way ANOVA + Bonferroni post *hoc* test).

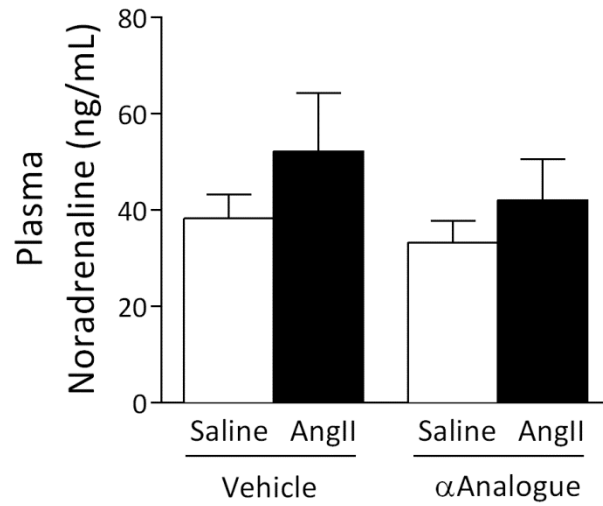


**Supplemental Figure 10. Effects of  $\alpha$ -CGRP analogue ( $\alpha$ Analogue) on vascular eNOS expression in mesenteric vessels.** Mice were treated daily with the  $\alpha$ -CGRP analogue (50nmol/kg, *s.c.*) or vehicle post AngII or saline infusion for 14 days. mRNA expression measured by qRT-PCR (n=4-6) and expressed as copy numbers per  $\mu$ l normalised to HPRT, B<sub>2</sub>M and  $\beta$ -actin. Protein expression normalised by GAPDH and shown by immunoblotting (top panel) and densitometry analysis (bottom panel). (**A**) mRNA and (**B**) protein expression of endothelial nitric oxide synthase (eNOS). Results show mean  $\pm$  SEM. ns  $p > 0.05$  (2-way ANOVA + Bonferroni *post hoc* test).

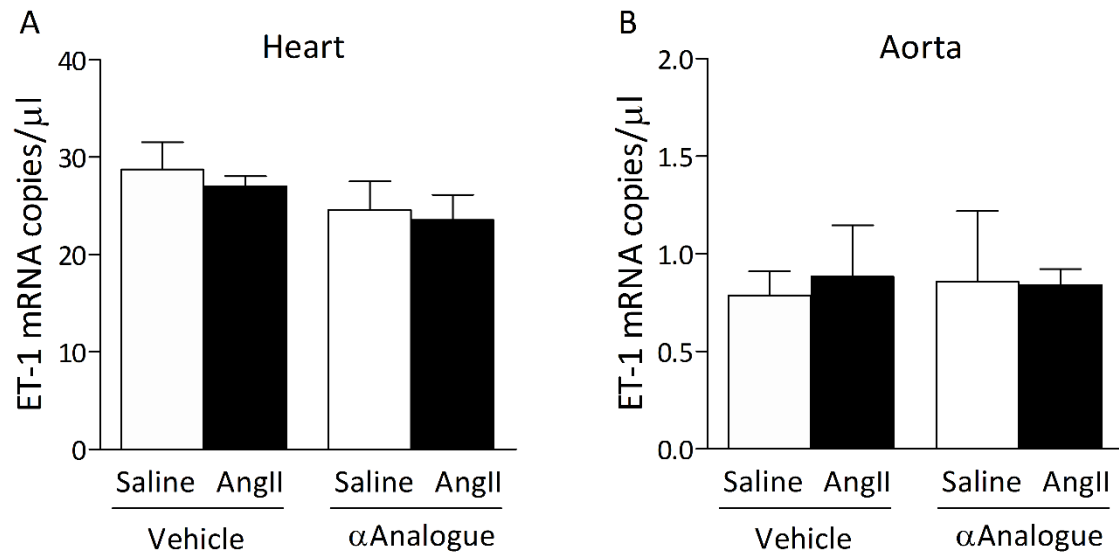


**Supplemental Figure 11. Effects of  $\alpha$ -CGRP analogue ( $\alpha$ Analogue) on morphological changes in the glomeruli in the kidney of Angiotensin II (AngII)-induced hypertension mice.** Mice were treated daily with the  $\alpha$ Analogue (50nmol/kg, *s.c.*) or vehicle post AngII or saline infusion for 14 days. **(A)** Representative image showing glomerular mesangial pathology using PAS staining (20 $\mu$ m, scale bar). **(B)** Summarized glomerular matrix expansion by semi-quantification of scores in different groups. Results show mean  $\pm$  SEM. \* $p$ <0.05 vs vehicle-treated (2-way ANOVA + Bonferroni *post hoc* test).

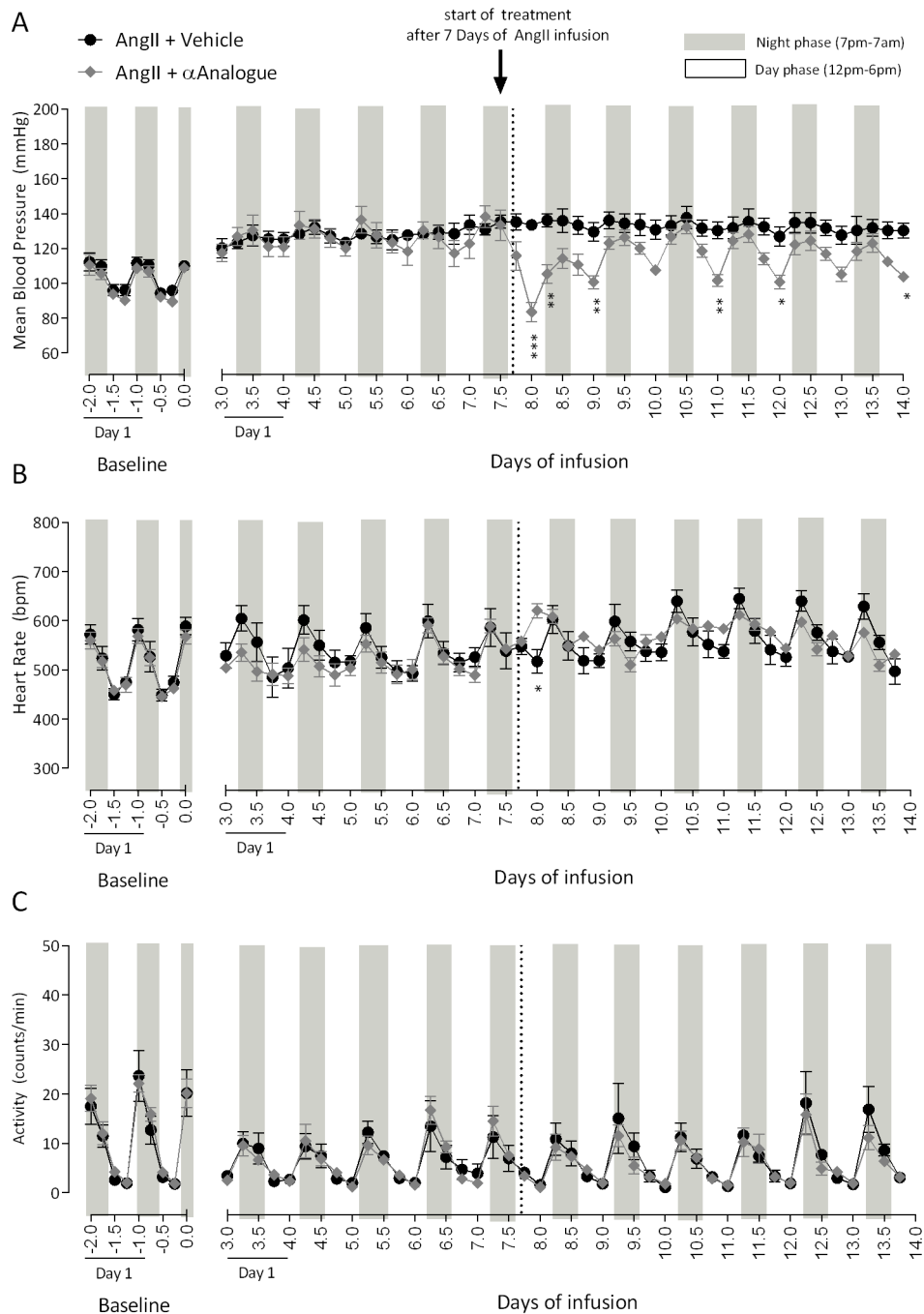




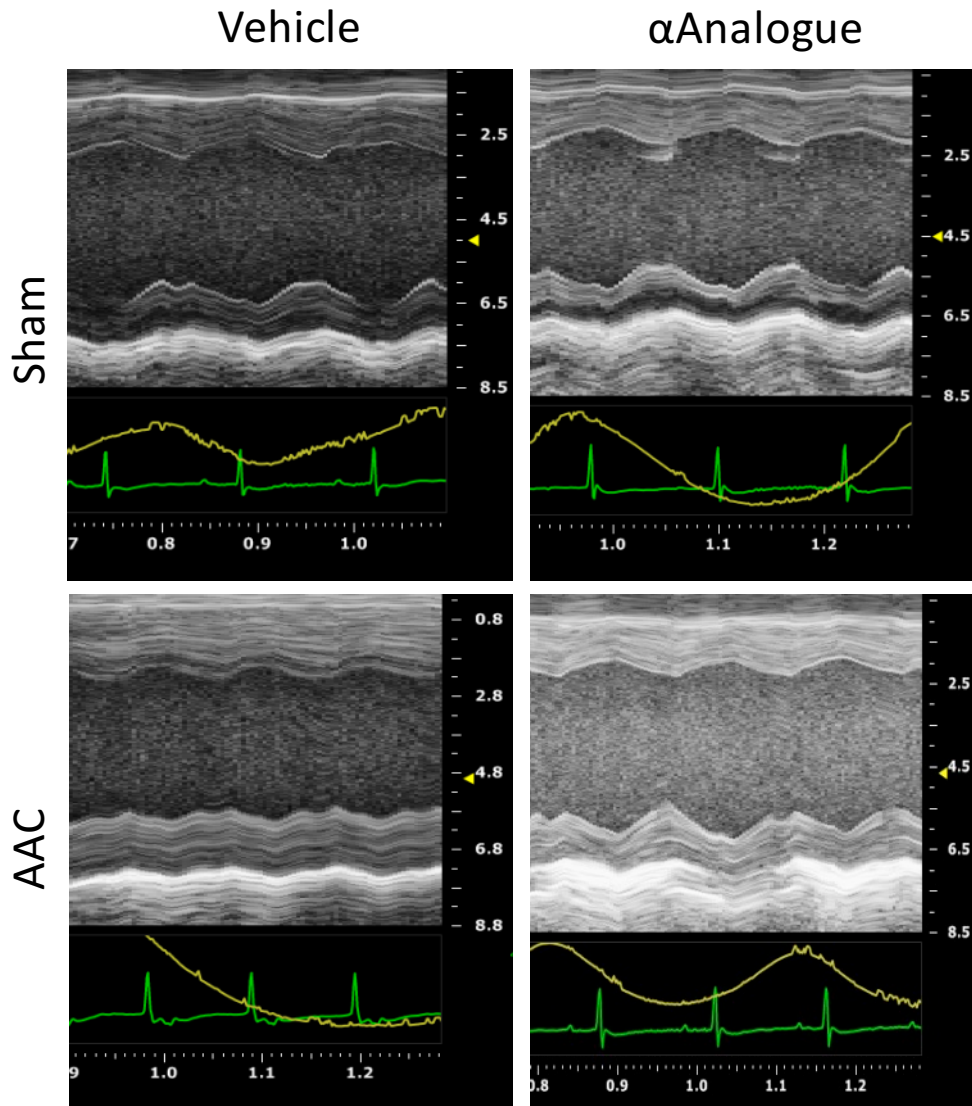
**Supplemental Figure 12. Effects of  $\alpha$ -CGRP analogue ( $\alpha$ Analogue) on plasma noradrenaline (NA) level in Angiotensin II(AngII)-induced hypertension mice.** Mice were treated daily with the  $\alpha$ Analogue (50nmol/kg, *s.c.*) or vehicle post AngII or saline infusion for 14 days. NA was quantified using ELISA (n=6-9). Results show mean  $\pm$  SEM. ns  $p>0.05$  (2-way ANOVA + Bonferroni *post hoc* test).



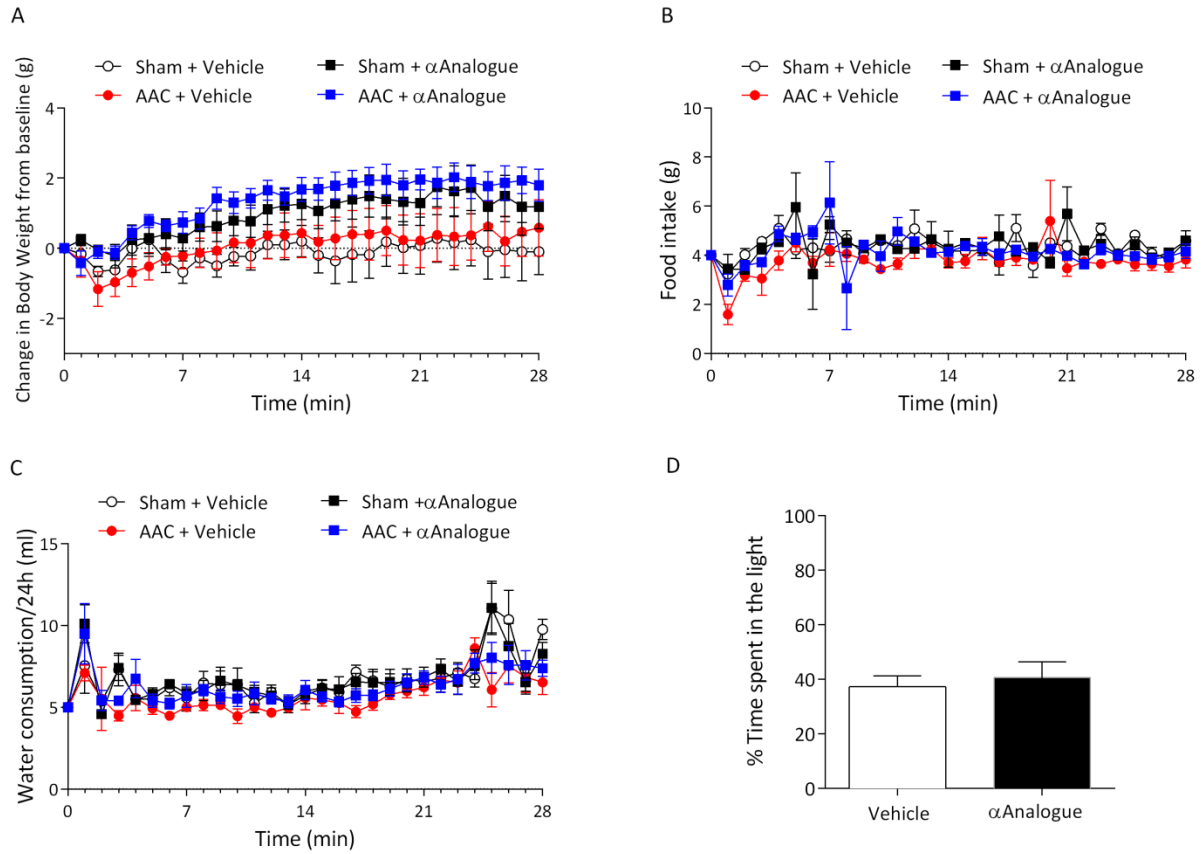
**Supplemental Figure 13. Effects of  $\alpha$ -CGRP analogue ( $\alpha$ Analogue) on mRNA expression of endothelial-1 (ET-1) level in Angiotensin II(AngII)-induced hypertension mice.** Mice were treated daily with the  $\alpha$ Analogue (50nmol/kg, *s.c.*) or vehicle post AngII or saline infusion for 14 days. mRNA expression measured by qRT-PCR (n=6-7) for ET-1 in **(A)** heart and **(B)** aorta (n=4-11). Results expressed as copy numbers per  $\mu$ l normalised to HPRT, B2M and  $\beta$ -actin. Results show mean  $\pm$  SEM. ns  $p > 0.05$  (2-way ANOVA + Bonferroni *post hoc* test).



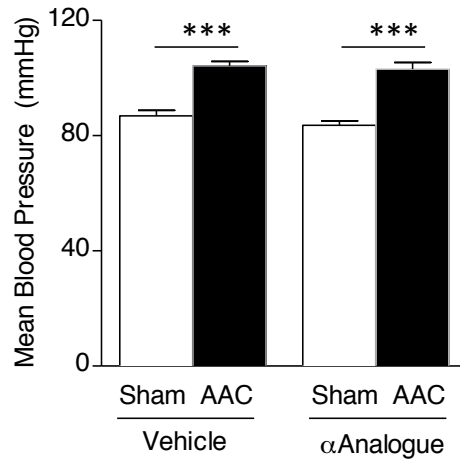
**Supplemental Figure 14. Effect of daily treatment with  $\alpha$ -CGRP analogue ( $\alpha$ Analogue, 50nmol/kg) on angiotensin II (AngII)-induced hypertensive mice.** Mice were infused with AngII (1.1mg/kg/day) osmotic pumps for 14 days and treated with vehicle or  $\alpha$ Analogue (50nmol/kg) on Day 7-14 (n=4). **(A)** Mean blood pressure, **(B)** heart rate and **(C)** activity were measured by radiotelemetry. Results show measurement taken every 10 min, expressed as 6h average. Mice experience a 12/12h light/dark cycle, with the dark cycle shown in the grey striped area. Arrow indicates the start of daily treatment with vehicle or  $\alpha$ Analogue. \*p<0.05, \*\*p<0.01, \*\*\*p<0.001 vs vehicle-treated AngII-infused mice (Repeated measures 2-way ANOVA + Bonferroni *post hoc* test).



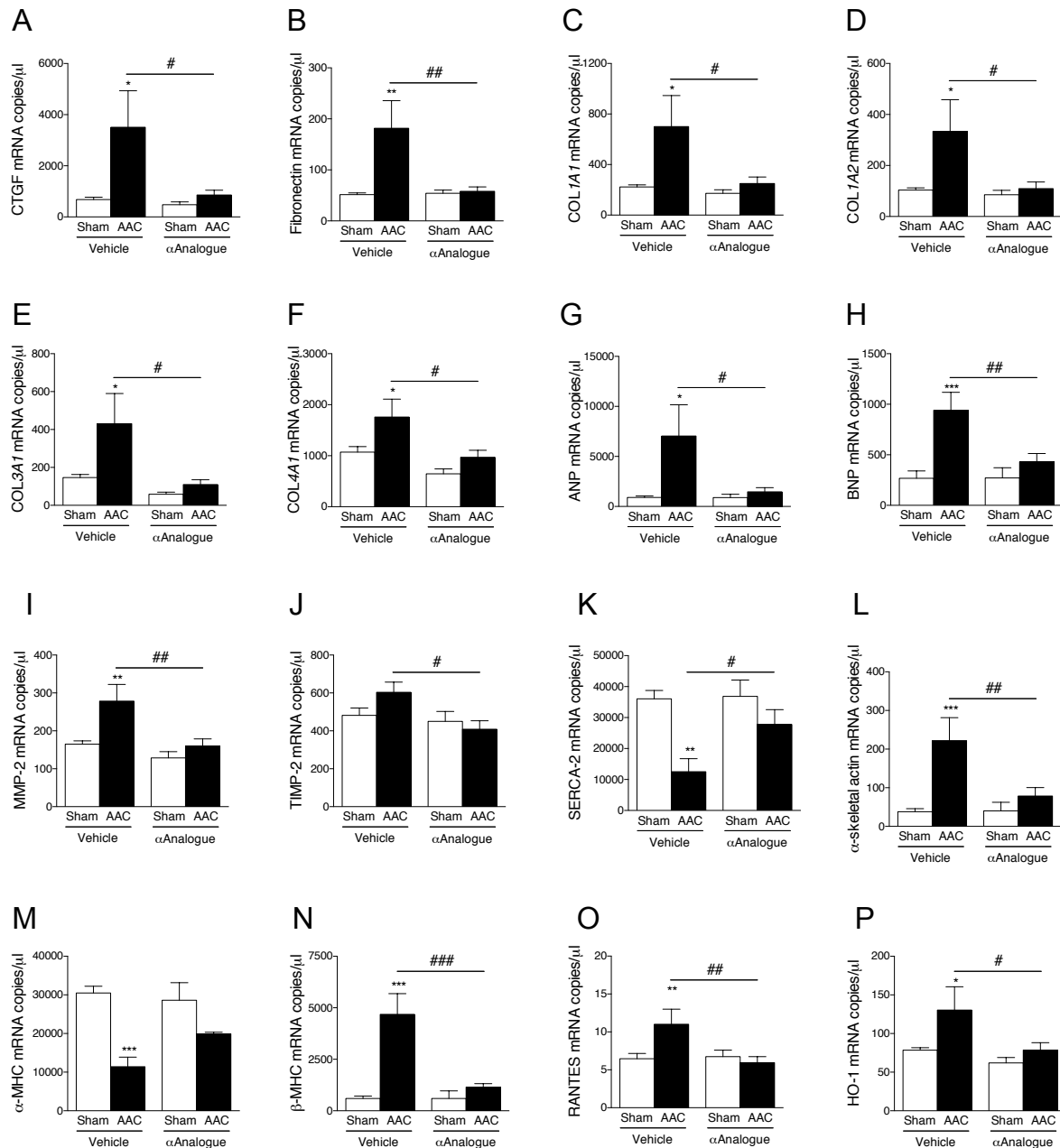
**Supplemental Figure 15. Effect of daily treatment with  $\alpha$ -CGRP analogue ( $\alpha$ Analogue) on abdominal aortic constriction (AAC)-induced cardiac hypertrophy and heart failure in mice.** Mice were treated with vehicle or  $\alpha$ Analogue (50nmol/kg, *s.c.*) for 5 weeks post-surgery and cardiac function was assessed using echocardiography at week 5. Representative images of cardiac function and dimension using M-Mode echocardiography in the parasternal long axis view in mice after sham or AAC surgery with or without treatment.



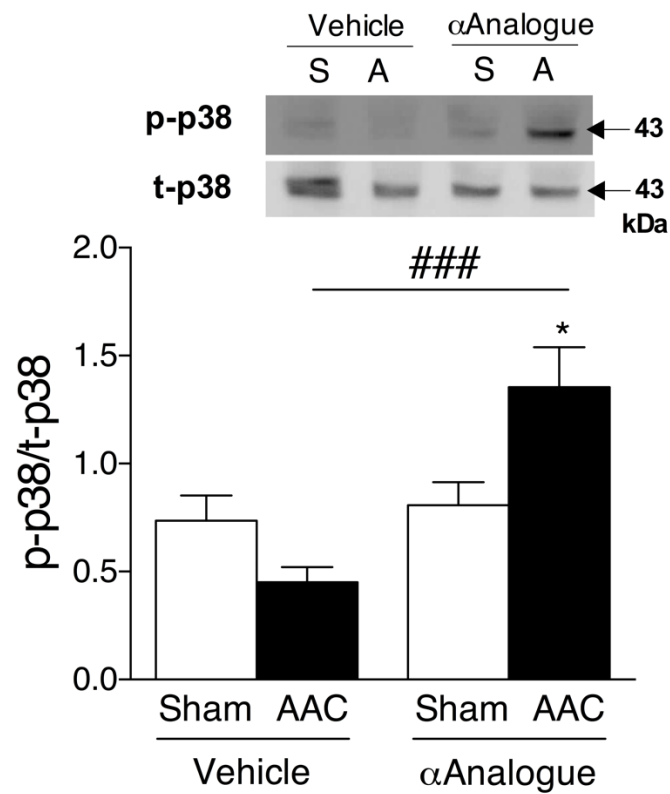
**Supplemental Figure 16. Effects of the  $\alpha$ -CGRP analogue ( $\alpha$ Analogue) or vehicle on (A) body weight, (B) food intake, (C) water consumption and (D) light aversion assay in abdominal aortic constriction-induced cardiac hypertrophy and heart failure. Mice were treated with vehicle or  $\alpha$ Analogue (50nmol/kg, *s.c.*) for 5 weeks post-surgery. Measurements were taken daily. Data are mean  $\pm$  S.E.M from n=6-8. ns  $p > 0.05$  (Repeated measures 2-way ANOVA + Bonferroni *post hoc* test).**



**Supplemental Figure 17. Changes in blood pressure in vehicle or  $\alpha$ -CGRP analogue ( $\alpha$ Analogue)-treated at 5 weeks following abdominal aorta constriction-induced cardiac hypertrophy and heart failure in mice.** Blood pressure measurement obtained by carotid artery cannulation in isoflurane-anaesthetised mice treated daily with the  $\alpha$ Analogue (50nmol/kg, *s.c.*) or vehicle for 5 weeks (n=7-8). Results show mean  $\pm$  SEM. \*\*\*p<0.001 vs vehicle treated sham mice (2-way ANOVA + Bonferroni *post hoc* test).



**Supplemental Figure 18. Daily systemic treatment with  $\alpha$ -CGRP analogue ( $\alpha$ Analogue) protects against abdominal aorta constriction (AAC)-induced cardiac fibrosis, hypertrophy, inflammation and oxidative stress.** Following AAC, mice were treated daily for 5 weeks with vehicle or  $\alpha$ Analogue (50nmol/kg, *s.c.*). mRNA expression measured by qRT-PCR (n=6-7) for (A) CTGF, (B) fibronectin, (C) collagen type 1  $\alpha$  (COL1A1), (D) collagen type 1  $\alpha$ 2 (COL1A2), (E) collagen type 3  $\alpha$ 1 (COL3A1), (F) collagen type 4  $\alpha$ 1 (COL4A1), (G) atrial natriuretic peptide (ANP), (H) brain natriuretic peptide (BNP), (I) matrix metalloproteinase-2 (MMP-2), (J) tissue inhibitor of metalloproteinase 2 (TIMP-2), (K) sarco-endoplasmic reticulum  $\text{Ca}^{2+}$  ATPase-2 (SERCA-2), (L)  $\alpha$ -skeletal actin, (M)  $\alpha$ -myosin heavy chain ( $\alpha$ -MHC), (N)  $\beta$ -myosin heavy chain ( $\beta$ -MHC), (O) chemokine RANTES and (P) heme oxygenase-1 (HO-1) in heart (n=6-7). Results expressed as copy numbers per  $\mu\text{l}$  normalised to HPRT, B2M and  $\beta$ -actin. Results show mean  $\pm$  SEM. \* $p$ <0.05, \*\* $p$ <0.01, \*\*\* $p$ <0.001 vs vehicle-treated sham mice; # $p$ <0.05, ## $p$ <0.01, ### $p$ <0.001 vs vehicle-treated AAC mice (2-WAY ANOVA + Bonferroni *post hoc* test).



**Supplemental Figure 19. Effects of  $\alpha$ -CGRP analogue ( $\alpha$ Analogue) on the phosphorylation of p-38 mitogen-activated protein kinases (MAPK) in the heart of abdominal aortic constriction-induced cardiac hypertrophy and hear failure in mice.** Mice were treated daily with the  $\alpha$ Analogue (50nmol/kg, *s.c.*) or vehicle post-surgery. Protein expression of phosphorylated p-38 was normalised to total p-38 (t-p38) and are shown by immunoblotting (top panel) and densitometry analysis (bottom panel) in heart tissues (n=6-8). Results show mean  $\pm$  mean. \*p<0.05 vs sham-treated, ###p<0.001 vs sham-treated (2-WAY ANOVA + Bonferroni *post hoc* test).



## Supplemental References

1. Aubdool AA, Graepel R, Kodji X, Alawi KM, Bodkin JV, Srivastava S, Gentry C, Heads R, Grant AD, Fernandes ES, Bevan S and Brain SD. TRPA1 is essential for the vascular response to environmental cold exposure. *Nat Commun.* 2014;5:5732. doi:10.1038/ncomms6732
2. Aubdool AA, Kodji X, Abdul-Kader N, Heads R, Fernandes ES, Bevan S and Brain SD. TRPA1 activation leads to neurogenic vasodilatation: Involvement of reactive oxygen nitrogen species in addition to CGRP and NO. *Br J Pharmacol.* 2016;173:2419-2433. doi:10.1111/bph.13519
3. Alawi KM, Russell FA, Aubdool AA, Srivastava S, Riffo-Vasquez Y, Baldissera L, Jr., Thakore P, Saleque N, Fernandes ES, Walsh DA and Brain SD. Transient receptor potential canonical 5 (TRPC5) protects against pain and vascular inflammation in arthritis and joint inflammation. *Ann Rheum Dis.* 2016;76:252-260. doi:10.1136/annrheumdis-2015-208886
4. Doods H, Hallermayer G, Wu D, Entzeroth M, Rudolf K, Engel W and Eberlein W. Pharmacological profile of BIBN4096BS, the first selective small molecule CGRP antagonist. *Br J Pharmacol.* 2000;129:420-423. doi:10.1038/sj.bjp.0703110
5. Starr A, Graepel R, Keeble J, Schmidhuber S, Clark N, Grant A, Shah AM and Brain SD. A reactive oxygen species-mediated component in neurogenic vasodilatation. *Cardiovasc Res.* 2008;78:139-147. doi:10.1093/cvr/cvn012
6. Nielsen AS, Kruse T, Kodra JT, Lau JF, Kofoed J, Raun K and Nilsson C, inventors; Novo Nordisk, assignee. Derivatives of cgrp. WO patent 2,011,051,312. May 5, 2011.
7. Smillie SJ, King R, Kodji X, Outzen E, Pozsgai G, Fernandes E, Marshall N, de Winter P, Heads RJ, Dessapt-Baradez C, Gnudi L, Sams A, Shah AM, Siow RC and Brain SD. An ongoing role of alpha-calcitonin gene-related peptide as part of a protective network against hypertension, vascular hypertrophy, and oxidative stress. *Hypertension.* 2014;63:1056-1062. doi:10.1161/HYPERTENSIONAHA.113.02517
8. Marshall NJ, Liang L, Bodkin J, Dessapt-Baradez C, Nandi M, Collot-Teixeira S, Smillie SJ, Lalgı K, Fernandes ES, Gnudi L and Brain SD. A role for TRPV1 in influencing the onset of cardiovascular disease in obesity. *Hypertension.* 2013;61:246-252. doi:10.1161/HYPERTENSIONAHA.112.201434
9. Leiper J, Nandi M, Torondel B, Murray-Rust J, Malaki M, O'Hara B, Rossiter S, Anthony S, Madhani M, Selwood D, Smith C, Wojciak-Stothard B, Rudiger A, Stidwill R, McDonald NQ and Vallance P. Disruption of methylarginine metabolism impairs vascular homeostasis. *Nat Med.* 2007;13:198-203. doi:10.1038/nm1543

10. Bodkin JV, Thakore P, Aubdool AA, Liang L, Fernandes ES, Nandi M, Spina D, Clark JE, Aaronson PI, Shattock MJ and Brain SD. Investigating the potential role of TRPA1 in locomotion and cardiovascular control during hypertension. *Pharmacol Res Perspect.* 2014;2:e00052. doi:10.1002/prp2.52
11. Zhang M, Brewer AC, Schroder K, Santos CX, Grieve DJ, Wang M, Anilkumar N, Yu B, Dong X, Walker SJ, Brandes RP and Shah AM. NADPH oxidase-4 mediates protection against chronic load-induced stress in mouse hearts by enhancing angiogenesis. *Proc Natl Acad Sci U S A.* 2010;107:18121-18126. doi:10.1073/pnas.1009700107
12. Murray TV, Smyrniak I, Schnelle M, Mistry RK, Zhang M, Beretta M, Martin D, Anilkumar N, de Silva SM, Shah AM and Brewer AC. Redox regulation of cardiomyocyte cell cycling via an ERK1/2 and c-Myc-dependent activation of cyclin D2 transcription. *J Mol Cell Cardiol.* 2015;79:54-68. doi:10.1016/j.yjmcc.2014.10.017
13. Crawley J and Goodwin FK. Preliminary report of a simple animal behavior model for the anxiolytic effects of benzodiazepines. *Pharmacol Biochem Behav.* 1980;13:167-170.
14. Thiels E, Hoffman EK and Gorin MB. A reliable behavioral assay for the assessment of sustained photophobia in mice. *Curr Eye Res.* 2008;33:483-491. doi:10.1080/02713680802130347
15. Kaiser EA, Kuburas A, Recober A and Russo AF. Modulation of CGRP-induced light aversion in wild-type mice by a 5-HT(1B/D) agonist. *J Neurosci.* 2012;32:15439-15449. doi:10.1523/JNEUROSCI.3265-12.2012
16. Ramachandran R, Bhatt DK, Ploug KB, Olesen J, Jansen-Olesen I, Hay-Schmidt A and Gupta S. A naturalistic glyceryl trinitrate infusion migraine model in the rat. *Cephalalgia.* 2012;32:73-84. doi:10.1177/0333102411430855
17. Papacleovoulou G, Abu-Hayyeh S, Nikolopoulou E, Briz O, Owen BM, Nikolova V, Ovadia C, Huang X, Vaarasmaki M, Baumann M, Jansen E, Albrecht C, Jarvelin MR, Marin JJ, Knisely AS and Williamson C. Maternal cholestasis during pregnancy programs metabolic disease in offspring. *J Clin Invest.* 2013;123:3172-3181. doi:10.1172/JCI68927
18. Alawi KM, Aubdool AA, Liang L, Wilde E, Vepa A, Psefteli MP, Brain SD and Keeble JE. The sympathetic nervous system is controlled by transient receptor potential vanilloid 1 in the regulation of body temperature. *FASEB J.* 2015;29:4285-4298. doi:10.1096/fj.15-272526

19. Looi YH, Grieve DJ, Siva A, Walker SJ, Anilkumar N, Cave AC, Marber M, Monaghan MJ and Shah AM. Involvement of Nox2 NADPH oxidase in adverse cardiac remodeling after myocardial infarction. *Hypertension*. 2008;51:319-325. doi:10.1161/HYPERTENSIONAHA.107.101980
20. Murdoch CE, Chaubey S, Zeng L, Yu B, Ivetic A, Walker SJ, Vanhoutte D, Heymans S, Grieve DJ, Cave AC, Brewer AC, Zhang M and Shah AM. Endothelial NADPH oxidase-2 promotes interstitial cardiac fibrosis and diastolic dysfunction through proinflammatory effects and endothelial-mesenchymal transition. *J Am Coll Cardiol*. 2014;63:2734-2741. doi:10.1016/j.jacc.2014.02.572
21. Liang L, Tam CW, Pozsgai G, Siow R, Clark N, Keeble J, Husmann K, Born W, Fischer JA, Poston R, Shah A and Brain SD. Protection of angiotensin II-induced vascular hypertrophy in vascular smooth muscle-targeted receptor activity-modifying protein 2 transgenic mice. *Hypertension*. 2009;54:1254-1261. doi:10.1161/HYPERTENSIONAHA.109.129783
22. Junqueira LC, Bignolas G and Brentani RR. Picrosirius staining plus polarization microscopy, a specific method for collagen detection in tissue sections. *Histochem J*. 1979;11:447-455.
23. Ducharme A, Frantz S, Aikawa M, Rabkin E, Lindsey M, Rohde LE, Schoen FJ, Kelly RA, Werb Z, Libby P and Lee RT. Targeted deletion of matrix metalloproteinase-9 attenuates left ventricular enlargement and collagen accumulation after experimental myocardial infarction. *J Clin Invest*. 2000;106:55-62. doi:10.1172/JCI8768
24. Riehle C, Wende AR, Zaha VG, Pires KM, Wayment B, Olsen C, Bugger H, Buchanan J, Wang X, Moreira AB, Doenst T, Medina-Gomez G, Litwin SE, Lelliott CJ, Vidal-Puig A and Abel ED. PGC-1beta deficiency accelerates the transition to heart failure in pressure overload hypertrophy. *Circ Res*. 2011;109:783-793. doi:10.1161/CIRCRESAHA.111.243964
25. Johnson RJ, Iida H, Alpers CE, Majesky MW, Schwartz SM, Pritzki P, Gordon K and Gown AM. Expression of smooth muscle cell phenotype by rat mesangial cells in immune complex nephritis. Alpha-smooth muscle actin is a marker of mesangial cell proliferation. *J Clin Invest*. 1991;87:847-858. doi:10.1172/JCI115089
26. Bank N, Klose R, Aynedjian HS, Nguyen D and Sablay LB. Evidence against increased glomerular pressure initiating diabetic nephropathy. *Kidney Int*. 1987;31:898-905.